CAPILLARY LIQUID TRANSPORT IN POROUS MEDIA

J. VAN BRAKEL

CAPILLARY LIQUID TRANSPORT IN POROUS MEDIA

PROEFSCHRIFT

TER VERKRIJGING VAN DE GRAAD VAN DOCTOR IN DE TECHNISCHE WETENSCHAPPEN AAN DE TECHNISCHE HOGESCHOOL DELFT, OP GEZAG VAN DE RECTOR MAGNIFICUS, Ir. H. B. BOEREMA, HOOGLERAAR IN DE AFDELING DER ELEKTROTECHNIEK, VOOR EEN COMMISSIE AANGEWEZEN DOOR HET COLLEGE VAN DEKANEN, TE VERDEDIGEN OP WOENSDAG 12 FEBRUARI 1975 TE 16.00 UUR

DOOR

JAAP VAN BRAKEL

scheikundig ingenieur
wijsgerig doctorandus
geboren te dordrecht

DRUKKERIJ J. H. PASMANS - 'S-GRAVENHAGE

DIT PROEFSCHRIFT IS GOEDGEKEURD DOOR DE PROMOTOR

PROF.DR.IR.P.M.HEERTJES

Solange ein Wissenszweig
Ueberflusz an Problemen bietet,
ist er lebenskräftig

D. Hilbert

Zeer velen hebben aan de totstandkoming van dit proefschrift hun bijdrage geleverd. Ik zeg hun daarvoor recht hartelijk dank.

TABLE OF CONTENTS

SUMMARY AND INTRODUCTION

The central theme of this thesis is to give an analysis of the phenomena that can be observed in capillary rise in porous media (e g , the capillary rise of water in coarse sand). These phenomena give rise to two problems:

(i) When, after capillary rise, equilibrium is reached between gravity and capillarity, sometimes a wide saturation gradient is observed, while in other cases no saturation gradient is observed. That is to say, sometimes there is a sharp separation between the dry part of the porous medium and the completely saturated part, and sometimes there is a very gradual change from the saturated to the dry part.

(ii) In some cases equilibrium is reached after a few minutes (for capillary rise of water in coarse sand). In other cases it may take several weeks before equilibrium has been reached.

The contents of this thesis can be divided into two parts. The first chapter is the text of a review article concerning the use of porespace models and other approaches to describe transport phenomena in porous media (emphasizing capillary liquid transport). On the one hand the first chapter is the introduction to the other four chapters, which treat the two problems mentioned above. On the other hand it is the endogeneous justification of the research described in the following chapters. The main conclusions of chapter one are:

(i) Capillary liquid transport in porous media cannot be described without taking into account the geometry of the porespace.

(ii) Different transport phenomena require different porespace models. This is the more important because the input parameters of the models are often determined by transport phenomena, which are different from those to which the model is applied.

(iii) Capillary rise is the most complicated transport phenomenon in porous media. This is illustrated by the fact that, of all porespace models proposed in the literature, none is capable of explaining, not even qualitatively, the phenomena observed with capillary rise.

The next chapters mainly concern capillary rise. In the second chapter the experimental techniques are described and the characteristics of the four kinds of capillary rise are elucidated by means of a large number of examples. Most experiments were performed with

sand, glass beads, or polystyrene spheres as the solid phase. Water and various organic liquids were used as the rising liquid. In the third chapter the more superficial hypotheses that could explain the different kinds of capillary rise are refuted (e g : homogeneity of the packing, air entrapment, capillary condensation).

The attempt to explain the observed phenomena is introduced in chapter four by establishing the following two empirical laws:

(1) The occurrence of a wide saturation gradient at equilibrium corresponds to a contact angle of about zero. A sharp liquid front at equilibrium corresponds to a contact angle above some critical value.

(2) The relatively slow capillary rise is caused by the fact that the contact angle decreases during capillary rise.

A large part of the fourth chapter is formed by a priori considerations concerning the contact angle of different systems. The resson for this is that a number of systems yield a contact angle larger than zero for combinations, such as glass-hexane, for which this would not be expected. One of the conclusions is that polymolecular adsorption films, with properties different from those of the bulk liquid, occur more often than is generally assumed. Further, a number of mechanisms is considered that might explain a decreasing contact angle. At present definitive conclusions regarding the interpretation of the above mentioned empirical law (2) are not yet possible.

In the final chapter the mechanism of a moving liquid front in an irregular sphere packing is analyzed, in order to explain the above mentioned law (1). This mechanism and the interpretation of law (1) can be summarized as follows:

(a) The liquid-vapour interface consists of concave and anticlastic parts. (Anticlastic means that the principal radii of curvature have an opposite sign). The anticlastic or α-menisci are contained by two spheres. The concave or γ-menisci are contained by three or more spheres.

(b) The porespace can be visualized as a number of cavities connected by windows. The mechanism of transport is governed by a continuous merging and generation of menisci. The continuity of transport is sustained by two intersupporting mechanisms:

(i) The filling of windows by merging α-menisci.

(ii) The filling of cavities when a number of windows are closed.

(c) Primarily, capillary rise is dependent on the α-menisci. The γ-menisci have a supporting function, and are necessary to fill the cavities, but they cannot, by themselves alone, maintain continuity of transport.

(d) In first approximation the saturation gradient at equilibrium is a function of the window-size distribution. In an irregular sphere packing there are a large number of minimum size (i e the window between three contiguous spheres). If the α-menisci, which fill these smallest windows, together with the γ-menisci, can maintain continuity of transport, then no saturation gradient will be observed.

(e) The dependence of the curvature on the contact angle is different for α- and γ-menisci. The contribution of the γ-menisci to the continuity of transport is more important at higher values of the contact angle. Above some critical value of the contact angle the maximum height of capillary rise is determined solely by the smallest window.

CHAPTER 1

PORESPACE MODELS FOR TRANSPORT PHENOMENA IN POROUS MEDIA[†]

Review and evaluation with special emphasize on capillary liquid transport

1.0. Summary

A classification and characterization is given of the more important transport phenomena in macroporous media (molecular diffusion, viscous flow, transport phenomena involving moving menisci: wetting, capillary rise, drainage, drying). Porespace models are used to obtain values for the transport coefficient (effective diffusion coefficient, permeability) and - when applicable - the driving force (capillary potential) in the transport equation. These models and this approach have to be distinguished from (i) models used in simulating particle packings, (ii) models used in determining the so-called pore-size distribution (suction technique, mercury porosimetry), (iii) analytic calculation of the transport coefficient, and (iv) overall description of the transport phenomena (in which the microscopic porespace structure is not accounted for).

An enumeration of almost all proposed models is presented and classified with reference to the porespace interconnectivity. This interconnectivity may be one-dimensional (tubes in parallel, in series; tubes with constrictions; random adjacent slices models), two-dimensional (network models), three-dimensional (regular sphere packings; tetrahedra networks; tubes and/or junctions randomly in space), and strictly zero-dimensional (simple capillary elements used in ad hoc explanations; independent domain theory).

In order to remove too optimistic ideas about the use of porespace models all models are checked against the phenomena of capillary rise (e g water in sand). The predictions of the models regarding the statics and dynamics of capillary rise are compared with the experimental facts and it appears that none of the models can even give a qualitative description of the observed phenomena. The situation is better for other transport phenomena than it is for capillary rise, but it should be realized that even slightly different transport phenomena ask for a different approach and

---

[†] The contents of this chapter are identical to that of a review article to appear in *Powder Technology*. A few notes have been added which refer to the subsequent chapters.

further, that improvement of porespace models should be directed by a more careful analysis of the non-macroscopic physical phenomena. It is the ghost of the concept of a pore-size (distribution) that plays a dominant role here. This concept is analyzed.

Finally a number of seemingly comparable phenomena or concepts are discussed: drainage - imbibition; suction - mercury porosimetry; molecular diffusion - viscous flow; capillary potential and permeability as a function of liquid content. Tacitly this comparison gives an evaluation of the porespace models for the transport phenomena involved. Suggestions for further research are given.

1.1. Introduction

Consider a plate of sand, a brick, or a mass of soil, saturated with water and subjected to drying conditions. First evaporation takes place at the outside surface, later on somewhere inside the porous medium. Several transport phenomena take place. Heat flows from the atmosphere to the place of evaporation. Diffusion of water vapour takes place in the opposite direction. As long as the liquid phase in the porous medium is continuous, there will be liquid transport to the place of evaporation, induced by capillary forces.

In order to describe these and other transport phenomena in porous media we have to know which processes take place, what the driving forces are, and what are the transport coefficients. The macroscopic transport coefficients and some driving forces (such as the capillary potential) are, among other things, a function of the geometries of the interfaces between the different phases in the porous medium. These geometries are, in general, very complex. Therefore, many models or theories have been proposed to describe one or more of the transport coefficients and the capillary potential as a function of structural parameters of the porous medium (such as porosity and specific surface).

The goal of this review is the classification and evaluation of these porespace models. As will appear, this objective covers a very broad area; therefore, a large number of restrictions are made to decrease the complexity of the systems to be described and compared. These restrictions include: the porous medium is statistically homogeneous and isotropic; the porespace is continuous, of a rather simple structure (no bidisperse porous media; porosity

30-60%), and the so-called pores are not too small (0.1 - 2000 μm); the solid surface is fixed (no swelling or consolidation) and inert to the other phases; the number of phases and components is restricted and only very simple initial and boundary conditions are considered (one dimensional transport only).

Further restrictions will be made as we proceed. As far as possible, reference will be made to reviews or selected papers that give an introduction to problems not discussed in the present review. In such cases the reference number is preceded by 'R'. In describing proposed models or theories we often use literal phrases from the original sources without quotation marks. Quotations marks are used only when a criticism follows.

1.2. Classification of transport phenomena in porous media

The literature concerning transport phenomena in porous media is scattered over a large number of areas. Many examples could be given of knowledge or experimental methods several times being proposed as novel in different applied sciences and/or geographic areas. In Table 1.1 the major contributing disciplines are given, together with selected references that give access to the literature. In the sub-sections that follow typical examples of the variety of transport phenomena in porous media are given.

TABLE 1.1

Major disciplines that contribute to the knowledge of transport phenomena in porous media

Description	Introduction	Books, reviews	Older English literature	German literature	Russian literature
transport phenomena in porous media, general (pretended)	[1]	[2-6]	[3]	[5,6]	[4,7]
characterisation of porous media; particle packing structure	[8]	[9,10]	[11]	[12,13]	[14]
flow in packed beds	[15]	[16,17]	[19]	[5]	
drying	[18]	[20,21]	[22]	[20]	[21,23,24]
heterogeneous catalysis	[25]	[26]		[13]	[27]
petroleum and groundwater engineering	[1,28]	[2,29]	[3,30]		[31]
soil physics	[32]	[33,34]	[35,36]		
building physics	[39]	[37,38]		[20]	[4]

When classifying transport phenomena in porous media we should first distinguish between capillary liquid transport and non-capillary liquid transport. More precisely: we should distinguish between transport phenomena that are partly determined by the geometries of liquid-vapour menisci present in the porous medium and those that are not. In the latter case the driving force is, in general, not a function of the structural properties of the porous medium and we are interested only in models for the porous medium that help in specifying the transport coefficients. From this class of transport phenomena, heat conduction, molecular diffusion, viscous flow, and dispersion are treated in the next four sub-sections. In the case of capillary liquid transport both the driving force and the transport coefficient are a function of the geometries of the porespace. From this class we will discuss capillary rise, wetting, infiltration, drainage, drying, and the transport phenomena that occur in the suction and mercury porosimetry measurement techniques. In Fig. 1.1 the transport phenomena to be discussed are represented schematically.

1.2.1. Heat conduction. Description of heat transport in porous media is of importance in many applied sciences. One may think of the thermal properties of dried products (especially foods), insulating systems, heat pipes, chemical or nuclear reaction in packed beds, etc. First we will restrict ourselves to conduction. In porous media convection will often be negligible and radiation is of importance only at high temperatures [R40]. When the isothermal lines are parallel we can write

$$q_h = -\lambda_{eff} \frac{dT}{dx} \tag{1.1}$$

which is Fourier's equation with an effective conductivity. The latter is a complicated function of the conductivities of the different phases present, and of the structural and surface properties of the porous medium.

Heat conduction is in some important aspects different from other transport phenomena in porous media. Most and for all this is due to the fact that transport takes place in all phases. In dry porous media the conductivity of the gas phase will often be negligible and knowledge about the resistance to heat flow at the contact points between the particles is necessary, especially in the case of evacuated insulation systems of hollow spheres [41]. Most research

carried out on the effective conductivity is empirical. Only in a few cases the models used are comparable with those used for other transport phenomena [41-43]. Therefore, in what follows, heat conduction will not often be mentioned.

1.2.2. Molecular diffusion. Diffusion of gas or vapour in porous media occurs in many circumstances: diffusion of water vapour, oxygen, and carbon dioxide in soils; transport of water vapour in construction materials (timber, brick, concrete) and reaction products in catalysts; during drying of granular materials or porous media and underground storage of (radioactive) gases. Knudsen diffusion, which occurs in microporous media, will not be considered. For binary gas diffusion we may write

$$j_A = -\mathcal{D}_{eff} \frac{d\rho_A}{dx} \tag{1.2}$$

hence Fick's law with an effective diffusion coefficient. In the discussions that follow we will always refer, tacitly, to the simple diffusion experiment depicted in Fig 1.1b. For ideal gases eq (1.2) can be derived from the kinetic gas theory [44,45], that is to say

$$\mathcal{D}_{eff} = Q\mathcal{D}_{AB} \tag{1.3}$$

where Q, the diffusibility, is only a function of the porespace geometry. For simple structures, like regular sphere packings, Q can be calculated [46]. It should be noted that such regular structures are always anisotropic.

The mechanism of molecular gas diffusion is akin or analogous to the conductivity of a non-conducting porous medium saturated with a conducting liquid and to the dielectric conductivity of the medium. The electric conductivity of porous media is used as a characterisation technique in geology (petroleum technology) to determine what is called the formation factor [R47].

Several attempts have been made to derive Q for one or more of these transport phenomena as a function of the porosity, ε, of some considered sphere packing [R43, R48, R49], but the assumptions

that have to be made are rather unrealistic. Recently it has been suggested that [43]

$$Q = \frac{2\varepsilon}{3-\varepsilon} \tag{1.4}$$

for the diffusion (and ionic conductivity) in any irregular sphere packing, independent of the particle size distribution or the number of contact-points. However, experimental values of Q do not seem to confirm eq (1.4), [49].

1.2.3. Viscous flow. The main areas where we meet mass transport by viscous flow are, firstly, the transport of ground water, petroleum, and natural gas in porous natural material (soil, limestone, sandstone, mica), and secondly, the flow through packed beds as encountered in chemical engineering [R17], water winning, and chromatography [R50]. We will not consider gas flow [R16], non-Newtonian flow [R51], or cases in which the inertia terms cannot be neglected [R17].

For the simple experiment as depicted in Fig 1.1a, Darcy [52] found

$$q = K \frac{\Delta P}{L} \tag{1.5}$$

with L the length of the porous medium, ΔP the pressure loss over the packing, and K a constant depending on the properties of the packing and the liquid. Darcy's law has the same form as the Poiseuille law for laminar flow in a cylindrical tube of radius r,

$$q = \frac{r^2}{8\eta} \frac{\Delta P}{L} \tag{1.6}$$

See for the connection between these two equations and the Navier-Stokes equation e g [333]. For easy comparison with other transport phenomena, we write eq (1.5) in the following form:

$$q = -k \frac{d}{dx}(\Psi + x\cos\alpha) \tag{1.7}$$

with Ψ the pressure head and $x\cos\alpha$ the elevation head. Many attempts have been made to derive eq (1.7) from the Navier-Stokes equation [R53], but the assumptions and the rigidity of the proposed derivations are still under discussion [54]. For regular sphere packings,

several approximate calculation methods for the permeability, k, have been proposed, e g [46,55,56].

1.2.4. Dispersion. Dispersion is the spreading of a tracer, a solute, or of heat carried by a fluid flowing in a porous medium, and is caused by the irregularities of the streamlines. Dispersion in packed beds is of importantce in chemical engineering [R57] and chromatography [R58]. In hydrogeological sciences dispersion plays a role in the transport of fertilizers, contaminants (underground waste disposal), and in the encroachment of salt water. Dispersion is related to miscible displacement in porous media; the latter will not be discussed [R3].

The dispersion coefficient can be introduced in different ways. One of them is the following. A fluid particle will undergo a certain displacement in a time interval τ. Each possible displacement has a certain probability. If the displacements are assumed to be independent and the standard deviation of the probability distribution displayed in the displacement is σ, then the dispersion coefficient, D, can be defined as $2\sigma^2/\tau$ [59-61].

The dispersion coefficient is also called the convective or mechanical diffusion coefficient. One of the main problems in modelling dispersion phenomena is that the longitudinal or axial dispersion coefficient is not equal to the transverse or lateral dispersion coefficient. When not indicated otherwise we always mean longitudinal dispersion when we speak of dispersion.

1.2.5. Capillary liquid transport. All the disciplines mentioned in Table 1.1 are concerned with capillary liquid transport in some way or another. Most liquid transport in soil involves capillary liquid [R33,R62]. In reservoir engineering one may be interested in the connate water distribution [R63] or the threshold pressure [64], but the main interest here is in the mechanism of the displacement of oil by water [R65]. In this review we will not consider liquid-liquid menisci, only liquid-vapour menisci. In chemical engineering capillary liquid transport takes place during drying [R18] or mechanical dewatering [R66,R67] of powders, sludge, etc. Further, to give just a few examples, knowledge of the mechanism of capillary liquid transport is of interest in such diverse applications as: porous electrodes [68], storage of liquids in the absence of gravity [69], wetting of fibres (paper, textile) [70], rain penetration in walls and roofs [71], and capillary rise in wood [72,73].

In 1907 Buckingham [74] proposed an equation for capillary liquid transport, which can be written in the same form as the Darcy equation,

$$q = -k \frac{d}{dx}(\Psi + x\cos\alpha) \tag{1.8}$$

in which, now, both k and Ψ are dependent in a non-unique way on the liquid content, u, of the porous medium, and Ψ is called the capillary potential (also: moisture potential, suction potential). In the neighbourhood of a meniscus Ψ is directly related to the capillary pressure:

$$\Psi = \frac{p_c}{\rho g} \tag{1.9}$$

and for p_c (Laplace equation for hydrodynamic equilibrium of a meniscus):

$$p_c = \gamma(\frac{1}{r_m'} + \frac{1}{r_m}) = \gamma C \tag{1.10}$$

where r_m and r_m' are the two radii of curvature of the meniscus. See for a review of the hydrodynamics and thermodynamics of capillary liquid [70,75]. The radii of curvature are a complicated function of the geometry of the porespace and the contact angle, θ. Hence, for capillary liquid transport, we need not only a model for the transport coefficient, k, but also for (part of) the driving force, i e the capillary pressure. In the equilibrium situation, after capillary rise in a cylindrical capillary, we have

$$\rho g h_c = -\gamma C = \frac{2\gamma\cos\theta}{r} \tag{1.11}$$

From the thermodynamic equilibrium condition for the phases at both sides of the meniscus, the Kelvin equation follows [R76,R77],

$$p_v = p_s \exp(\gamma CM/\rho RT) \tag{1.12}$$

Hence, when transport takes place in a partly saturated porous medium, the presence of a capillary potential gradient is accompanied with a vapour pressure gradient. The difference between p_v and p_s can, in general, be neglected when $|C| > 10^7 m^{-1}$.

1.2.6. Wetting, capillary rise, infiltration. When an initially dry porous medium is wetted by a moving liquid front, this is called capillary rise, infiltration, or (horizontal) wetting, depending on the value of α in eq (1.8). The three processes are illustrated in Fig 1.1, picture c, e, and f. Wetting and capillary rise have been studied mainly with respect to powders and fibres. In soil science much work has been done in solving eq (1.8), assuming $k(u)$ and $\Psi(u)$ to be known [R78].

The rate of movement in a cylindrical capillary is easily derived from a macroscopic energy balance [cf eq (1.6)],

$$\frac{dx}{dt} = \frac{r^2}{8\eta} \frac{h_c - x\cos\alpha}{x} \cdot \rho g \; ; \tag{1.13}$$

Probably, this equation was first derived in 1918 by Lucas [79]

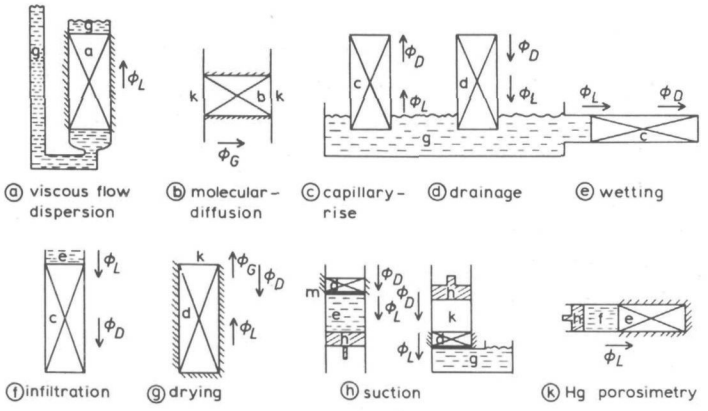

Fig 1.1. Schematic view of some transport phenomena in porous media. Nomenclature: a, b, c, d: porous medium; a: filled with liquid; b: filled with gas; c: initially filled with gas; d: initially filled with liquid; e: wetting phase; f: non-wetting phase; g: liquid connected to free liquid surface kept at constant level; h: piston; k: stationary gas phase; m: membrane, only permeable to wetting phase; $\emptyset_L$: flow of liquid; $\emptyset_D$: flow of fluid that displaces or is displaced by the liquid; $\emptyset_G$: molecular transport caused by concentration gradient in gas phase.

and independently by Washburn in 1921 [80]. When $\alpha = 90^0$ or $h_c >> x\cos\alpha$ we obtain

$$\frac{dx}{dt} = \frac{r^2}{8\eta}\frac{h_c}{x}\rho g \equiv \quad x^2 = \frac{r^2}{4\eta} h_c t \cdot \rho \cdot g \tag{1.14}$$

which equation is known as the Washburn equation, though it was already derived and verified in 1906 [81]. Several assumptions are made in the derivation of eq (1.13) [82-86], but we do not know of any experimental evidence that indicates these assumptions to be unwarranted.

If we assume a sharp liquid front advancing in a porous medium, we can write for eq (1.8):

$$\varepsilon\frac{dx}{dt} = -k\,\frac{\Psi + x\cos\alpha}{x} \tag{1.15}$$

which has much in common with eq (1.13), but it must be emphasized that eq (1.8) is not more than an hypothesis. We will presently return to the question whether there is any experimental support for eq (1.8) or (1.15).

1.2.7. Drainage and suction. Drainage is called the process in which liquid drains from an initially completely saturated porous medium until equilibrium is reached between capillarity and gravity (Fig 1.1d). For an infinitely porous medium and an infinite reservoir of liquid the wetting and infiltration process never reaches equilibrium. In the case of capillary rise and drainage, equilibrium is reached when for each x

$$\Psi + x\cos\alpha = 0 \tag{1.16}$$

where $x = 0$ at the level of the free liquid surface.

Suction is a technique to measure Ψ as a function of u [R87-89]. Probably the technique was first used by Versluys in 1916 [328]. The saturated porous medium is connected to a liquid reservoir by way of a membrane. A pressure difference, ΔP, is created by external means between the gas phase above the menisci in the porous medium and that above the free liquid surface, e g as depicted in Fig 1.1h. At each equilibrium point this pressure deficiency is equal to Ψ (it is assumed that $x\cos\alpha \simeq 0$). When the liquid content of the porous medium is determined at each ΔP, one obtains a Ψ-u

relationship. The liquid displacement between a change of one ΔP to another is, in general, not reversible. Hence, there exist an infinite number of Ψ-u functions.

1.2.8. Mercury porosimetry. If an evacuated porous medium is impregnated with mercury in small steps by means of an external pressure (cf Fig 1.1k), we obtain a Ψ-u relationship as well. The technique was proposed by Washburn in 1921 [329]. The family of Ψ-u functions obtainable by mercury porosimetry and that obtainable by suction cannot be correlated in a simple way. We will return to this point in section 1.10.6.

After its introduction in 1945 [90], mercury porosimetry has found wide application as a characterization method for porous media [R91,R92], in particular for catalysts, adsorbents and other microporous media.

1.2.9. Drying. For the transport mechanisms described in the three preceding subsections, the direction of flow of the displacing and the displaced phase is the same, when considered at a macroscopic level. This is, in general, not the case during drying where, as represented in Fig 1.1g, liquid or vapour leaves the porous medium in one direction and air enters the porous medium in the opposite direction. In the sense that drainage is the opposite of capillary rise drying may be compared with the wetting of a dry porous medium completely immersed in a liquid, though in the latter case the porous medium can explode [93,94].

The way in which the air replaces the liquid is of considerable importance in explaining the macroscopic drying behaviour. For example, in explaining the occurrence of a period of constant drying rate at diminishing liquid content, the occurrence of air entrapment has been postulated [21]. Though air entrapment has been observed under special circumstances [95] and the occurrence of discontinuous redistribution of menisci - Haines jumps - has been confirmed experimentally [75,96], the period of constant drying rate can also be explained without invoking the occurrence of air entrapment [97,98].

1.2.10. Other transport phenomena. In the evaluation of the porespace models for transport phenomena in porous media, we restrict ourselves to the transport phenomena mentioned in the preceding subsections and consider them only under the simple initial and boundary conditions as illustrated in Fig 1.1. Because models are often

proposed for more than one transport phenomenon, we will occasionally refer to the statics and dynamics of sorption isotherms for microporous media [R9,R99] and the combined transport of liquid and vapour [100,101]. It may be noted that for non-isothermal transport [R4,R20,R102], the dependency of Q, k, and Ψ on the interface geometries within the porous medium remains the same.

Let us finally mention some phenomena that may occur during vapour or liquid transport and can be responsible for apparently anomalous behaviour: the existence of liquid water with other properties than normal water [R103,R104] and the occurrence of film flow caused by surface tension gradients [R105] or disjoint pressures [101,106].

1.3. Non-porespace models

Before we enter into a discussion of the porespace models that have been proposed to relate the transport coefficients and the capillary potential to structural properties of the porous media, we mention some alternative approaches in this section. The last two sub-sections of this section are rather polemical and somewhat biased. This was thought necessary to counterbalance the bias to the other side now in fashion.

1.3.1. Empirical correlations. From the earliest studies there has been the wish to express the transport coefficients as a function of the porosity. Probably the first to determine such a correlation was Buckingham [107], who, in 1904, found for soils $\mathcal{D}_{eff} \propto \varepsilon^2$ and $k \propto \varepsilon^{6-7}$. Since then for $\mathcal{D}_{eff}$ many [R49] and for k numerous [R17, R108] empirical correlations with ε have been published. Since 1960 proposals have been made concerning the mathematical form of the $\Psi(u)$ and $k(u)$ functions, as determined empirically (e g [109-111]). Often such correlations are presented as following from a dimensional analysis, especially for Ψ [112] and k [108]. (In the latter case fluidization and sedimentation may be included [113].) However, because important variables like ε and u are dimensionless, a geometric analysis seems more appropriate than a dimensional one.

Of course the distinction between formal models, such as empirical correlations, and conceptual models, such as porespace models, is not sharp; especially when the latter contain one or more parameters obtained by curve fitting.

1.3.2. Discrete particle models. These models, which are used in describing flow through porous media, do not picture the system as a porous medium through which a fluid flows but as an assembly of particles submerged in a flowing fluid [R3,R17,R114].The analogy with sedimentation or elutriation is clear. Typical examples of this approach [115,116] are those in which it is assumed that two concentric spheres or cylinders describe a typical cell in a random cluster that is considered to have many cells. Each cell contains a particle surrounded by a fluid envelope, i e , the entire influence due to each particle is confined to the cell of fluid with which it is associated. See for an evaluation of this class of models [114,117] and also the recently proposed model of Neale and Nader [43,334], which predicts $\mathbb{D}$ and k for random sphere packings solely as a function of ε and d.

In a methodological sense, we may compare the discrete particle models for viscous flow with the dusty gas model for diffusion [118]. In the dusty gas model the solid phase of the porous medium is introduced in the kinetîc gas theory as an assembly of very large molecules.

1.3.3. Continuum models. There is a tendency in the literature to distinguish between models that treat the transport phenomena on an average basis, while ignoring local structural details, and models based on an assumed porespace structure - which can be done - and to consider these as alternative approaches, e g [2,3,119] - which is uncorrect. Of the different continuum models we will subsequently discuss statistical dynamics (analogy with kinetic gas theory), classic continuum theory, and application of the thermodynamics of irreversible processes. Finally we will make some remarks on the form of the transport equation for capillary liquid transport.

Statistical dynamics. Scheidegger [59] discards porespace models, because 'it is unavoidable to introduce fudge factors ... [and this] ... nullifies the very purpose of introducing the models'. We should develop a statistical dynamics comparable to Gibbsian statistical mechanics. (The analogy being between fluid-particles and molecules.) Though many articles have been written since 1954 [R120]. the practical usefulness of this approach seems limited. In particular it is difficult to understand in what sense this approach is an alternative to considering porespace models, if in statistical dynamics a variable B occurs which 'at every point will depend on the shape and size of the opening through which the fluid packet passes' [59].

Continuum approach. In this approach the actual porous medium filled with a flowing homogeneous fluid is replaced by a fictitious continuum, to each mathematical point of which (whether in the solid or in the porespace) medium parameters such as ε or k can be assigned. The essential point is the definition of a representative elementary volume, or physical point, over which averages of medium, fluid, and flow properties are performed [121]. The main proponent is Bear [2]. Though he acknowledges the need of porespace models (for example in the specification of the source function that occurs in his model of overlapping or interpenetrating continua for polyphase flow in porous media [121]), this is not wholeheartedly. Thus, on page 134 of his [2], he speaks of his own approach, yielding a relationship 'in which permeability is related to porosity, to tortuosity and to conductance of the elementary matrix channels', as being *purely theoretical*. Such in contrast to the *semi empirical* approach of the porespace models for which 'numerical coefficients must be determined experimentally'. But such a contrast is not permitted because his purely theoretical approach does not yield in any way whatsoever, e g, the value of the conductance of the elementary matrix channel.

Especially with respect to capillary liquid transport the sense of a continuum approach seems disputable. According to Bear ([2], page 25 and 446) parameters like k and Ψ are parameters of ignorance, which must be deduced from actual experiments. But in the case k and ψ are unknown non-unique functions of u, as they are, it would seem that any continuum theory going further than stating eq (1.8) is inopportune. The same criticism can be levelled against the local averaging approach when the equations of change contain Ψ [122].

Irreversible thermodynamics. This approach, it is said, 'affords insight into *all* factors affecting transfer within the medium' ([123], italics added). The main proponent is Luikov, whose account of capillary liquid transport will be discussed in the next sub-section. The phenomenological equations presented in the publications using this approach (e g [4,123,129]) are mainly of two kinds: they already occur in [124] or they are postulated (and hence do not belong to the theory of irreversible thermodynamics). Further, as with the other overall approaches, when it comes to a

specification of the transport coefficients or the thermodynamic potential, porespace models are necessary [125,126].

The form of eq (1.8). In simple as well as sophisticated overall descriptions of capillary liquid transport, eq (1.8), neglecting the gravity term, is often rewritten in the following way [4,20, 127,128,etc]:

$$q = -\mathcal{D}_u \frac{du}{dx} \tag{1.17}$$

in which $\mathcal{D}_u$, the moisture diffusivity, $= k d\Psi/du$.

The inclination to use du/dx as the driving force, in stead of $d\Psi/dx$, has to be strongly advised against. In no sense of the term can the liquid content be regarded as the driving force. Moreover, it leads to the confusion that $\mathcal{D}_u$ is, at the least approximately, a constant. Energy is spent in providing explanations or solving equations in which it is assumed that $\mathcal{D}_u$ is a constant [24,130,131], while the data available in the literature show it to change, in general, several orders of magnitude as a function of u.

1.3.4. Luikov's metaphysics. Luikov considers eq (1.17) as a phenomenological equation in the sense of the thermodynamics of irreversible processes. Because it appears that for capillary liquid transport $\mathcal{D}_u$ is not a constant Luikov proposes to replace eq (1.17) by [24,132-134]

$$q = -\mathcal{D}_u \frac{du}{dx} - \tau_{rm} \frac{dq}{dt} \tag{1.18}$$

in which τ_{rm} is the relaxation time or period of propagation of moisture transport in capillary-porous media. A second reason to use eq (1.18) would be that τ_{rm} is much greater than the period of propagation for heat transport. (It may be noted that eq (1.18) is not intended to account for the inertia terms in the Navier-Stokes equation.) For the following reasons we think there is no ground for introducing eq (1.18):

(i) Luikov has never presented a derivation of eq (1.17); it is introduced ad hoc, invoking the analogy with Fourier's and Fick's law. It seems certain that it cannot be derived from irreversible thermodynamics alone [126]. But apart from that, there is no reason to introduce eq (1.18) on the basis that $\mathcal{D}_u$ is not a

constant. This might just mean that du/dx is not the correct thermodynamic driving force. Moreover, there is a difference between $\mathcal{D}_u$ being a function of u and $\mathcal{D}_u$ being a function of du/dx.

(ii) The physical meaning of τ_{rm} is unclear. Luikov gives the definition $\tau_{rm} = \mathcal{D}_u/w_{rm}^2$, where w_{rm} is the rate of propagation of mass. An estimate of w_{rm} is obtained from the 'capillary velocity in mono-capillary-porous bodies', for which [133] $w_{rm} = a_o/x$ [cf eq (1.14)]. Apparently, in that case the rate of propagation of mass is the same as the thermodynamic flux, i e $q = \varepsilon w_{rm}$, which seems a strange conclusion. Further, by this definition, τ_{rm} is certainly not a constant. Moreover, the choice of w_{rm}, as obtained on a certain system, i e sand-water [135], is completely arbitrary. Particularly as the values of $\mathcal{D}_u$, used to make an estimate of τ_{rm} [which estimate is part of the argument to introduce eq (1.18)], have been obtained on other systems.

(iii) Luikov [132] reports confirmation of eq (1.18), but this verification seems completely accidental when it is noted that: Firstly, capillary rise experiments are performed with systems for which, at least in some cases, the gravity term cannot be neglected. Secondly, part of the confirmation is provided by the same experiments from which the values of w_{rm} are obtained. But in that case the fact that, as is reported, $w_{rm} = a_o/x$ implies that eq (1.17) is, at least qua form, the correct one (with $\mathcal{D}_u = \varepsilon a_o$ and a sharp liquid front, which was assumed). And finally it seems a somewhat contradictory result in the context of relaxation phenomena that eq (1.17) is a good approximation of eq (1.18) at short times [134].

More criticisms can be made but the above should suffice to show that 'the theory of similarity, which is the study of methods of scientific generalization of the data of a single experiment' ([4], page 74), sometimes suffers from losing contact with reality.

1.4. One-dimensional porespace models

In this and the subsequent three sections a systematic inventory is given of the porespace models that have been proposed. One-dimensional models entail that transport is possible in one direction only. Two-dimensional models permit transport in a plane containing the macroscopic transport direction. Three-dimensional models permit transport also in a plane perpendicular to the macroscopic transport direction. Within this main classification further refinements

are made. Every model has been given a number that refers to its place in the classification scheme. As is usual in such cases, some models fit in the adopted structure better than others. The policy has been that, in order to get a general view, it is better to force the existing models in the best possible scheme than to admit exceptions or intermediate cases. Elements of several one-dimensional porespace models are represented in Fig 1.2.

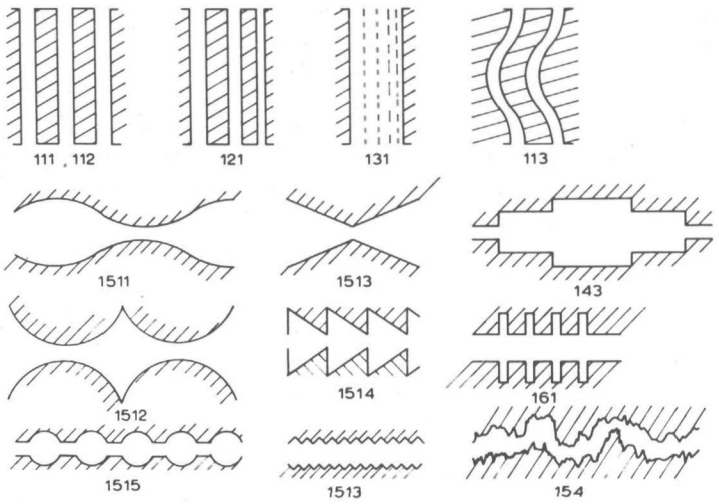

Fig 1.2. Elements of porespace models with one-dimensional connectivity.

1.4.1. Parallel tubes with fixed radius (11). The following models come under this category: equivalent radius (*111*), hydraulic radius (*112*), tortuous cylinders (*113*). The porespace is pictured by a bundle of parallel uniform tubes, which may be tortuous. See Fig 1.2.

Equivalent radius (111). If an equivalent radius exists then the values of the macroscopic transport coefficients and the capillary potential can be calculated from the available equations for cylindrical capillaries and the fact that the number of tubes in a unit volume, N, follows from $\varepsilon = N\pi r^2$. One may, of course, assume that only part of the porespace is available for the equivalent tubes in the transport direction considered [136].

Slichter [137], in 1899, related the equivalent radius to the particle size by considering what tubes can be recognized in

regular sphere packings. He assumed that there exists a unique $r(d,\varepsilon)$ function; this is not the case [11]. In most cases the equivalent radius is determined by one transport phenomenon and used to predict another. For example, the equivalent radius of a filter may be determined by the breakthrough pressure, p_b, which is the pressure necessary to force air through a saturated porous medium. According to model *111* the equivalent radius follows from eq (1.11) where $p_b = \rho g h_c$.

In contact angle determinations of the Washburn or Bartell type [80,138-140] model *111* is used tacitly, in the sense that it is not necessary to know the value of the equivalent radius.

Hydraulic radius (112). This model can be considered as a model for *111*. For non-circular tubes the hydraulic radius, r_h, has been defined as the ratio between the cross section and the perimeter of the tube. The analogous definition for the porous medium then yields, with s the specific surface in (m^2 solid surface)/(m^3 solid phase),

$$\frac{r}{2} = r_h = \frac{\varepsilon}{(1-\varepsilon)s} \tag{1.19}$$

From which it follows that, for the equilibrium after capillary rise or drainage,

$$p_b = \rho g h_c = \gamma \frac{(1-\varepsilon)s}{\varepsilon} \cos\theta \tag{1.20}$$

an equation popularized by Carman [141], but it was already used in 1905 by Mitscherlich [142] to determine the particle size from capillary rise experiments (for spheres $s = 6/d$). Eq (1.20) has been proposed as a possibility to determine s from h_c [70,141-146] and has been used as a justification of methods to determine θ [147,148]. Carman has later mitigated the validity of eq (1.20) [149].

From eqs (1.6), (1.7) and (1.19), together with the fact that the superficial and interstitial velocity differ a factor ε, it follows that [150,151]

$$k = \xi_1 \frac{\rho g}{\eta} \frac{\varepsilon^3}{(1-\varepsilon)^2 s^2} \tag{1.21}$$

ξ_1 is a function of the form of the tubes, for cylinders $\xi_1 = 0.5$.

Values for various other forms have long been known [152], but they are all too high to fit experimental data, Therefore, ξ_1 is considered to be an empirical constant.

Sometimes the hydraulic radius concept is used by authors who pretend not to make any assumption about the porespace geometry. For example, Fricke et al [67] write: 'This equation [stating the equilibrium between centrifugal and capillary forces] requires no assumption about the shape and size of the capillary or the number of capillaries.' Since the capillary force is supposed to act on the three-phase line in a partially saturated packing, it will be clear that, the moment the length of this three-phase line is related to the particle size, an assumption is made concerning the nature of the meniscus and thus of the porespace.

Tortuous tubes (113) Model *113* is the accepted model for diffusion [25,153-155],

$$\mathbb{D}_{eff} = \frac{\varepsilon}{\tau^2} \mathbb{D}_{AB} \tag{1.22}$$

τ is the tortuosity, which can be defined as the ratio between the actual tube length and its projection on the transport direction. The value of τ can be determined from the ionic conductivity of a porous medium, using an analogon of eq (1.22).

For viscous flow eq (1.21) becomes, for model *113*,

$$k = \xi_2 \frac{\rho g}{\eta} \frac{\varepsilon^3}{\tau^2 (1-\varepsilon)^2 s^2} \tag{1.23}$$

We will call eq (1.23) the Kozeny equation, although Kozeny [82], in 1927, had τ in stead of τ^2. This was corrected later by Carman [19]. We need the square of τ because it enters not only in the actual tube length but also in the superficial velocity. As before, according to the derivation, ξ_2 is about 0.5. If it is assumed that $\tau \simeq \pi/2$, this yields $\tau^2/\xi_2 \simeq 5$, which is in agreement with the experimental values obtained for rotund-particle packings.

For viscous flow we may also use model *113* with an equivalent radius. For example, when it is assumed that the equivalent radius is the same for viscous flow and for the breakthrough pressure, it follows from eqs (1.20) and (1.23) that [156,157]

$$k = \xi_3 \frac{\rho g}{\eta} \frac{\varepsilon}{\tau^2} \frac{\gamma^2}{p_b^2} \tag{1.24}$$

when $\cos\theta = 1$. This equation has also been applied to viscous flow in partly saturated media with ε the fraction of the liquid phase and τ a function of u, to be determined from conductivity measurements [158,159].

Model *113* has been applied to capillary liquid transport by Kozeny [82],

$$\frac{dx}{dt} = \frac{k}{\varepsilon} \frac{h_c - x\cos\alpha}{x} \tag{1.25}$$

in which h_c follows from eq (1.20) and k from eq (1.23).

1.4.2. Tubes of different radii in parallel (12). Cylinders (121). This is the basic model underlying the techniques to determine the so-called pore-size distribution. When suction or mercury porosimetry is applied to model *121* (cf Fig 1.2) the experimental data provide the percentage of the tubes with radii in the interval $r_i - r_j$, where r_i and r_j correspond to Ψ_i and Ψ_j according to eqs (1.9) and (1.11). The model has been used in the description of all transport phenomena in which menisci play a role (cf Table 1.2).

Sometimes model *121* is approximated by an equivalent radius [160]. In such a context the equivalent radius is different for different transport phenomena or geometrical definitions because it is a function of different moments of the tube radii distribution [161,162,321].

Tortuous tubes (122). When the tubes of model *121* are assumed to be tortuous eq (1.24) becomes [163,164]:

$$k(u) = \xi_4 \frac{\varepsilon\gamma^2}{\rho g \eta \tau^2} \int_{u=0}^{u} \frac{du}{\Psi^2} \tag{1.26}$$

Eq (1.26) was first derived in 1949 by Purcell. It can be refined further by introducing $\cos\theta$ [165,166] or by using a more correct averaging technique [167]. Some of the proponents of eq (1.26) have later doubted its reliability [168], because it appeared that ξ_4 is a function of ε for certain systems.

It has also been argued [156,159] that at each u the equivalent radius is the one that follows from the corresponding value of Ψ. Hence

$$k(u) = \xi_5 \frac{\varepsilon u}{\rho g \eta \tau^2} \frac{\gamma^2}{\Psi^2} \tag{1.27}$$

(for u = 100 %, $\Psi = -p_b/\rho g$). Eq (1.27) is of interest because several inconsistent models are combined: (i) Ψ depends on u following model *121*. (ii) Eq (1.27) is incorrect for viscous flow in model *122*; it is defended with reference to a model of tubes with constrictions [156]. (iii) It is assumed, and found, that τ is a function of u (this is the case for eq (1.26) as well). This implies that the model itself is a function of u. To prevent this, it has been suggested we should consider τ to be a function of the tube radius [165].

Model *122* has also been used for the description of dispersion [169], and diffusion in the transition region [170].

1.4.3. Parallel tubes with ideal connections (13). The disadvantage of the models *12*, described in the preceding sub-section, is that they do not imply that Ψ is constant in a plane perpendicular to the transport direction. The assumption of ideal connections accounts for this. Probably the model was proposed for the first time in 1938 by Krischer [20]. Model *13* has been used mainly in describing capillary liquid transport, as in capillary rise [171,172], suction [173] and during drying [20,174]. For a given radii distribution, the model predicts the same equilibrium situation after capillary rise and drainage, as does model *12*. However, the kinetics are different. It is not always easy to conclude from a paper whether model *12* or *13* was used, as shown in a recent discussion [175].

It has been argued [176] that the ideal-connection assumption is unrealistic, but it seems to us that it is not more unrealistic than the parallel tube model itself. Experiments with connected capillaries of different radii show that they behave virtually as one capillary as long as there are no menisci in equilibrium [171].

1.4.4. Tubes in series (14). *Random adjacent slices.* Elements of two tubes of different radii in series (model *14*) have been used to explain the effect of constrictions in the porespace (cf Table 1.2). The idea was first applied to diffusion by Adzumi, in 1937, who also considered elements of tubes of different radii in series and parallel [177]. The serial analogon of model *121*, the converging-divergent duct (model *143*, cf Fig 1.2) has been proposed to describe both Knudsen and bulk diffusion [178]. This model, however contains a rather large number of parameters to be obtained by curve fitting and needs a large computer to apply it.

Random adjacent slices. These models are constructed as follows

[179]: Consider a bundle of tubes whose radii are given by the radii size distribution $f(r)$. Imagine the bundle to be cut into a large number of thin slices. When the short pieces of tube in each slice are then arranged randomly, the re-assembled slices constitute the model of the porous medium. The first model of this kind (*145*) was proposed in 1950 by Childs and Collis-George [180], their incentive being that the Kozeny equation is invalid in case "pores" of different cross section are present. They obtain an expression for $k(u)$ in the following way. A cross section of the porous medium, of area A, will exhibit two similar faces showing a similar $f(r)$. If we take the random juxtaposition of these two faces, this yields the probability of different tube sequences, while the total pore-space area in contact will be $\varepsilon^2 A$. The resistance to viscous flow is, by definition, confined to the smaller tube in the sequence. It then follows that

$$k(u) = \xi_6 \frac{\rho g}{\eta} \sum_{r_i = 0}^{r_i = R} \sum_{r_j = 0}^{r_j = R} r_i^2 \, f(r_i)\delta r \quad f(r_j)\delta r \qquad (1.28)$$

in which r_i and r_j are the radii of two tubes forming a sequence, r_i being the smaller of the two; $f(r_i)\delta r$ and $f(r_j)\delta r$ are the fractions of the cross sectional area taken up by tubes of radius range from r to $r+dr$. The tube radius distribution, $f(r)$, has to be determined by suction (assuming model *121*) and R is the radius of the largest tube filled at u. The constant ξ_6 has to be determined experimentally.

In later refinements of this approach, which all specify ξ_6, two points mainly emerge. Firstly, in stead of the radius of the smaller tube in any sequence, r_i, several authors [179,181] take $r_i\sqrt{\varepsilon}$ as the effective radius because of the poor fit of one tube to the next. Secondly, to specify ξ_6 one needs the effective area available for transport per unit area. The original model takes this to be ε^2 and this is also assumed by Wyllie and Gardner [179], who consider the difference between the geometric and hydrodynamic pore area as the physical nature of τ. Their model (*147*) can then be seen as an improvement of model *122*, cf eq (1.26), because no determination of τ is necessary any more. Because it was realized that the model does not give a very good account of the three-dimensional connectivity of the porespace, other exponents of ε have been suggested. Marshall [181], model *146*, uses ε and Milling-

ton $\varepsilon^{4/3}$, model *148*. The latter value is obtained assuming spherical pores [182]. Later Millington & Quirk [183] envisaged the porous medium as consisting of solid spheres that interpenetrate each other, separated by spherical pores that also interpenetrate. This model gives ε^n for the effective area, with $0.6 < n < 0.7$ for $0.1 < \varepsilon < 0.6$. (We may again note an example of the combination of three different models to describe one transport phenomenon.)

The random adjacent slices models have been developed and tested mainly in connection with $k(u)$. Millington [184] applies his model also to diffusion. Childs [33] still keeps to his model. Both Marshall [185] and Millington [186] have later doubted the underlying assumptions.

1.4.5. Tubes with periodic constrictions (15). There are many reasons to introduce models containing tubes with constrictions: Because of the extra resistance offered to viscous flow and molecular diffusion. To explain hysteresis in adsorption isotherms or suction and, more generally, to explain the influence of the accessibility of different porespace regions, for example the influence of the exposed surface to the displacing fluid during suction [187]. And further, to explain certain aspects in deep-bed filtration and dispersion, such as clogging [188] and the assumed occurrence of cells in the porespace in which there is complete mixing.

Simple elements (151). Some examples are given in Fig 1.2. Model *1511* has been used in describing combined liquid-vapour transport in soils [100] and, in sinusoidal form, for the calculation of $\mathcal{D}_{eff}$ [189]; that is to say eq (1.22) is rewritten as

$$\mathcal{D}_{eff} = \frac{\varepsilon\delta}{\tau^2}\,\mathcal{D}_{AB} \qquad (1.29)$$

in which δ is the constrictivity factor defined as $(\mathcal{D}_{eff}/\varepsilon\mathcal{D}_{AB})_{\tau=1}$. It is difficult to state the distinction between τ and δ in a clear way, because in a real porous medium they are always both present. Their separation is acceptable only if they can be determined or estimated independently [49]. The value of δ has also been calculated for model *141* [190] and for a hyperbola of revolution (*1512*), [191].

Model *1513* and the analogon with a circle segment as the basic element have been used to calculate the extra energy dissipation caused by constrictions during viscous flow [20,119,314]. These

models and many others, such as *1515* and *1514*, have been used to explain hysteresis in adsorption-desorption [192], in drainage - capillary rise [171,193-194] in mercury porosimetry [195] and in two-phase flow [196].

Tortuous tube with varying radius (154). Astbury [197] used a model in which the porous medium consists of a number of parallel tortuous circular tubes of randomly varying radius. The parameters of the model are obtained from electrochemical measurements on non-stationary wetting experiments. Cf also [326].

Constricted tubes of different dimensions (155). In the model presented by Payatakes et al [198], the porous medium is represented by a unit bed element, which consists of a number of unit cells in parallel. Each unit cell resembles a piece of constricted tube (parabola of revolution). The model is applied to describe visous flow in particle packings without neglecting the inertia terms.

Overlapping non-uniform spheres (156). This model is used by Batel [143,199] to obtain a modified Kozeny equation for viscous flow and capillary rise. The hydraulic radius for a porespace constituted by spheres is (cf eq (1.19))

$$r_{hs} = \frac{3\varepsilon}{s(1-\varepsilon)} \qquad (1.30)$$

This radius has also been applied to Knudsen diffusion [200]. Batel uses a more complicated function, making further assumptions concerning the measure of overlap.

1.4.6. Dead-end porespace regions (16). Turner [169] described the dispersion in a packed bed by means of a bundle of equal length parallel tubes, with dead-end spaces of various sizes leading off from the tubes (model *161*). Aris [201] extended the model to a continuous distribution of tube sizes. Similar models are used to advocate the use of an effective porosity [119] or to explain the entrapment of air during a wetting process [202].

1.5. Two-dimensional porespace models

1.5.1. Networks, junctions not specified (21). The conception of a network of tubes to picture the porespace of a porous medium was introduced by Fatt in 1956 [203-208]. The model consists of short cylindrical tubes of different radii distributed randomly over a regular net-

work. The network is characterized by the β-factor, β being the number of tubes to which each tube is connected. In Fig 1.3 some examples are given: the single hexagonal network (*211*) with β = 4, the square network (*212*) with β = 6, and the triple hexagonal network (*213*) with β = 10. According to the definition model *13* has β = ∞ and model *14* has β = 2.

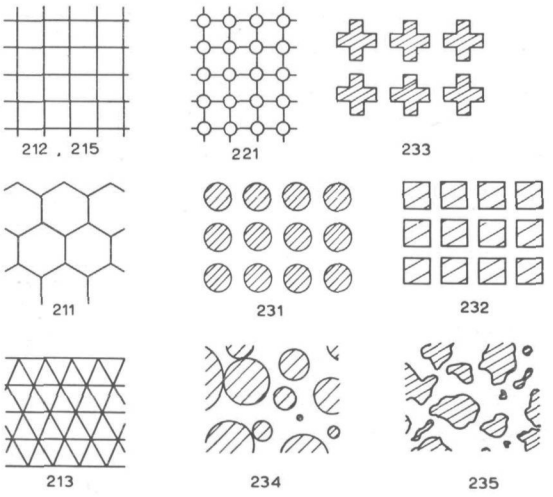

Fig 1.3. Elements of porespace models with two-dimensional connectivity.

The model has been applied to viscous flow, diffusion [204], and ionic conduction in partly saturated media. The tube radii distribution is obtained from a suction or mercury porosimetry experiment, the data of which are interpreted using the same model (i e , contrary to model *12*, there is an accessibility effect). The volume of the junctions between the tubes is assumed to be zero and the length of the tubes is given by $l = r^{-1}$ (and hence the tubes have to be tortuous to fit in the regular network). It is said that the predictions of the model hardly change if a random distribution is assumed for l. The β-factor can be estimated from photomicrographs [205]. When $k(u)$ is calculated from the measured $\Psi(u)$, experimental data (for porous media encountered in petroleum geology) fit best for β = 10. The calculations are made using an analog computer (analogy: laws of Poiseuille, Fick, and Ohm).

There are several reasons to prefer model *21* to models such as *12* or *14*. The higher connectivity gives better agreement with experimental data. For two-phase flow the model predicts relative permeabilities whose sum is not equal to 1 [206], as is also observed in practice. Further the model can be extended to account for the entrapment of the displaced phase [207,209]. Harris [210], using a Latin square as a model (*215*, $\beta = 8$), has shown that the choice of the entry-exit arrangement, i e the specification of how the two fluid phases leave and enter the model, has a considerable influence on the predictions of the model.

1.5.2. Networks, junctions specified (22). Model *21* would become more realistic if the junctions between the tubes have a certain volume. For example, one could assume that the junctions are spherical (model *221*, see Fig 1.3). We do not know of any attempts to make calculations on such a type of model.

1.5.3. Solid phase elements (23). In stead of specifying the geometry of the porespace in the model, one can specify the solid phase. Models of this kind have been used mainly for qualitative explanations. We give a few examples (see Fig 1.3). Model *231*, array of circles, has been used to argue that, in a suction experiment, one may assume that the accessibility of different layers is hardly influenced by their distance from the entry face of the displacing fluid [211]. Model *232*, array of squares, has been used in modelling diffusion in bidisperse media [212] and in describing non-creeping laminar flow [213]. Model *233*, array of crosses, was put forward to explain blocking in deep bed filtration [188]. The models may be considered three-dimensional when it is assumed that the two-dimensional representation is an intersection through a three-dimensional array of solids. In that case they have the disadvantage of assuming isolated solid phase elements floating in the porespace. One may compare these models with two examples of intersections through real porous media, as depicted in Fig 1.3, models *234* and *235*.

1.6. Three-dimensional porespace models

1.6.1. Regular sphere packings (31). Sphere packings have been used as a model for almost any transport phenomena in porous media. In this sub-section we discuss some regular sphere packings. It should be noted that all regular packings are anisotropic. Hence, when

used as a model, an average has to be taken over all direction. or the model has to be restricted to a specified position of the packing with respect to the transport direction.

Cubic and hexagonal array (*311* and *312*; see Fig 1.4). These packings have been used to make estimates of the equivalent radius (for viscous flow) as a function of the particle size [11,137], to make estimates of the tortuosity and the constrictivity of monosized sphere packings [46,49,214], and to calculate the thermal conductivity [41]. However, the main application has been to capillary liquid transport. In two important papers of 1927 and 1930, Haines described the behaviour of the cubic and hexagonal sphere packing in a suction experiment [215].

When suction is applied to a hexagonal packing, saturated with water, the air will enter when the suction is equal to the capillary pressure of the meniscus between three contiguous spheres. If it is assumed that the curvature of this meniscus is equal to that of the sphere that just passes the window between the three spheres, we have for the entry pressure of air

$$\Delta P = \frac{26\gamma}{d} \tag{1.31}$$

with d the sphere diameter and $\cos\theta = 1$. At this suction the packing drains completely except for the pendular rings (the liquid remaining around the contact-points of the spheres). When the pressure is now released, Haines assumed that the re-entry pressure of the liquid is determined by the curvature of the pendular rings on the moment they make contact. Then

$$\Delta P = \frac{9\gamma}{d} \tag{1.32}$$

For a cubic packing comparable calculations can be made. For an arbitrary sphere packing the entry and re-entry pressures will cover a certain range and Haines showed, experimentally, that this range lies between the extreme values for the cubic and hexagonal packing. However, it should be noted that eq (1.32) can be applied only when it is assumed that liquid is transported to the isolated pendular rings via the vapour phase or a liquid film on the particles. If ever present, these are both very slow transport processes in macroporous media and can therefore be neglected. The re-entry

pressure and also the driving force during wetting processes will be determined by another mechanism. Whether the radius of the largest spheres that can be described in the porespace of the sphere packing is a reasonable measure for the equivalent radius for wetting, is highly disputable, although often assumed.†

Haines' approach has been refined on minor points later on [216] and has also been applied to the description or explanation of sorption isotherms [217], capillary liquid transport in porous electrodes [68], mercury porosimetry [218], and drying [219,220].

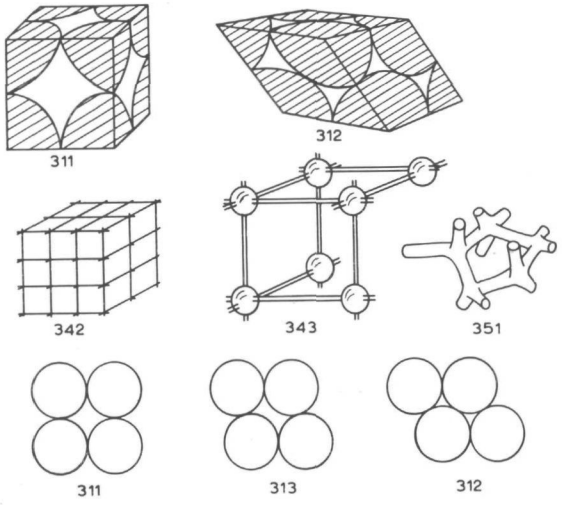

Fig 1.4. Elements of porespace models with three-dimensional connectivity; model *351* from [60].

Intermediate packings (313). To apply the considerations for the cubic and hexagonal packing, which have a porosity of 48 % and 26 % respectively, to sphere packings of arbitrary porosities, one may assume the latter to be a mixture of cubic and hexagonal elements. In fact this was what Haines did, and also Smith before him [221]. Another possibility is the following. In a cubic packing the angle formed by connecting the centres of three adjacent spheres, when not 180^0, is 90^0; in a hexagonal packing it is 60^0. By taking intermediate angles, one obtains regular packings of porosities varying

† See section 5.2.

from 26 to 48 % (cf Fig 1.4). This was the model used by Slichter [137] to obtain the $r(d,\varepsilon)$ function mentioned in the paragraph on the equivalent radius model (*111*). The work of Slichter was later extended by Smith [222], who aldo applied this model to capillary rise and drainage in a series of papers [193], which have undeservedly been neglected by much later workers. Furthermore the model has been used in the description of the $\Psi(u)$ functions obtained with mercury porosimetry [223-225] or suction [226].

1.6.2. Regular packing of other elements (32). The use of other elements than spheres has been restricted to specific areas. For fibres a model consisting of a bundle of solid cylinders is more appropriate than one consisting of spheres [70,227]. Princen [227] has given a detailed account of capillary rise in such a model. In the interpretation of sorption isotherms, regular packings of several other solids have been used [192,228].

1.6.3. Tetrahedra model (33). Any particle packing can be described more or less roughly by means of a Delauney graph, which consists of the lines joining the centres of touching or nearly touching particles. These lines can be considered as the edges of tetrahedra. Only in the case of a dense random packing of polysized spheres, defined as the packing for which for every tetrahedron every one of its spheres touches every other one, is the Delauney graph unique [229,230]. But in practice such packings will not be formed for the same reasons as no dense regular packing is formed for monosized spheres. There will always be a number of near-contacts. Experimental data are available on the number of near-contacts in random packings, as obtained by normal packing techniques [231,232]. Using such data together with an assumed sphere size distribution Mason [233] generated, on a computer, tetrahedra networks that have porosities reasonable in agreement with those found in practice.

Assuming that the distribution of tetrahedra volumes is independent of the edge length distribution and further that drainage is governed by the inscribed circles in the tetrahedral faces and imbibition by the inscribed spheres in the tetrahedra, Mason could give an a priori description of the wetting and drainage behaviour of irregular sphere packings. Assuming that the resistance to flow is located in the tetrahedra faces, the model also gives a prediction of $k(u)$. As it is worked out, Mason's model has a two-dimensional connectivity only because, in account-

ing for the accessibility of the tetrahedra, he assumes that the packing consists of layers of tetrahedra, while each tetrahedron is connected to tetrahedra in adjacent layers only, i e they have no connections to tetrahedra in their own layer.

1.6.4. Fixed networks (34). In this category we place all three-dimensional models that consist of elements that are arranged regularly in a lattice or network. As in the case of the two-dimensional networks (*21*) the values of one or more properties of the elements are randomly distributed over the elements.

Lattice of black boxes (341). Because the internal geometries of the lattice elements are not specified in detail, we have no true porespace model in this case. The macroscopic transport coefficients are a function of the transport coefficients of the lattice elements. The model has been used as a generalization of the random adjacent slices model by Marshall [185]. He assumes lattice elements that are cubes to which equivalent radii, and hence local permeabilities, are assigned randomly from a given distribution. Further the model has been used for viscous flow in packings of particles with a polydisperse size distribution [234].

Network of tubes (342). The idea of a three-dimensional network of tubes is, of course, very old ([5], page 404). With the exception of models for microporous media [228,235], in almost all cases the tubes are assumed to be cylindrical, as in the two-dimensional networks. The most natural network is that with $\beta = 10$ (cf Fig 1.4). This model was used by Ksenzhek [236] to determine the accessibility effect on the distribution of the non-wetting phase entering a porous medium. The radii of the tubes are distributed randomly over the network and the junctions are assumed to have zero volume (as in the Fatt models). The model was generalized to a variable number of tubes per junction by Nicholson, who applied it to sorption isotherms [237], viscous flow [238], and anisotropic media [238]. The latter is achieved by eliminating tubes from the network in some systematic way.

The difference between two- and three-dimensional network models was analysed by Rose [239]. For the same β the connectivity of grid points via more than one tube is different for two- and three-dimensional networks. Rose used a three-dimensional tetrahedral network, for which $\beta = 22$, to describe $k(u)$ and $\tau(u)$ as a function of $\Psi(u)$. The model can also be used to obtain a connectivity distribution by knocking out tubes (by specifying zero size).

Lattice of connected cavities (343). Because these models have been developed mainly in connection with transport phenomena that are governed by the windows (= connections) between the cavities, the dimensions of the latter are seldom specified. And when it is done, it is done in a very general way [240]. All the existing models from this category assume that the cavities are arranged in a simple cubic array and that each cavity is connected to its six neighbours. The only distinction with the tube networks described above is that the porespace volume is now ascribed wholly to the junctions. To obtain the equivalent radii distribution, to be assigned to the windows, in many cases [241-244], more or less tacitly, a displaced hexagonal sphere packing is assumed. That is to say model *313*, but with a random distribution of the sphere distances (as is done in the tetrahedra model). In one case the distribution is obtained from data concerning the relative occurrence in irregular sphere packings of cavity-windows formed by three to six spheres [245].

The model has been applied to viscous flow [245], electric conductivity [244], drainage [241], suction [243], and mercury porosimetry [242]. In all cases the description of the accessibility of the cavities is of major importance. Probably the theory of branching random processes can be of help in a more general description of the properties of this model [246].

1.6.5. Random networks (35). In the random network approach, the porous medium is visualized as a lattice in which a randomly distributed set of points are connected to their neighbours by tubes, in most cases cylinders. As in the case of many other models the idea as such can be traced back to the beginning of this century [136], but the first specification of such a model had to wait until 1958. Such a specification is also necessary for qualitative explanations. For example, when it is said that many solids can be considered to contain a very large number of interconnected capillaries of all sizes extending in all directions [247], this may sound rather trivial. It is only after a detailed specification of such a description that the unrealistic assumptions emerge.

Random network models have been developed mainly in relation to dispersion. De Josselin de Jongh [60,248] represents the porespace by a network of tubes of uniform length and radius, uniformly distributed in all directions, and $\beta = 6$ (model *351*, see Fig 1.4).

Assuming that the path of a fluid particle consists of a sequence of statistically independent steps, each step corresponding to passing one tube, expressions for the dispersion coefficient are obtained. Independently Saffman [249] gave a more general description of the same model. Bear [2] applied the model also to viscous flow and diffusion. It should be noted that the model contains no constrictivity effect (as in the regular networks the junctions do not have specified dimensions). The tortuosity is the same for all transport phenomena.

The model was further generalized by Greenkorn et al [250, 251], who assign a distribution to both the radius and the length of the tubes. It is assumed that radius, length, and orientation are independent (this is not true for isotropic, homogeneous media). The model is applied to dispersion, viscous flow, and suction (for suction the tubes are assumed to be directly accessible, hence in fact model *12* or *13*). An interesting result of the model is that, for the equivalent radius for viscous flow in a sphere packing, it predicts a value lower than the inscribed circle between three spheres [198]. In later publications of Greenkorn et al, the assumptions, underlying this and similar approaches [3,59,252], have been seriously criticized, in particular the assumption, more or less hidden in the statistics, that the residence time is the same in each tube [253,254,323].

Roughly the same model has been used for diffusion [330] and in describing the change in tube size distribution due to a dissolving solid surface, as encountered in acid injection during oil recovery [255]. Other related models include the random lattice of interconnected ideal mixers, or cavities, e g of spherical form, as applied to deep bed filtration [61], dispersion [256], or Knudsen diffusion [200]. In the latter case diffusion is regarded as a random walk from cavity to cavity.

1.7. Pseudo-porespace models

1.7.1. Simple elements. Models are classified as pseudo-porespace models when the capillary structure that functions as the model cannot be multiplied in a simple way to obtain an extended porespace. Such models are used in ad hoc explanations, for didactic purposes, or as a conceptual model of a formal model of some transport phenomena.

In Fig 1.5 a few examples are given. Model *411* is used in describing capillary liquid transport to a drying surface [4,7]. It represents a homogeneous medium by an inhomogeneous model. Models *421*, *422*, and *423* are used to explain different hysteresis phenomena. Model *421* explains both static and kinetic hysteresis in capillary liquid transport [173] as well as the entrapment of the displaced phase [63,265]. Model *422* is the so-called pore-doublet used to explain trapping of oil in secondary recovery operations [262,263], and hysteresis phenomena in suction [112] and imbibition processes [202]. This model has been generalized to a two-dimensional network model to describe hysteresis in two-phase flow [264]. The network consists of rows of doublets in parallel, the rows put in series with mixing zones. Model *431* is used to elucidate the occurrence of Haines jumps [75]. When the model drains, a Haines jump occurs when the meniscus in the right leg reaches a bulb. On that moment the system becomes unstable and the liquid from the bulb jumps to the other leg. During imbibition the same kind of redistribution phenomena occur.

1.7.2. Independent domain theory. The notions accessibility, independent domain, and ink-bottle pore are closely related. The ink-bottle pore (model *423*) was introduced in connection with the hysteresis loop in sorption isotherms. The idea was generalized to the independent domain theory [R9,R75], which states that the pore-

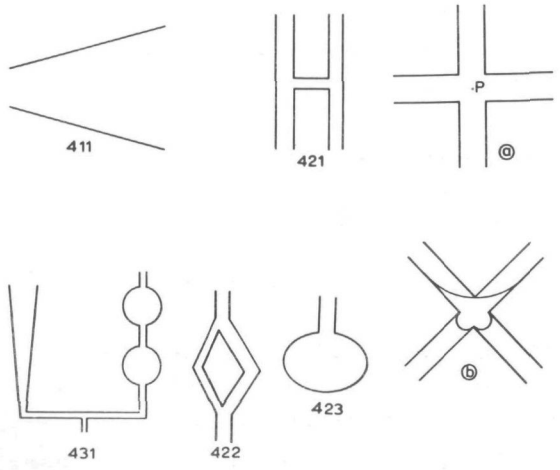

Fig 1.5. Simple capillary models used in explanations of specific behaviour of porous media.

space can be divided into domains or regions that behave independently. To each domain two equivalent radii can be assigned, one for capillary condensation and one for capillary evaporation. Later the theory has been taken over to explain hysteresis in $\Psi(u)$ and $k(u)$.

We think that the independent domain theory has had more attention than it deserves. Hysteresis can be explained in many, more realistic, ways than by picturing the porespace as a set of independent ink-bottles. Even in a cylindrical capillary,sorption behaviour may show hysteresis [266]. The theory is often assumed or applied, recently e g [33,195,267,332], when there is no experimental evidence that it is true. The scanning curves (that is, the $\Psi(u)$ curves within the hysteresis loop) obtained in a suction or mercury porosimetry experiment can be used to test the theory. As might be expected the theory turned out not to be valid [92,268-270], although, initially, some confirmatory results were reported in the case of suction [271].

The general problem that the independent domain theory and its successors [270,272] intend to solve is that of giving an account of the accessibility of an arbitrary region in the porespace. This accessibility is not a property of the porespace alone. It also depends on the kind of transport phenomena, and on the initial and boundary conditions that specify in which way different phases leave and enter the porous medium. A general theory of accessibility has yet to be developed. The first steps on the experimental [273,274], modelling [241,320], and mathematical [246] components of this theory have been made.

1.8. Input parameters porespace models

1.8.1. General remarks. In Table 1.2 an enumeration is given of the various porespace models. In the left part of the table examples are given of models worked out in sufficient detail to guess what are meant to be the input and output parameters. In the right part some idea is given of the transport phenomena to which models of a certain category have been applied. Many models or protomodels described in the literature function basicly as a qualitative elucidation of something that is observed in a particular case. We evaluate the models only with respect to their predictive power regarding a specified class of phenomena. In this review we are not concerned with the considerations of those who comment on

the (experimental) refutation of a model that 'We are not interested here in these models to predict directly.' [253].

Concerning the input and output parameters as given in Table 1.2, the following may be remarked. Each model gives the predicted parameters as a function of the input parameters. When $\Psi(u)$ occurs under both this means that the measured $\Psi(u)$ is interpreted using the model. In the other cases $\Psi(u)$ is interpreted according to model *121*. Seldom is it clearly stated in which way the $\Psi(u)$ function has to be determined, because this is considered trivial. Under input parameters we do no mention the physical properties of the phases present in the porous medium, nor the porosity. By $\overline{d}$ is meant average particle size, and by d particle size distribution; δ is the constrictivity factor as determined by mercury porosimetry [49]. The difference between an estimated parameter and one obtained by curve-fitting is that between a priori and a posteriori. The amount of reliable experimental data is scarce, therefore on this point, an evaluation of the different models is hardly possible. In the next sub-sections we will briefly discuss the available methods to determine the input parameters.

1.8.2. Statistical geometry. Statistical geometry is the geometry of random (sphere) packings. It should provide us the possibility of calculating parameters like porosity, average number of contacts, size distribution of interstices, etc, as a function of the particle size (distribution) and a few other assumptions. The incentives for studying statistical geometry are many, an important one being the development of structural models for simple liquids, monoatomic glasses, and amorphous metallic alloys, to help predict their thermodynamic properties.

All models require, directly or indirectly, the location of the sphere centers in the packing. These may be obtained experimentally or by computer simulation (of the compression of a hard sphere gas, the swelling of spheres at random points in a box until they touch, the packing of spheres in a box at random, rejecting spheres that overlap, etc [R10,R275-277]). The packing is described by the Delauney graph, already mentioned in the sub-section on tetrahedra models, [275,278] or Voronoi polyhedra [276,277]. (A Voronoi polyhedron for a given sphere is that region of space composed of points which are closer to the centre of that sphere than to the centre of any other sphere in the structure.)

TABLE 1.2

Application of porespace models

(i) typical example for each category of models

Models						input parameters			
category	description	year	author	predicted parameters	solid phase	Ψ	τ	curve-fitting	estim-ated
111	equivalent radius	1899	Slichter [137]	k,τ	$\overline{d}$			?	
112	hydraulic radius	1905	Mitscherlich [142]	h_c	$\overline{d}$				
113	tortuous tubes	1927	Kozeny [82]	k, h_c	s			τ	ξ
113	tortuous tubes	1949	Rose and Bruce [156]	$k(u)$		p_b	$\tau(u)$		ξ
12	cylinders, radii distribution	1949	Purcell [163]	$k(u),\Psi(u)$		$\Psi(u)$	$\tau(u)$		ξ
13	*121*, ideally connected	1938	Krischer [20]						
141-143	tubes in series	1937	Adzumi [177]						
145	random adjacent slices	1950	Childs and George [180]	$k(u)$		$\Psi(u)$		k	
148	random adjacent slices	1959	Millington and Quirk [182-184]	$k(u),\mathbb{D}(u)$		$\Psi(u)$			
151	tubes with constrictions	1974	van Brakel and Heertjes [49]	$\mathbb{D}$		δ			τ
154-156	random assemblies of *151*	1973	Payatakes et al [198]	k	d	$\Psi(u)$			
21	network of tubes	1956	Fatt [203]	$k(u),\mathbb{D}(u),\Psi(u)$		$\Psi(u)$			β
31	regular sphere packings	1927	Haines [215]	$\Psi(u)$	d				
33	tetrahedra	1972	Mason [233]	$\Psi(u),k(u)$	d				
34	fixed network	1957	Rose [239]	$k(u),\tau(u)$		$\Psi(u)$		β	
35	random network	1970	Haring and Greenkorn [250]	k,D		$\Psi(u)$		?	

TABLE 1.2

Application of porespace models

(ii) occurrence in the literature for various transport phenomena

category	$\mathbb{D}$, $\mathbb{D}(u)$	k	$k(u)$	wetting, cap rise	suction, drainage	mercury porosimetry	others
111		[11]		[80,138-140]	[160]		
112		[150,151]		[147,257]	[67,141]		
113	[25,153-155]	[19]	[157-159]	[148]			
113							
12	[4,132,133]		[164-167]	[4,132]	[6,259,325]	[90,163]	Knudsen diffusion [170,258]; dispersion [169,201]
13			[20]	[171,172]	[173]		drying [20,174]
141-143	[177,178,190]	[260,261]			[89]	[237]	Knudsen diffusion [237,260]
145							
148	[179,181-185]						
151	[189,191]	[20,119,198]	[196]	[21,171,193]	[171,187,194]	[195]	sorption [192]
154-156	[197]	[143,199]		[143,197,199]			Knudsen diffusion [200]
21	[204]		[206]		[209,210]		
31	[46,49,214]	[11,137,222]		[193]	[193,226]	[223-225]	drying [219,220], sorption [217]
33							
34	[244]	[234,238,245]	[185]		[236,241,243]	[236,242]	sorption [228,235,237]
35	[2,330]	[2,251]					dispersion [2,60,248,249]

Some parts of the developing statistical geometry are of interest for the description of transport phenomena in porous media. However, it is of importance to realize the distinction between models for particle packings and models of the porespace used in describing transport phenomena in porous media. The tetrahedra model discussed above is a case in point. When it is applied to give $\Psi(u)$ or $k(u)$ as a function of the particle size distribution, additional assumptions have to be made, which reduce the model to one more or less identical with Fatt's two-dimensional network.

Stereology. Stereology is the discipline concerned with the interpretation of (two-dimensional) photomicrographs in terms of the (three-dimensional) structural properties of the porous medium [252,R279,R331]. The specific surface and the particle size are the only input parameters that can be measured via photomicrographs. One may speculate that it must be possible to define parameters such as τ, δ, β, or even $\Psi(u)$ in such a way that they can be obtained from photomicrographs, but at the moment no established methods are available. Recent developments are mainly concerned with the problem of giving criteria for randomness and of giving the variation of the local porosity in a random packed bed as a function of the overall porosity and the particle size distribution [280-282]. This can be of use in the description of viscous flow in porous media [108,281] or sedimentation and filtration [283].

As far as we know tomographic techniques (e g [284,285]) have not been used as yet to obtain input parameters for porespace models.

1.8.3. Input parameters obtained from transport phenomena. In many cases the input parameters of a porespace model for a transport phenomenon in porous media are obtained by measurement techniques that make use of another transport phenomenon. Therefore, in many applications the porespace model is less a picture of the physical porespace than a formalism that provides, perhaps, a correlation between different transport phenomena. This has several consequences, to which we shall return presently. Here we give only an enumeration of the techniques most often used.

The equivalent radius, the hydraulic radius, and the specific surface can be determined by measuring the permeability [R3] or by measuring the maximum capillary rise from a dynamic [144-146] or static experiment [70,141,286,287]. The latter experiments are also used to determine the contact angle [80,138,139,147], a para-

meter that is needed for each transport coefficient model that uses $\Psi(u)$ as an input parameter.

The tortuosity is often estimated or obtained by curve-fitting. The measurement technique via the ionic conductivity [R47,R288] has found acceptance only in petroleum geology. It should be noted that $\tau(u)$ as measured by ionic conductivity relates to the liquid phase. When we speak about $\mathbb{D}(u)$ this concerns the gas phase. Recently several measurements techniques have been proposed that combine viscous flow and diffusion phenomena [187,289,290].

As already remarked, the suction [R6,87,R291] and mercury porosimetry [R91,R92] technique were developed specifically to determine $\Psi(u)$. In particular in soil science, several techniques have been developed to measure Ψ in situ [R291]. Apart from the procedures illustrated in Fig 1.1, $\Psi(u)$ is also measured by subjecting a porous medium to increasing centrifugal forces [20, 66,259]. There are developments to combine mercury porosimetry with the interpretation of photomicrographs taken at various saturations [273,327].

All transport coefficients and other parameters that are determined as a function of the liquid content, i e $\Psi(u)$, $\tau(u)$, $k(u)$, $\mathbb{D}(u)$, show hysteresis, that is to say, the dependence on the liquid content is a function of the history of the system.

1.8.4. Comparison of different measurement techniques. An evaluatory article should be written on the different techniques to measure r_h, τ, $\Psi(u)$ and such like, with special emphasize on the experimental difficulties involved and the comparability of their results. Here we can give some examples only of such comparisons. We do not mention the result of the comparison, because, without going into detail, qualifications like "reasonable" or "not very good" do not say much, and furthermore the interpretation offered is often disputable. Of the latter we may give as an example that it is as yet impossible to determine the contact angle in a reliable way independently of the transport phenomena studied. This fact explains why it is reported [89,293] that different liquids give, in a suction experiment with the same porous medium, different results for $C'(u)$, where $C' = \rho g \Psi / \gamma \cos\theta$, but also [292] that different liquids give the same $C'(u)$. (It should be noted that there is no a priori reason that C' is not a function of θ [294]†.)

† See now also chapter 5.

As to the hydraulic or equivalent radius, comparisons have been made between permeability and capillary rise [295,300], permeability and mercury porosimetry [153], permeability and photomicrographs [164], imbibition and mercury porosimetry [146]. For τ comparisons have been made between diffusion, conductivity, and viscous flow [R16]. For $\tau(u)$ between conductivity (salt solution or mercury) and diffusion (in the gas phase) [296,297]. Comparisons between different techniques to determine $\Psi(u)$ are seldom made, and when they are made it is done on porous media with a very complicated porespace configuration [301]. An exception is [324]. The results of mercury porosimetry have been compared with those of photomicrographs [298,327], suction [163], centrifugal drainage [259], liquid-liquid displacement [299], and for microporous media very often with the results of sorption isotherms.

1.9. Porespace models and capillary rise

In this section we check the predictions of the different models against the experimental facts with respect to the statics and dynamics of capillary rise in porous media. As will appear the observed phenomena of capillary rise cannot be explained even qualitatively by any of the models.

1.9.1. Predictions of the models. In Table 1.3 the predictions of the models are given regarding two points. The first is whether the model implies an equation of the form

$$\varepsilon \frac{dh}{dt} = \frac{k}{h} (h_c - h) \tag{1.33}$$

with k and h_c constants, i e dh/dt plotted vs $1/h$ should give a straight line. The second point is whether the model predicts the presence of a saturation gradient in the equilibrium situation.† In Table 1.3 the difference in prediction for a capillary rise and a drainage experiment is also given. We will compare the

† A saturation gradient is absent when there is a sharp front between the dry part and the saturated part of the porous medium. A saturation gradient is present when there is a gradual change from the completely saturated part to the dry part of the porous medium. Hence, models *12* predict a saturation gradient and models *11* do not predict a saturation gradient. See section 2.3 for the operational definition of a saturation gradient.

TABLE 1.3

Predictions of the models for capillary rise

Category	description	$dh/dt \sim 1/h$	saturation zone	hysteresis
11	hydraulic radius	linear	no	no
12	radii distribution	meaningless	yes	no
13	ideal connections	linear	yes	no
14	tubes in series	meaningless	very narrow	yes
151	constrictions	linear	no	yes
21, 342	fixed network	no cap rise	only with drainage	yes
311	cubic sphere packing	no cap rise	no	yes
312	hexagonal sphere packing	linear	no	yes
343	window distribution	linear	only with drainage	yes
343	cavity distribution	linear	only with cap rise	yes

predictions with the observations for capillary rise only. Most predictions follow from the models directly. Maybe the following points should be elucidated.

(i) For models *12* and *145-148* eq (1.33) is not defined, because from the very first moment of capillary rise a saturation gradient is present. In the other cases the applicability of eq (1.33) is, of course, restricted to the period during which there is a sharp, moving, liquid front.

(ii) If the tubes are ideally connected, as in model *13*, or reasonably, as in most two- and three-dimensional models, there will be a rather sharp liquid front as long as the (maximum) capillary rise in the largest tube in the model, $h_{c\ min}$, is not reached. For model *13* we have

$$\frac{dh}{dt} = \frac{\frac{dV}{dt}}{\sum_i \pi r_i^2} = \frac{\sum_i \{\pi r_i^2 \frac{\rho g}{8\eta} \frac{r_i^2}{h} (h_{ci} - h)\}}{\sum_i \pi r_i^2} = \tag{1.34}$$

$$\frac{dh}{dt} = \frac{\rho g}{8\eta} \frac{\sum_i \pi r_i^4 h_{ci}}{\sum_i \pi r_i^2} \frac{1}{h} - \frac{\rho g}{8\eta} \frac{\sum_i \pi r_i^4}{\sum_i \pi r_i^2}$$

Hence dh/dt vs $1/h$ should give a straight line until $h_{c\ min}$ is reached, then a saturation gradient develops.

(iii) For models containing tubes with constrictions, eq (1.33) is also valid. For a tube with periodic constrictions we have

$$\frac{dh}{dt} = \frac{k}{h}(\overline{h}_c - h) \qquad h < h_{c\ min}$$

$$\frac{dh}{dt} = 0 \qquad h > h_{c\ min} \tag{1.35}$$

in which $h_{c\ min}$ is the capillary rise in the widest section of the tube. See also Fig 1.6. On a microscopic scale the rise velocity oscillates between line p and line q. Macroscopically we observe line r.

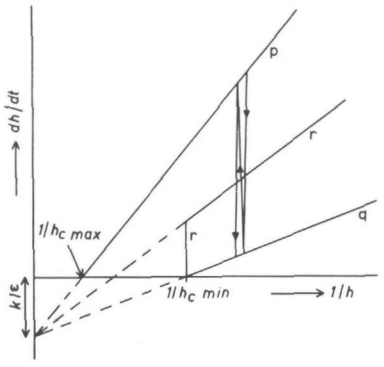

Fig 1.6. Velocity of capillary rise vs inverse height for models of type *151* and others containing channels with periodic constrictions.

(iv) Two- and three-dimensional models contain junctions or cavities whose dimensions are seldom specified in detail. The symmetry that is generally assumed greatly diminishes the capillary rise. If six tubes meet at a grid point of a cubic three-dimensional network, the model predicts no capillary rise (cf Fig 1.5a). A meniscus rising from below P can never reach P because ther are no walls to support it. In general, the curvature of the meniscus that can pass a junction depends on the precise geometry of the junction and the number of menisci that meet at the junction. It should be noted that this curvature has nothing to

do with the inscribed sphere of the cavities. It is very difficult to illustrate this in three-dimensional space. An example for two-dimensional space is given in Fig 1.5b. One meniscus cannot pass the junction. When two menisci meet, they will pass with a maximum curvature of $r(1+\sqrt{2})$. When three menisci meet this maximum curvature is r. The inscribed circle is $r\sqrt{2}$.

1.9.2. Comparison with the observations. In Table 1.4 a number of observations, as reported in the literature, have been compiled. Apart from the validity of eq (1.33) and the presence of a saturation gradient, it is also mentioned whether the correct permeability was observed (correct = correct order of magnitude). This is included because, when only three or four observations

TABLE 1.4

Observed phenomena in capillary rise

year	author	model	eq (1.33) valid	correct k	saturation zone	materials solid-liquid
1921	Hacket [302]	*11*	no	no		sand-oil
1949	Porhaev [84]	*11*	yes			sand-water
1962	Koida [145]	*11*	yes			minerals-water
1966	Tanaeva [135]	*11*	yes	yes ¶	yes ¶	sand-water
1969	Kuz'min [146]	*11*	yes			ceramics-kerosene
1970	Smith [303]	*11*		yes	no	ice-water
1973	Schindler [304]	*11*	no ¶			glass-various
1920	McLaughlin [305]	*12*	no ¶	no	sometimes	sand-water
1966	Luikov [132]	*12*	yes ¶	yes ¶	yes	sand-water
1971	Sommer [176]	*12*	no ¶	no ¶		glass-water
1961	Braslavskii [171]	*13*			yes	polymer-oil
1963	Cammerer [172]	*13*	no ¶	no ¶	yes	glass-water
1970	Heizmann [72]	*13*	no ¶	no ¶	yes	glass-water
1949	Puri [36]	*313*	no ¶	no ¶	sometimes	sand-water
1900	Krawkow [306]	-	sometimes ¶			sand-water
1906	Bell [81]	-	no			paper-various
1918	Attenberg [307]	-	no ¶	no	yes	sand-water
1931	Wadsworth [308]	-	no ¶	no	yes	sand-water
1934	Peck [309]	-	yes	no ¶		paper-water
1958	Youngs [109]	-			sometimes	(infiltration)
this laboratory [294,310]			sometimes	sometimes	sometimes	various

have been made during one experiment, it is dangerous to draw a conclusion concerning the linearity of $dh/dt - 1/h$. For systems such as sand and glass beads, the value of k, as a function of the particle size, is firmly established. If a qualification is followed by ¶, this means that the qualification follows from the data presented, but that it is not stated explicitly by the author(s) in question. In many cases the observations do not confirm the model adopted by the author. This is due to the fact that the model is seldom stated in a precise way, let alone that its consequences are realized.

It will by now be clear why the models were only checked against two qualitative properties. Other, or more detailed predictions are irrelevant, because none of the models can account for the fact that sometimes eq (1.33) is valid and sometimes it is not, or that sometimes a saturation gradient is observed and sometimes it is not. This is not the place to discuss the possible explanation(s) of the, at first sight perhaps anomalous, phenomena observed during capillary rise. However, it should be noted that there is an important difference between the eq (1.33) problem and the saturation gradient problem. The first is due to other transport phenomena being rate determining (which may also happen in cylindrical capillaries) while the second is a direct consequence of the mechanism of capillary rise [294]†. The reason that all models fail in describing the mechanism of capillary rise is twofold. Firstly, all models assume that there exist a large number of isolated menisci in the porous medium while in fact there is one meniscus only. Secondly, all models assume that the curvature of the meniscus or menisci can be characterized by one (average) radius of curvature. This cannot be done, primarily because the average curvature is no simple function of the contact angle.

1.10. Further evaluation of the models

1.10.1. Models and models. In the preceding section it appeared that the existing porespace models are of little use in describing capillary rise in porous media. The situation is better for other transport phenomena, but the failure of the models to describe

† See now chapters 4 and 5.

capillary rise emphasizes two things. Firstly, different transport phenomena ask for different models and secondly, reliable data must be available to check the models. More generally, the conceptual model should not lose contact with the physical phenomena it intends to describe. For this reason we have no high opinion of combinations of more than one model, of which we have already given some examples. We may add two recent examples of a mixture of models, which can be confirmed by experiment only by accident, and whose inconsistency as a physical model speaks for itself.

Dodds and Lloyd [278], in describing a suction experiment, use a two-dimensional network. The tube radii distribution of this network is obtained from the tetrahedra model of Wise [229], but because Wise's model has a fixed porosity, much lower that that obtained in practice, a correction is made using the hydraulic radius model.

As a second example we choose (cf [92]) the proposals to determine the particle size distribution from mercury porosimetry [311,319]. Here it is assumed that an irregular polysized sphere packing can be considered as an assembly of independent regions of regular monosized sphere packings according to model *313*.

As a further evaluation of the porespace models we will first give a criticism of the concept of a pore-size distribution. After that a number of transport phenomena are compared in pairs to elucidate further the need of different approaches for different transport phenomena.

1.10.2. The concept "pore-size distribution". Some readers may have found it cumbersome that, in the preceding sections, we have never used the term pore-size distribution, but instead spoke of tube radii distribution, which refers to a model, or geometries of the porespace, which refers to the porous medium, or the $\Psi(u)$ function, which refers to a measurement technique. This was done because we seriously believe that the use of terms such as pore, pore-size, or pore-size distribution, hinders progress in the field of research under discussion. Of course, from time to time the concept of a pore is criticized [312,313], and, of course, we all know that the porespace has a very complicated structure. Nevertheless, when phrases still occur in the literature such as 'it has not yet been possible to define precisely what is meant by the size of a pore' [255], though we actually know, our common sense concep-

tion of a porous medium apparently still prevents us from drawing the right conclusions.

A porous medium consists of a solid phase dispersed in such a way that a non-solid phase remains in between. The latter we call the porespace and we restrict ouselves to a continuous porespace. Continuous means that any two points in the porespace can be connected by a line that does not pass the solid phase. The porespace does not consist of interconnected pores because a pore is, according to any established meaning, something having a certain length and recognizable walls. Such things are not present in a normal porous medium. As fas as geometric elements are recognizable in a porous medium, these are particles. Therefore, many porespace models turn into much more realistic pictures of the porous medium if the porespace in the models is taken to represent the solid phase.

If there are no pores in a porous medium there is, of course, neither a pore-size distribution. This does not imply that the term pore-size distribution, as used in the literature, is completely void of meaning. In fact, it can mean very different things, including:

(i) Distribution of radii of inscribed spheres in the porespace (e g [3,315]). Although this is a rather clear definition it is unclear in which way the distribution could be determined and in which theoretical or applied context it fits. In particular for capillary liquid transport, this notion is without any significance, because the inscribed sphere touches the solid phase in a few *points*, while a meniscus needs one or more three-phase *lines* to support it.

(ii) Distribution of the lengths of the line sections in the porespace that result when a straight line is placed at random in a porous medium. This distribution can be obtained from photomicrographs [277,316,327]. It is clear that this distribution provides some information on the geometric properties of the porespace but it must be emphasized that the same length distribution is a property of very different kinds of porous media. For example, the intersections, given in Fig 1.3, models *234* and *235*, might yield the same length distribution.

(iii) Curvature of the meniscus as a function of the liquid content, i e $C(u)$ as determined under some specified conditions. In almost all cases such a $C(u)$ or $\Psi(u)$ function is transformed, by

means of a model, into a tube radii distribution, which is then used in the same or another model to predict a transport coefficient. This is not necessary, leads to confusion, and disguises critical assumptions. It leads to statements such as 'Since a variety of different capillary shapes may give rise to the same capillary pressure, the pore dimensions calculated from capillary pressure measurments are also somewhat qualitative.' [9], which statement, to say the least, completely disguises what the problem is in calculating no matter what from capillary pressure, i e $\Psi(u)$, measurements. Slips of the pen, such as that we can 'relate the capillary pressure to the mean radius of curvature, to the air-water interfacial tension and to the contact angle' ([2], page 476), suggest that in due course the concept of a meniscus curvature will have disappeared completely, giving place to the all embracing cylindrical tube radius.

1.10.3. Molecular diffusion and viscous flow. In the preceding sections the term tortuosity and the symbol τ has not been used in a consistent way. Both $\mathbb{D}_{eff}$ and k depend on some kind of τ; whether this is the same τ depends on its definition. If τ is defined as a geometric property of the porespace, keeping to model *113* as close as possible [49], it is the same τ that enters into the expressions for $\mathbb{D}_{eff}$ and k. But, in a real porous medium, such a tortuosity is always combined with a constrictivity factor. And the latter is not the same for molecular diffusion and viscous flow because of the different influence of constrictions on the integration of the respective differential equations [46].

In most applications τ is used as a factor that accounts for both tortuosity and constrictivity. This is the case when τ is used as a fudge factor as well as when determined from ionic conductivity measurements. This τ is not the same for molecular diffusion and viscous flow. Determination of τ or $\tau(u)$ (from conductivity measurements) to predict k or $k(u)$ is possible only when a model is assumed that does not contain tubes with constrictions.

1.10.4. The interrelationship of $k(u)$ *and* $\Psi(u)$. For capillary liquid transport the hypothesis is used that [cf eq (1.8)]

$$q = -k(u)\,\frac{d}{dx}\{\Psi(u) + x\cos\alpha\} \qquad (1.36)$$

To test this equation we need $k(u)$, $\Psi(u)$, and the data of a displace-

ment experiment yielding $u(t,x)$. Experimental data available have been obtained mainly on drainage and infiltration experiments [268, R62,R269]. Normally, the procedure is to measure $u(t,x)$, $\Psi(t,x)$, and q and to calculate then, numerically, $k(u)$ from eq (1.36). It appears that there is strong hysteresis in $\Psi(u)$ and some in $k(u)$. Independent measurements of $k(u)$ hardly exist. The experimental difficulties are considerable, nevertheless a check of applicable models against these data should be worthwhile. On the other hand it should be noted that, although eq (1.36) is almost universally accepted [32,33, 78], there is in fact little or no evidence that it is true [317]. The fact that $k(u)$ and $\Psi(u)$ are non-unique functions for a given porous medium and liquid is of course one of the main difficulties.

1.10.5. Imbibition and draining. The difference between capillary rise, wetting, and infiltration on the one hand, and drainage and suction on the other is generally recognized and some of the distinctions have been mentioned above. We may note here that imbibition curves in a suction experiment (i e imbibition of a partly saturated medium) are not comparable with imbibition of a dry porous medium. Further that, although drainage and suction have much in common (and, by the way, should be clearly distinguished from drying), there are still differences caused by kinetic and accessibility aspects. See, e g , the data on imbibition, drainage, and suction in [322]. Because so little is known about the mechanisms of capillary liquid transport this is not the place to dwell further on these differences.†

1.10.6. Suction and mercury porosimetry. The $\Psi(u)$ curves obtained by a suction experiment and those obtained by mercury porosimetry may seem directly comparable. In both cases a non-wetting phase displaces a wetting phase. However, even in this case, there are important differences, which have hardly been analyzed.

In a suction experiment one side of the porous medium is connected with the wetting liquid, the other with air. During mercury impregnation the evacuated porous medium is completely surrounded by mercury. This difference in initial and boundary conditions causes a different continuity of the two fluid phases during the experiment. When the impregnation curve, for mercury or air, is followed by a retraction curve, the difference becomes even more pronounced. In the case of mercury porosimetry the na-

† See however section 5.4.4.

ure of the retraction curve depends strongly on the high pressure point from which it starts, because the release of mercury from the cavities depends on the number of closed near-contacts [92]. The higher the number of near-contacts closed during impregnation, the more difficult is the retraction.

1.11. Concluding remarks

Even when much of the criticism presented in the preceding sections is accepted, the question remains whether there is an alternative. Now we have not the intention to judge the practical usefulness of models, empirical correlations, or mathematical solutions, for some specialized applied science. That can be done only by those, if any, who make use of those models, correlations, and solutions in practice. Any criticism is levelled against claims of knowledge, in the sense of a priori predictability, and against the priorities chosen to obtain such knowledge. From the criticism and the analysis of the problem situation, the priorities for further research follow. The following list can be considered as the alternative asked for above.

(i) We have restricted ourselves to simple porespace structures. For this case the values of $\mathbb{D}_{eff}$, and k for a saturated porous medium, are more or less established via eqs (1.22) and (1.23). The usefulness of the parameters τ and δ should be studied, i e they should be defined and made measurable in a simple way. Special attention should be given to the statistical analysis of photomicrographs.

(ii) As to dispersion and $k(u)$ there is no need for more models. Experimental data on simple systems, such as glass beads and coarse sand, are hardly available, and they should be collected first.

(iii) For capillary liquid transport, the major drawback is that almost nothing is known about the form of the menisci that may be present in a porous medium. Though this certainly is not an easy matter, it must be possible, e g , to give a reasonable account of the menisci that can be formed in a hexagonal sphere packing. We expect that, when the latter problem is solved, this will have a severe influence on all descriptions of capillary liquid transport and several other areas such as agglomeration. Perhaps it is worthwhile to stimulate mathematicians to consider this problem.

(iv) The quantity and quality of experimental data on $u(x,t)$ obtained in capillary rise or drainage experiments is low. We expect that accurate $u(x,t)$ measurements on simple systems under different conditions will provide much understanding of the nature of capillary liquid transport. A review of the existing data is needed, especially because there is hardly any contact between the research carried out in soil science (which is mainly published in English) and the research done in building physics (which is mainly published in German).

(v) For imbibition processes (capillary rise, infiltration, wetting) no progress can be made before (iii) has been solved. For draining processes the approach using models such as *341* [241] and *33* [233] seems to give a reasonable approximation. It seems advisable to check the models against drainage experiments in the first place.

(vi) The interpretation of the scanning curves obtainable by suction and mercury porosimetry can be of heuristic value for a general understanding of the behaviour of menisci in porous media. The combined study of suction and mercury porosimetry can add to this. It may be noted that the fact that these experiments are rather time consuming has never been explained. Study of the kinetics of reaching the equilibrium points can help to gain insight in $k(u)$ and the little studied phenomenon of meniscus redistribution.

(vii) Finally, we may emphasize two related problem areas that are directly relevant to the problem of obtaining reliable experimental data. First, we need techniques to make homogeneous porous media and techniques to check this homogeneity [318]. Secondly we need a reliable technique to measure the contact angle of porous media.

From these priorities it will be clear that we do not share the prejudice that a scientific publication *must* contain a mathematical model, which can only be expressed in tensor notation and solved only by a large computer, while it *may* contain experimental data (but one experiment at a maximum).

CHAPTER 2

A PROBLEM IN CAPILLARY RISE IN POROUS MEDIA

2.1. Introduction

From the review presented in the preceding chapter, it appears that none of the existing porespace models can describe the phenomena observed during capillary rise in porous media. The data gathered in Table 1.4 show that the common sense description of capillary rise in porous media is inadequate. There is no obvious reason why we should sometimes observe a linear relationship between dh/dt and $1/h$ and sometimes not [cf eq (1.33)], and why we should sometimes observe a saturation gradient in the equilibrium situation and sometimes not.[1] And again, as will appear, why these different phenomena can be observed on porous media with the "same" porespace geometry.

In this and the following chapters the discussion is restricted to capillary rise in porous media. The phenomenon of drainage is treated en passant. That is to say, the experimental results and the interpretation for drainage have a function in elucidating the more complex phenomenon of capillary rise. In the present chapter the experimental techniques and a classification of the observed phenomena are given. In chapter 3 a number of refuted or non-confirmed hypotheses are discussed. Chapters 4 and 5 concern possible solutions to the problem as stated in section 2.4.

2.2. Experimental techniques

2.2.1. General remarks. Capillary rise experiments were performed by submerging a porous medium in a liquid and observing the capillary rise visually, yielding $h(t)$, and/or by means of an X-ray absorption technique, yielding $u(h,t)$. Drainage experiments were carried out by draining a completely saturated porous medium and observing $u(h,t)$.

A large number of experiments were performed with different solid and liquid phases and under different conditions. Each experiment has a many symbol name, which gives information about the most

---

1. Cf section 1.9 and the SUMMARY AND INTRODUCTION.

important parameters. The meaning of the symbols is given in the Appendix.

In this section the main outline of the experimental techniques is given. Details relevant to specific hypotheses are given in the subsequent chapters where such a hypothesis is discussed.

2.2.2. Materials used. For obvious or practical reasons most experiments were carried out with glass beads or sand as the solid phase and water or toluene as the liquid phase. Other solid phases include: mixtures of sand and glass beads, crushed glass, fused silica particles, copper spheres, and polystyrene spheres. Other liquid phases include *n*-hexane, *n*-heptane, paraffin oil, ethyl alcohol, glycol, dichloroacetic acid, acetonitrile, and nitromethane. These other solid and liquid phases were used to test specific hypotheses. The organic liquids were, in general, of reagent quality and used without further treatment. See section 4.6.4 for the influence of the purity of the wetting liquids. Glass beads and sand from various sources were used and different pre-treatment procedures were applied such as heating, cleaning with detergents and/or acids, and etching. Further details on this are given in section 3.3.

2.2.3. The porous medium. The porous media are prepared by packing the particles in a vessel using a special technique. This technique consists of a controlled deposition of the particles in a vessel that is subjected to a controlled horizontal vibration. In this way reproducible and homogeneous packings are obtained. The homogeneity, defined as the scatter in $\varepsilon(h)$, is measured using an X-ray absorption technique. In the case of glass beads, experiments were also carried out with consolidated porous media, i e the particles are sintered together without noticeable disturbance of the packing or deformation of the particles. The packing technique, the homogeneity measurement by means of X-ray absorption, and the sintering technique have been described in detail elsewhere [318].

In almost all cases the porous media used were cylindrical, usually with a diameter of 23 mm and a height of 10-25 cm. The non-consolidated porous media were supported by glass cylinders with a glass filter at the bottom. The supporting cylinders with filter were cleaned with detergent, water and dried with reagent acetone. The influence of the homogeneity, the filter, the wall effect, etc, is discussed in section 3.2.

2.2.4. Experimental conditions. All experiments were conducted at (20 ± 0.5)°C. The experiment is started by submerging the porous medium 2 mm below the liquid surface. Depending on the duration of the experiment and the vapour pressure of the liquid, precautions are necessary to ensure a constant level of the free liquid surface.

The liquid front at the wall was observed visually. In selected experiments the capillary rise was also followed by means of X-ray absorption. In this case the saturation of the porous medium is measured as a function of time in 1 mm sections of the medium. Usually, the height of the column was scanned with steps of 2.5 mm. The relation between the logarithm of the transmitted intensity, I, an the liquid content, u, is linear [318], but, because of the $\varepsilon(h)$ fluctuations, the constants differ for different heights. Therefore it is necessary to know, for each height, the intensity at zero and complete saturation, I_0 and I_{100} respectively. No attempt was made - given the problem situation - to make very accurate u measurements; the error is in the order of 3-5 % absolute. During capillary rise there will be some air entrapment (cf section 3.4). Nevertheless, all results are calculated and reported as if the porous medium is completely saturated below the sharp wetting front. Further, in most cases, I_{100}, for heights not completely saturated at equilibrium, is calculated from I_0, assuming a constant I_{100}/I_0 ratio for the porous medium and the X-rays used.

A number of experiments were performed under special boundary conditions with respect to the partial pressure of air in different parts of the system. These are described in sections 3.4.1. and 3.6.

2.3. Classification of the observed phenomena[2]

2.3.1. Terminology. An experiment is performed upon a certain system. A system consists of a combination of a solid phase and a wetting (liquid) phase. The solid phase is a homogeneous packing of particles of a certain narrow size distribution. When the solid phase

2. The experimental results on capillary rise and drainage, to which we refer in this and the next chapters, were gathered over a number of years. The greater part of the experimental work was carried out by Monsieur D.R.Y. Karboviac. Further, a large number of students contributed to specific parts as part of their undergraduate course work.

TABLE 2.1

Occurrence of different capillary rise phenomena as a function of the solid - liquid combination

	Solid phase	Class Ia $dh/dt = C/h$ Sat gradient	Class Ib $dh/dt \neq C/h$ Sat gradient	Class IIa $dh/dt = C/h$ no gradient	Class IIb $dh/dt \neq C/h$ no gradient
This laboratory	glass beads	toluene, hexane	ethylalcohol (?), glycol (?), water (?)	paraffinic oil	toluene, hexane, water
	sand	water, toluene, paraffinic oil		water	water
	crushed glass	water, toluene			
	fused silica	toluene			
	polystyrene	heptane, ethylalcohol	ethylalcohol (?), acetonitril (?)	glycol	nitromethane
The literature	glass beads		water [72,172]		(?) water [176,304]
	sand	water [36,132,135,335-338] oil [302]	water [308,397]	water [306,338]	(?) water [306,322,339]

is from a different source or has been subjected to different surface treatments, or when the experimental conditions are different, this is still called experiments upon the *same* system or combination. When all known parameters are the same, as far as is known, this is called experiments upon *identical* systems.

The observed phenomena suggest a classification as follows (the times given refer to the capillary rise of water in 350 μm sand particles[3] or glass beads):

Class Ia. At first there is a rapid capillary rise of a sharp liquid front, for which eq (1.33) is valid (i e dh/dt vs $1/h$ is linear). After some minutes a saturation gradient starts to develop. Equilibrium is reached after 1-3 days.

Class Ib. At first there is a very slow capillary rise of a sharp liquid front, for which eq (1.33) does not hold. After several days a saturation gradient develops. An equilibrium situation is reached after several months or years.

Class IIa. Equilibrium is reached in a few minutes. A saturation gradient does not develop, i e , no saturation gradient wider than $10d$. The capillary rise obeys eq (1.33).

Class IIb. Eq (1.33) does not hold, except for the very first moments of capillary rise. Equilibrium is reached after several weeks. No saturation gradient develops.

Ia, Ib, etc are used as adjectives in phrases like 'Ia system' and 'this system shows a Ia behaviour', which mean: when an experiment is performed upon this system the phenomena characteristic for class Ia are observed. The equilibrium height is the maximum height of capillary rise for complete saturation. The equilibrium time is the approximate time it takes to reach a height less than 0.5 mm below the equilibrium height.

In Table 2.1 the combinations that show a certain class behaviour are presented. Some data from the literature are included. It should, however, be noted that of the 18 references given only *one* [171] provides enough information to decide, beyond doubt, which behaviour was observed.

2.3.2. Class Ia behaviour. Ia systems display rapid rise and a saturation gradient at equilibrium. Figs 2.1-3 show dh/dt vs $1/h$ for some representative cases: toluene and hexane in glass beads

3. All experiments were performed with sieve fractions (see Appendix). They are denoted by the average particle diameter (median).

(Fig 2.1); toluene and water in sand (Fig 2.2); and toluene in crushed glass and copper spheres (Fig 2.3). For sand - paraffin oil see Fig 2.9. From the data for toluene in glass beads and sand, it can be seen that the reproducibility is good for identical sys-

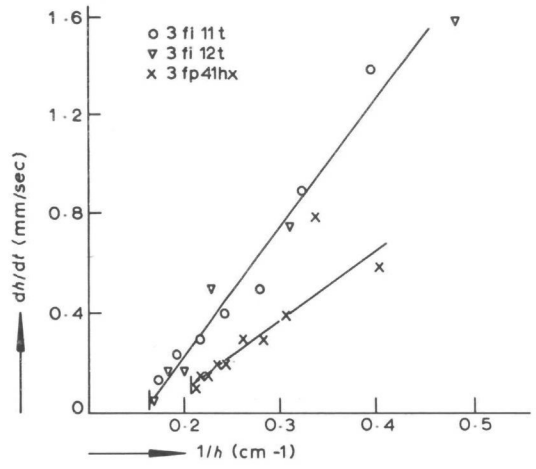

Fig 2.1. Class Ia. Capillary rise of toluene (▽, o) and hexane (x) in 350 μm glass beads.

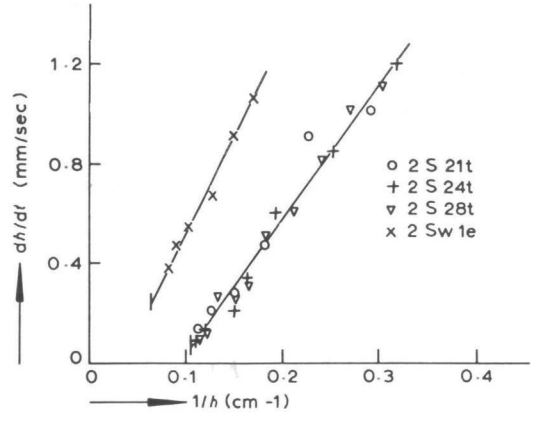

Fig 2.2. Class Ia. Capillary rise of toluene (o, +, ▽) and water (x) in 325 μm sand.

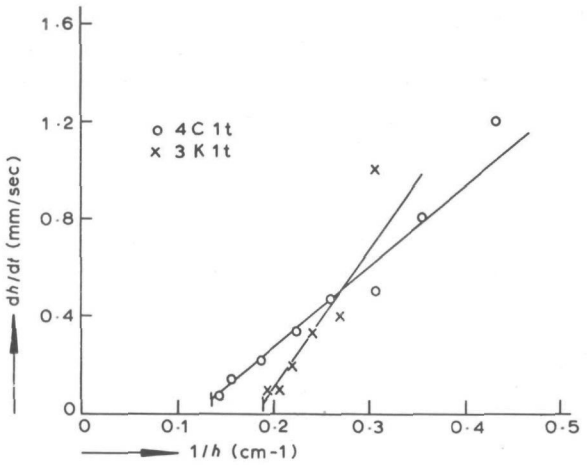

Fig 2.3. Class Ia. Capillary rise of toluene in 360 μm crushed glass (o) and 360 μm copper spheres (x).

tems.[4] The vertical stroke at the lower end of each straight line indicates the point at which the saturation gradient starts to develop. This point was determined by means of X-ray absorption, except in the case of copper where it was estimated visually. The values of k obtained by extrapolation of the straight lines are of the same order of magnitude as those calculated from eq (1.23) [cf section 3.2].

The height above which a saturation gradient develops is always higher than the equilibrium height of the same system that comes under class IIa or IIb. Three examples of a developing saturation gradient are given in Fig 2.4 (toluene - glass beads), Fig 2.5 (water-sand), and Fig 2.6 (heptane-polystyrene). It was assumed that equilibrium had been reached when there was no change in the measured $u(h)$ for ten days. The reproducibility of the saturation gradient is good for identical systems.[5]

---

4. The scatter of the points is due to the inaccuracy in reading the height of the wetting front. This accuracy might, in principle, be improved by filming the capillary rise. However, at very high velocities the liquid front becomes rather irregular, for understandable reasons, and there is therefore not much sense in carrying out a more severe testing of eq (1.33).
5. Cf: (i) Experiments 2Pk3k and 2Pk4k in Fig 2.6 and (ii) experiment 3fi22t in Fig 2.4 and 3fp32t in Fig 2.15. The saturation gradient after drainage is reproducible as well: see Fig 2.10.

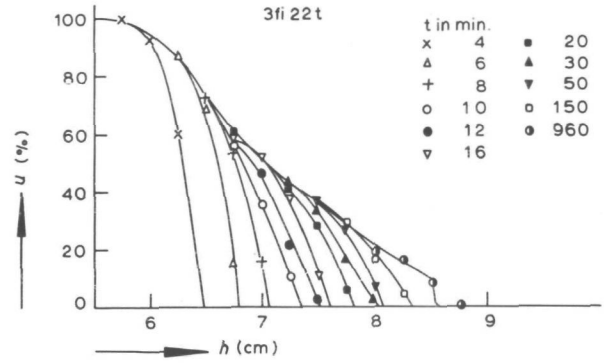

Fig 2.4. Class Ia. Development of the saturation gradient for capillary rise of toluene in 350 µm glass beads.

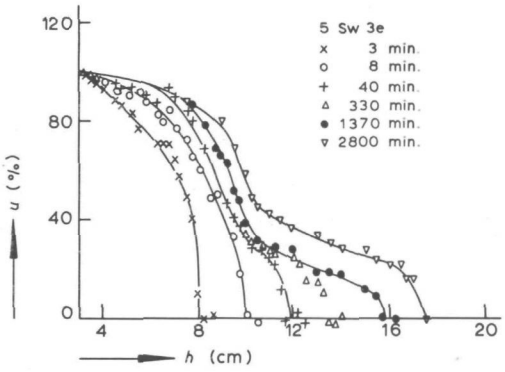

Fig 2.5. Class Ia. Development of the saturation gradient for capillary rise of water in 550 µm sand.

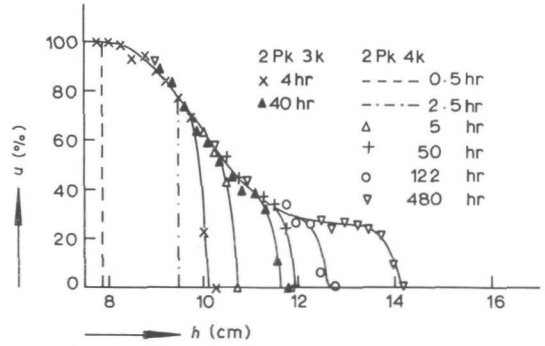

Fig 2.6. Class Ia. Development of the saturation gradient for capillary rise of heptane in 215 µm polystyrene spheres.

Drainage experiments performed upon Ia systems always yield a saturation gradient at equilibrium, which is reached rapidly. An example, for toluene-sand, is given in Fig 2.7 (cf also Fig 2.10).[6]

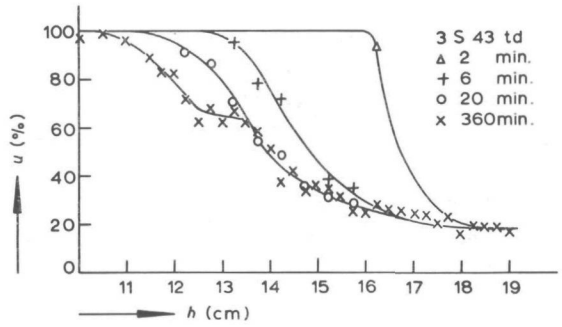

Fig 2.7. Class Ia. Development of the saturation gradient during drainage of toluene from 360 μm sand.

2.3.3. Class Ib behaviour. Ib systems display very slow rise and a saturation gradient at equilibrium. At this laboratory Ib behaviour has never been observed with certainty.[7] It is, however, clear from the literature that such systems exist. See Table 2.1. The only sophisticated experiment reported is that of Cammerer [171]. He finds, for water in 200-300 μm glass beads, a sharp rising front for the first 10 days or so. Then, at a height of about 12 cm a saturation gradient starts to develop. After 128 days there was still no equilibrium and a saturation gradient from 13 to 20 cm. We have no reason to suppose that Ib behaviour is more rare than that of the other classes.

2.3.4. Class IIa behaviour. IIa systems display rapid rise and no saturation gradient after capillary rise. Fig 2.8 shows dh/dt vs $1/h$ for water-sand. The points given for $dh/dt = 0$ refer to the equilibrium heights. In Fig 2.9 the results are given for paraffin oil in glass beads (class IIa) and in sand (class Ia). The

---

6. One should not be confused by the difference in the equilibrium time for 3S43td (< 360 min) and 9Sw2ed (< 3 min). The difference in particle size entails a difference in the permeability for saturated flow by a factor 30.
7. Possible Ib systems are discussed in section 5.4.3.

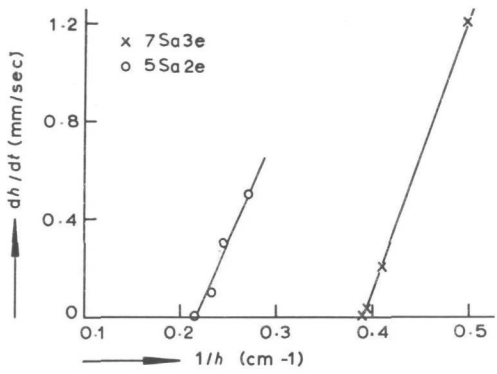

Fig 2.8. Class IIa. Capillary rise of water in 550 µm sand (o) and 780 µm sand (x).

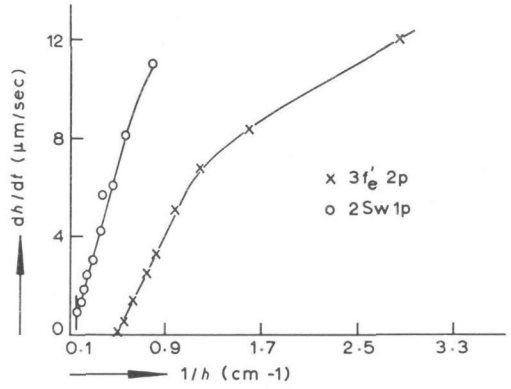

Fig 2.9. Capillary rise of paraffinic oil in 350 µm glass beads (x), class IIa, and in 325 µm sand (o), class Ia.

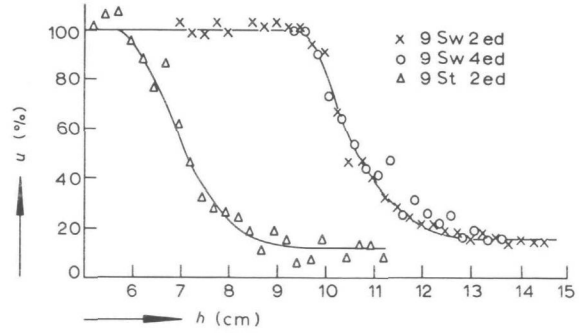

Fig 2.10. Saturation gradient after drainage of water from 925 µm sand. Class Ia (x, o) and class IIa (Δ).

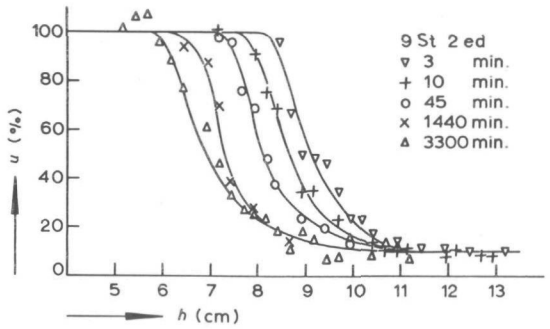

Fig 2.11. Class IIa. Development of the saturation gradient during drainage of water from 925 μm sand.

concave part of the curve at low heights is due to the supporting filter (cf section 3.2).[8]

In Fig 2.10 the saturation gradient after drainage is given for a Ia and a IIa system water-sand. The general form of the gradient is the same, but there is a large difference in the equilibrium time. Fig 2.11 shows the development of the saturation gradient (during drainage) for the IIa system. The equilibrium time is in the order of two days, to be compared with less than 3 min for the (same) Ia system.

2.3.5. Class IIb behaviour. IIb systems display slow rise and no saturation gradient after capillary rise. In Figs 2.12-14 three examples are given of dh/dt vs $1/h$. Because the velocity of capillary rise decreases strongly with increasing height the scale for dh/dt is changed, first from mm/sec to mm/min and then from mm/min to mm/hr, to obtain a good discrimination.[9] The concave

8. Because no saturation gradient is present and eq (1.33) is obeyed, equilibrium is reached very rapidly. In the case of water-sand, measurements are hardly possible, equilibrium being reached in a few minutes or less. For paraffin oil - glass beads, a height of 1.95 cm had been reached after 17 min. The equilibrium height of 2.00 cm did not change over the next 40 days (after which no further readings were taken).

9. Although it is not a normal procedure to spread the data of one experiment over different scales it seems the best method in the present case. Various scales were tried, but in no case did we obtain curves of reasonable form and discrimination over the whole range of measurements. Further, for reasons of comparison and interpretation, dh/dt vs $1/h$ on linear scales has several advantages.

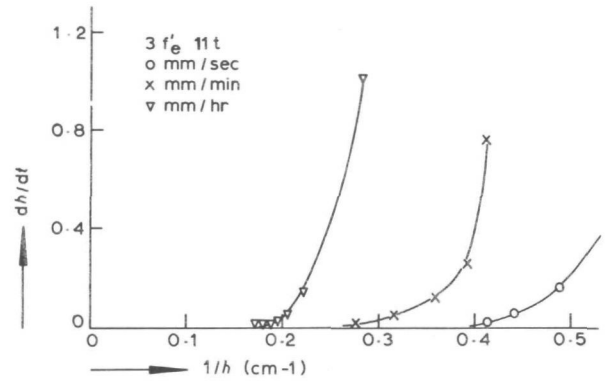

Fig 2.12. Class IIb. Capillary rise of toluene in 350 µm glass beads.

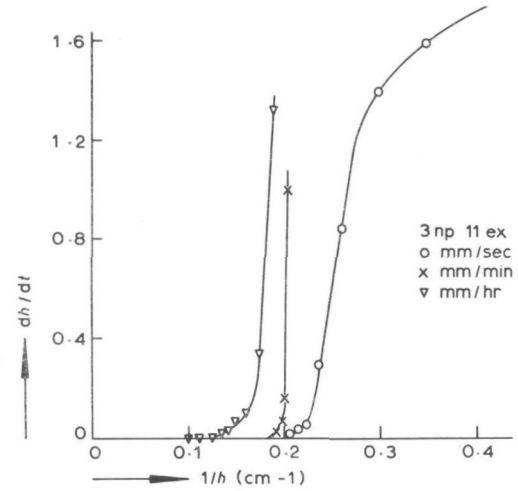

Fig 2.13. Class IIb. Capillary rise of water in 350 µm glass beads.

part at short times in Fig 2.13 (for water - glass beads) is due to the resistance of the supporting filter. Fig 2.14 for water-sand is an example of the fact that a number of points on a straight line do not permit the conclusion that capillary rise can be described by eq (1.33). For almost all IIb systems, the part of the dh/dt - $1/h$ function at low heights can be approximated by a straight line, i e , Fig 2.14 is the representative case and Fig 2.12 is the exception. The value of k, obtained by extrapolation of this straight line, is comparable with that obtained for Ia and IIa systems (cf section 3.2). For identical IIb systems the re-

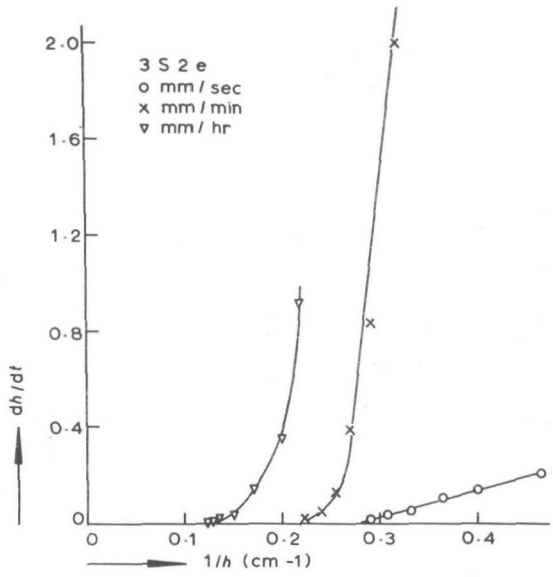

Fig 2.14. Class IIb. Capillary rise of water in 360 µm sand.

producibility is good for toluene - glass beads, but not for water - glass beads (see also section 3.3.1).

In Table 2.2 some equilibrium heights are given. For water - glass beads and toluene - glass beads the range given indicates the minimum and maximum values found in a series of about ten experiments with the same system (see also section 3.3). For the other combinations one typical example is given. The numerals between parentheses in the last column refer to the number of days after which no further readings were taken.

TABLE 2.2

Equilibrium heights and times for IIb systems (d = 350 µm; last three examples perhaps Ib, cf section 5.4.3)

Combination	equilibrium height (mm)	equilibrium time (days)
glass beads - water	77 - 113	21(173) - 85(142)
glass beads - toluene	32 - 58	5(40) - 34(82)
sand - water	73	66(114)
glass beads - dichloroacetic acid	42	>180
glass beads - glycol	85	300(1000)
polystyrene -alcohol	57	3(60)

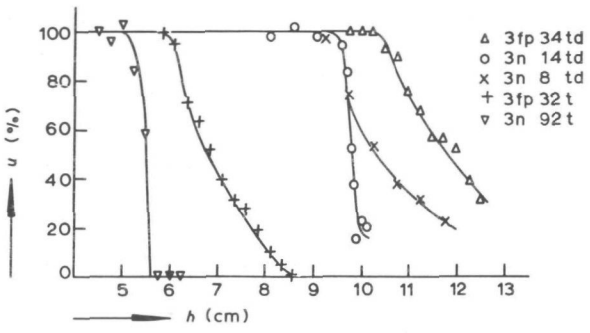

Fig 2.15. Saturation gradients at equilibrium for 350 μm glass beads-toluene. Capillary rise: class IIb (▽), class Ia (+). Drainage: class IIb (o, x), class Ia (Δ).

In Fig 2.15 saturation gradients after capillary rise and drainage are depicted for toluene - glass beads, which combination shows both Ia and IIb behaviour. In general the form of the saturation gradient after capillary rise or drainage for Ia systems and after drainage for IIb systems is the same.[10]

2.4. Statement of the problem

From the contents of section 2.3 it follows that there are two problems: (i) presence or absence of a saturation gradient and (ii) rapid or slow capillary rise. These two bipartitions give rise to four classes of phenomena. The fact that all four possibilities occur supports the hypothesis that the two problems are not directly related. More precisely the problems can be formulated as follows.

PROBLEM I (regarding the statics of capillary rise in homogeneous packings of rotund particles): *What is the reason that in some experiments a saturation gradient (much wider than 10d) is observed, while in other experiments, not necessarily with other solid-liquid combinations, such a gradient is not observed.*

---

10. The almost absent saturation gradient found for 3n14td is the exception, but not due to some error. Experiment $3f_e^1 12td$ (also class IIb) yielded a saturation gradient of 0.7 cm. All other drainage experiments that were carried out with 350 μm particles (about 30) yielded a gradient of at least 2 cm.

PROBLEM II (regarding the dynamics of the sharp, rising, liquid front during capillary rise in homogeneous packings of rotund particles): *What is the reason that in some experiments the capillary rise velocity decreases linearly with the inverse height, which, according to the classical theory, one would expect, while in other experiments, not necessarily with other solid-liquid combinations, the rise velocity decreases much more slowly.*

Problem I is dealt with in chapter 5 and problem II in chapter 4. In chapter 3 a number of refuted or non-confirmed hypotheses are discussed. The following remarks further define the subject of the subsequent chapters.

(i) In general there were no problems in classifying the experimental results. Either a saturation gradient was not obeserved, or a saturation gradient was observed with a width of at least a third of the equilibrium height. Either eq (1.33) was obeyed or there were large deviations. Although the experiments cover a broad range of liquids and solid phases, it is of course possible that for certain systems there is a much more gradual change from one kind of behaviour to another. In fact, the solutions offered in chapters 4 and 5 predict such a gradual change. For reasons of clarity most of the subsequent considerations are however couched in terms that presuppose a sharp distinction between the four classes.

(ii) It is almost trivial to remark that the properties of the solid surface and its interaction with the liquid, especially at the three-phase line, will be relevant to the explanation of the observed phenomena. It should, however, be noted that we are not concerned with differences in the quantity of capillary rise but with differences in the nature of capillary rise. Further, problem I might suggest the existence of two different mechanisms of capillary rise, and problem II might suggest that other transport phenomena intervene. However, the suggestions could be interchanged as well. Therefore it is not immediately clear in what way, if any, different surface properties would cause different phenomena.

(iii) The problems have been stated in qualitative terms. The discussion in the following chapters is restricted to possible transport mechanisms, and not, in general, concerned with their quantitative description. This implies, among other things, that

we do not here consider the kinetics of the developing saturation gradient, nor its detailed form, but are only concerned with explaining the presence or absence of a gradient. Likewise, we do not discuss the kinetics of Ib/IIb behaviour but only possible explanations of the failure of eq (1.33).

(iv) Again, the discussion is restricted to homogeneous monodisperse porous media. For inhomogeneous porous media or solid phases that display no homogeneous wettability, and probably also for very irregular porespaces, a saturation gradient will always be present, usually from the very first moments of capillary rise.

(v) The existence of the two problems has not been reported as such in the literature. Nevertheless, the problems, in particular problem II, could have been recognized long ago, given the experimental data reported. There are several reasons that explain that this did not happen. These will not be discussed here.

(vi) The existence of the two problems has several consequences, e g for the techniques using capillary rise to determine physical constants, such as the contact angle. This aspect will be discussed elsewhere.

(vii) On earlier presentations of the two problems we have occasionally met strong scepticism with regard to their existence. For example it was said that inhomogeneous media would give saturation gradients while homogeneous media should not give a saturation gradient; or that air entrapment might strongly reduce the capillary rise velocity. For this and other reasons we discuss a number of possible errors, secondary phenomena, and such like in some detail in the next chapter.

CHAPTER 3

REFUTED AND NON-CONFIRMED HYPOTHESES

3.1. Introduction

In this chapter more details are given concerning the systems that display a certain class behaviour. This information is couched in a discussion of several secondary phenomena that might cause apparent anomalous behaviour. As said before, the existence of the two problems in capillary rise can be doubted by invoking ad hoc hypotheses, mostly to the effect that the solution of some experimental problem would resolve the problem.[1] This is one of the reasons that a number of possible secondary phenomena will be discussed in some detail, although, in almost any case, the rejoinder, to the contention that a parameter beyond control causes the class behaviour, is that a large number of experiments have been carried out under more or less identical circumstances and that it is highly improbable that the results fall apart into four classes without, in general, any intermediate cases, or showing different behaviour for identical systems.

On the other hand, the data reported in this chapter provide further insight in the phenomena as such, as well as the raw material the hypotheses presented in the next chapters have to fit. In the sections that follow, we discuss possible disturbances caused by inhomogeneous porous media (section 3.2), the properties of the solid surface (section 3.3), the displaced phase (section 3.4), and transport phenomena of the wetting phase other than capillary rise (section 3.5). In section 3.6 experiments with counter-pressure are discussed, the results of which bear upon several of the points mentioned before.

3.2. Homogeneity of the porous medium

Alle experiments were performed with porous media made out of sieve fractions. Because the same sieve fractions of the same particles

1. It may be of interest to note that from discussions regaring problem I it has appeared that some think that a saturation gradient at equilibrium is the normal case, while others consider the absence of the gradient as normal.

come under different classes, the size distribution is not a relevant parameter. Of course, a narrow sieve fraction may yield a less wide saturation gradient, if such a gradient is present, but that is not our main concern here.

The homogeneity of all porous media, except those of high-density glass and copper, was checked by means of X-ray absorption. Homogeneous media display a scatter in $\varepsilon(h)$ of 0.1-0.4 % absolute. See [318] for details and examples of $\varepsilon(h)$. No correlation exists between homogeneity and class behaviour. Stronly inhomogeneous media, no matter of which class, yield an inhomogeneous saturation gradient, which is easily distinguished from a Ia saturation gradient.

Each particle packing in a vessel has higher porosities at the wall than in the bulk of the packing, the influence of which, on the moving liquid front, is negligible. Visual measurements at the wall and X-ray measurements yield identical results (within 0.5 mm), provided the wettability of the wall is not much different from that of the solid phase. In the visual measurements the top of the liquid front is observed, as appears when a saturation gradient develops. An example is given in Fig 3.1. With some experience visual estimates of the width of the saturation gradient are reasonably possible.

The wetting process might disturb the particle packing (cf consolidation of a filter cake). For this reason experiments were also carried out with porous media consisting of sintered glass beads. The sintering produces a porous medium in which the particles

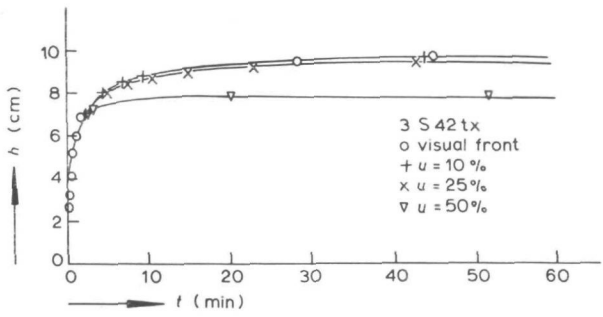

Fig 3.1. Capillary rise of toluene in 360 µm sand (class Ia). Comparion of visual and X-ray absorption measurement.

are definitely fixed relative to each other, but without significant deformation of the particles. No correlation was found between sintering and class behaviour.

A second reason to perform experiments with sintered packings is the possible influence of the supporting filter, necessary for non-sintered packings. Experiments were carried out with fine filters (Jena P4), with coarse filters (Jena P0), with home-made filters consisting of the same spheres as the non-sintered packing, and with completely sintered media. No influence of air (entrapment) below, in, or just above, the filter could be detected. The fine filter has a rather strong influence on the resistance to flow at low heights (high velocities). This causes a concave part in the dh/dt vs $1/h$ curve (cf Fig 2.13). Most experiments were performed with a coarse filter. This filter still causes a small extra resistance observable at high rise velocities. This is apparent form Table 3.1, in which k is given, as calculated from eq (1.23), and as obtained by extrapolation from the straight (part of the) dh/dt vs $1/h$ line at low heigths. It can be seen that for d = 350 μm and water or toluene as the wetting liquid the experimental k's lie in a range somewhat below the values predicted by eq (1.23). The range indicated for the theoretical values corresponds to the

TABLE 3.1

Permeability during the first moments of capillary rise (no difference between different classes)

	system solid - liquid	permeability, $k\|_{t\to 0}$ (10^{-4}m/sec)	
		experimental	eq (1.23)
NOT SINTERED	350 μm glass beads - water	1 - 6	7 - 13
	350 μm glass beads - toluene	2 - 11	11 - 16
	325 μm sand - water	1 - 2	5 - 13
	325 μm sand - toluene	1 - 5	8 - 19
	125 μm glass beads - toluene	1 - 3	1 - 3
	325 μm sand - paraffinic oil	0.1 - 0.2	0.1 - 0.3
SINTERED	350 μm glass beads - water	7 - 8	7 - 13
	350 μm glass beads - toluene	11 - 13	11 - 16

width of the sieve fractions. For smaller particles, high viscosity liquids, or sintered porous media, the experimental values lie in the predicted range. The experimental k, as defined above, is not dependent on class behaviour.

3.3. Properties of the solid surface

3.3.1. Surface treatment: sand. The behaviour of sand is rather straightforward when compared with glass (see below). A Ia behaviour is found for toluene (most experiments with non-treated sand), as well as for water when the sand has been subjected to a heat treatment at 250-500 ^{0}C. Contaminated sand displays a non-Ia behaviour with water.

The capillary rise of water was observed in sand rinsed with either pure toluene or acetone, and dried at 80^{0}C. When treated with toluene some sands display IIa, others IIb behaviour. When treated with acetone or mixtures of acetone and toluene, various kinds of complicated behaviour are observed (see section 5.5.2). Sand treated with toluene shows a slow drainage of water (cf Fig 2.11). These results support the hypothesis that Ia vs IIa/IIb behaviour correlates with a difference in the contact angle, θ.[2]

3.3.2. Surface treatment: glass beads. A very large number of experiments were performed with beads of soda-glass (ρ=2.49) and lead-glass (ρ=2.93). Some details of the surface treatments that were applied are given in Table 3.2. On treatments involving HF see also next sub-section. There is no correlation between surface treatment and class behaviour as is clear from Tables 3.3-4. In Table 3.3 classifications given between curved brackets are based on an inference by analogy. For the Ib classifications given between

---

2. Treatment with reagent toluene or acetone may not seem the most elegant way to change θ. It should, however, be noted that (i) There is no way to measure θ on sand, or, for that matter, on any other particulate material, independent of the problem under discussion. See also section 3.3.4 . (ii) Sand does not have a smooth surface. Hence, prediction of θ after a specified treatment is not possible on theoretical grounds (would that ever be possible; cf section 4.3). See also section 3.3.3. (iii) It is of independent interest to know that rinsing with reagent acetone can change the wettability of an oxide surface.

square brackets, the saturation gradient was observed visually only.[3]

TABLE 3.2

Different surface treatments of glass beads

Surface treatment	rinsing	drying
2 - 5 %vol detergent (1 - 24 hr)	water, acetone	air, 75°C
2 - 5 %vol detergent (2 x 1 hr)	water, acetone water	air, 20°C, 600°C vacuum, 50°C
detergent, boiling S-Cr acid (10-60 min)	water, acetone water	air, 75°C air, 75°C vacuum, 50°C
detergent, warm HNO_3 (30-60 min)	water, acetone	air, 75°C
detergent, 5% HF (30-90 min)	water, acetone	air, 75°C
detergent, 5% HF (2x30 min)	water	vacuum, 50°C
detergent, 65% HF (15 min)	water	air, 75°C
vacuum: 180°C, water, NaOH/ alcohol, water S-Cr acid	water water, toluene	pure N_2 (99.998%)

TABLE 3.3

Class behaviour of glass beads after different surface treatments

system	class Ia after treatment with	class Ib after treatment with	class IIb after treatment with
soda glass - water	(none)	(heat)	detergent, HNO_3
lead glass - water		[none], [heat], [detergent]	HF, toluene
soda glass - toluene	(heat), HF	(HNO_3), (HF)	(heat), detergent, S-Cr, HNO_3, HF, (toluene)
lead glass - toluene		[detergent], [HF]	HF, toluene

3. One of the reasons that such a large number of experiments were performed is that, chronologically, the experiments with glass beads were performed first, while it was thought that Ia/IIa behaviour is more natural than IIb (or Ib) behaviour. This also partly explains that we have until now failed to observe an explicit Ib behaviour. All planned attempts (about 15) to discriminate between Ib and IIb behaviour yielded no saturation gradient at equilibrium, but from this it should not be concluded that IIb behaviour occurs more often than Ib (cf section 5.4.3).

In Table 3.4 data are given for the equilibrium height and the driving force at low heights, for capillary rise of toluene in 350 μm soda-glass beads. Different batches (i e as obtained from different factories or from the same factory at different times) are indicated by α, β, ... From the results it is clear that the unknown part of the history of the surface is more important than the average chemical constitution or the surface treatment.[4]

After experiments with water, and often also with toluene, the sodaglass beads were sintered together. Partly for this reason experiments were carried out with glass beads of alumina silicate (ρ=2.8) and a borosilicate (Pyrex; ρ=2.9), because these glasses are assumed to be more inert. With toluene the alumina silicate displayed IIb and the borosilicate Ia behaviour.

3.3.3. Roughness of the surface. Surfaces can be geometrically or energetically inhomogeneous [340]. Although the notion of roughness is not particularly clear [341,342], the experimental evidence [342-345] seems to support that for $\theta < 90^0$, θ decreases with increasing roughness, while for $\theta > 90^0$ it increases with roughness. Further, grooves may be present on a rough surface. Capillary rise may take place along these grooves, thus creating a partially wetted surface.

Both these aspects of roughness might explain Ib/IIb behaviour, when this is taken to be the display of an effective contact angle decreasing with time. When we assume the liquid having a finite θ on its adsorbed layer or the solid surface, capillary rise in grooves would decrease the effective θ. And as to the other case: a meniscus might pass through successive metastable states of decreasing θ. That is to say, the capillary rise is governed by the advancing contact angle at the very beginning of rise. Then, the advancing θ slowly changes in the receding θ. This can be a discontinuous process, e g caused by vibrations, or a continuous process. (Mechanisms that might cause the latter are discussed in the next chapter.) However, the experimental results do not sus-

---

4. A second reason (cf preceding note) to do such a lot of experiments with glass beads is that soda- and lead-glass beads are the only wettable spheres available at modest prices and therefore used in many model studies involving transport phenomena in porous media. The results presented in Tables 3.3-4 suggest that glass should be the last material to choose for any study to which surface phenomena are relevant. But, in fact, there are no clear alternatives.

TABLE 3.4

Influence of surface treatment on capillary rise of toluene in 350 μm glass beads

batch	treatment and number of experiments performed	equilibrium height (cm)	$h_c\|_{t\to 0}$ (cm)
	detergent (4)	>5	3.8
soda α	heat (8)	>5	3.2 - 3.8
	HF (11)	class Ia	6.3 - 7.4
	detergent (4)	3.8 - 4	2.8 - 3.2
	S-Cr acid (2)	>3.9	2.3
soda β	HNO_3 (19)	3.9 - 5.2	2.1 - 2.9
	HF (5)	4.1 - 6	
	toluene (1)	4.6	2.4
soda γ	HNO_3 (1)	>5.5	
	HF (6)	> 5	2.5 - 4
soda δ	HF (1)	> 6	3.1
lead α	detergent (10)	>5.5	2.6 - 3.3
lead β	detergent (2)	4.4 - 4.6	2.2 - 2.5
	HF (3)	4.8 - >6.5	2.8

tain a correlation between roughness and Ib/IIb behaviour. Most glass beads display IIb (or Ib) behaviour. Most sands display Ia/IIa behaviour. The same polystyrene yields different behaviour for different liquids.

Etching of a glass surface, e g with HF, would decrease θ for organic liquids [346]. Although two batches of soda-glass (125 μm and 350 μm) displayed Ia behaviour, when treated with HF, it was not possible to reproduce this effect with other batches. All further attempts, with various treatment procedures (cf Table 3.2), to induce a Ia behaviour failed.[5]

5. When HF treated Ia glass beads were retreated with detergent or sulfo-chromic acid, they lost their Ia properties, now showing IIb behaviour. This is not due to general contamination during handling because Ia glass beads kept in open air and dried up to 120°C did not lose their properties. Furthermore, when those retreated glass beads were treated for the second time with HF, in the same way as originally caused a Ia behaviour, the IIb behaviour persisted.

3.4. Presence of displaced phase

In a normal capillary rise experiment the wetting liquid displaces air. The resistance of the air flow is easily shown to be negligible, but the presence of air may have, in principle, several disturbing effects: the entrapment of air might cause an extra resistance to flow, the air might interfere with the formation of a saturation gradient, and the desorption of air might be a rate determining step. However, from the data presented below, it appears that the presence of air does not interfere in any significant way with the capillary rise phenomena.

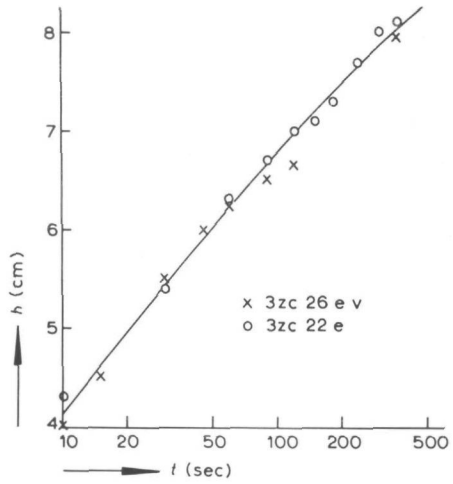

Fig 3.2. Capillary rise of water in 350 μm glass beads (class IIb). Comparison of a measurement at atmospheric and at low pressure.

3.4.1. Experiments at low pressure. Experiments were performed at a pressure equal to the saturated vapour pressure of water plus that of the wetting liquid (when not water).[6] No difference was found between the results of experiments carried out in air and at low pressure. In Fig 3.2, h vs t is given for a IIb system and

6. Experiments with organic liquids in the absence of water have not been performed. To obtain reliable results for such systems, from which water molecules are absent, the experimental problems are enormous. Given the interpretation offered in chapters 4 and 5, water-free inorganic surfaces are expected to yield a Ia behaviour with organic liquids.

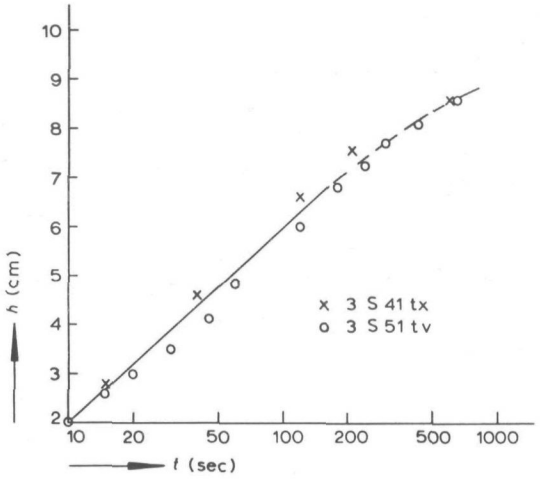

Fig 3.3. Capillary rise of toluene in 360 μm sand (class Ia). Comparison of a measurement at atmospheric and at low pressure.

in Fig 3.3 for a Ia system. In some cases IIb systems tended to rise more rapidly at low pressure, but without losing their IIb behaviour.

3.4.2. Air entrapment. Air entrapment is an often invoked ad hoc hypothesis, although reports that it scarcely influences capillary liquid transport exist [355]. From the data for k, given in Table 3.1, it follows that the air entrapment does not cause a noticeable extra resistance. Because, furthermore, no significant difference was found between experiments in air and at low pressure, no attempt was made to determine the quantity of air entrapment very accurately. After capillary rise or infiltration, air entrapment was found to be in the range of 5-12 % porespace volume. For practical reasons it is the remaining 88-95 % that is defined as u=100%. There were no indications that the amount of air entrapment is a function of the height.[7] See on air entrapment also section 3.6.

7. As to a possible relation between air entrapment and the presence or absence of a saturation gradient, it should further be noted that the entrapped air is surrounded by an isolated meniscus, which is not connected to the meniscus at the liquid front (no matter whether the latter displays a saturation gradient or not).

3.4.3. Continuity in the partly saturated region. For Ia systems the saturation gradient develops so rapidly that we may assume the liquid phase to be continuous. With regard to the continuity of the air phase, experiments were carried out in which a saturation gradient, being at equilibrium, is displaced by raising the level of the free liquid surface. An example is given in Fig 3.4, in which case the free liquid surface was raised 2.5 cm. The saturation gradient is reproduced very well, except that there is 10% air entrapment in the region of complete saturation. This (extra) air entrapment is due to the fact that the moment the free liquid level is raised the liquid in the existing gradient starts moving at all heights; this will cause random enclosures of air.

A discontinuous air phase has to be present in the form of bubbles larger than the narrowest passages in the packing. In particular when $\theta=0$, they cannot leave the packing in any intelligible way (except for the, very slow, diffusion via the liquid phase). We may therefore conclude that the air phase in the region of the saturation gradient is continuous.

3.5. Secondary transport phenomena of the wetting phase

3.5.1. Evaporation. Liquid will evaporate from the rising meniscus to the atmosphere (because the experiments are not performed in a saturated atmosphere). This implies that the equilibria reported for IIb systems (cf Table 2.3) are not true equilibria. But, of course, evaporation cannot explain why the different classes of behaviour exist.[8]

---

8. If we assume $p_v \simeq p_s$ at the liquid front and $p_v \simeq 0$ at the top of the porous medium, calculation shows that for water as well as toluene the evaporation, expressed in terms of the velocity of the rising front, is of the order of 0.5 mm/day. Although for class IIb much lower rise velocities are observed before equilibrium is reached, we may assume that also in IIb systems the liquid is transported to the liquid front by means of a hydrostatic pressure difference. For $d \simeq 300$ μm the pressure difference to supply the evaporating liquid is of the order of 1 μm liquid height. Because this pressure difference is much smaller than the particle size it is highly improbable that the evaporation flux from the meniscus surface interferes with any mechanism that might explain IIb behaviour. See for evaporation from adsorbed films section 4.8.5.

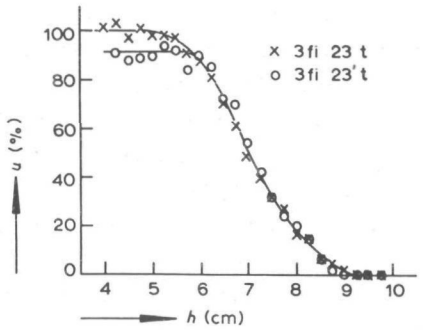

Fig 3.4. Saturation gradient after capillary rise of toluene in 350 μm glass beads (class Ia). The same after raising the free liquid surface 2.5 cm.

A small number of experiments were performed with IIb systems in an atmosphere almost saturated with the wetting liquid. Before the experiment was started the porous medium was kept in this atmosphere for a few days. No difference in behaviour was observed.

3.5.2. Capillary condensation. In the preceding considerations it was assumed that the capillary rise in a porous medium reaches (hydrodynamic) equilibrium by transport of the (bulk) liquid phase alone. If we consider thermodynamic equilibrium capillary condensation has to be taken into account.

Above a wetting front in a porous medium, capillary condensation will occur at the contact-points of the particles, thus forming pendular rings. It is possible that the pendular rings formed just above the continuous meniscus (of the bulk liquid front) make contact with the latter. This might cause a more favourable curvature for the continuous meniscus, which then rises about one particle diameter, after which the process repeats itself. The possibility of this mechanism was first proposed by Smith in 1933 [193]. Such a mechanism might explain the formation of a saturation gradient in case hydrodynamic capillary rise would yield no gradient. The formation of a Ia saturation gradient, however, takes place too rapidly to be ascribed to vapour transfer to pendular rings.

Capillary condensation seems more probable for the explanation of Ib/IIb behaviour. It explains that the rise velocity decreases strongly with the height: the higher the front rises, the larger

the pendular rings have to be to make contact with the continuous meniscus. On the other hand, if this hypothesis is true, the existence of class Ia and, in particular, class IIa is difficult to understand.

From analyses of the above mechanism [216,347], though based on uncorrect assumptions regarding the curvature of the continuous meniscus, it appears that the assumption of thermodynamic equilibrium would, indeed, predict a IIb (or more probably Ib) behaviour. The kinetics of this mechanism are difficult to evaluate. Capillary condensation in pendular rings just above the continuous meniscus is only possible as long as the curvature of the rings is lower than that of the continuous meniscus. If we assume that the air is saturated with the liquid vapour, calculation shows that the diffusion flux from the continuous meniscus to the pendular rings (being on a distance of about 0.03-0.3 d and extending from the contact point also 0.03-0.3 d) could well have the right order of magnitude to account for a IIb behaviour. However, because the experiments are not carried out in a saturated atmosphere, the vapour pressure on the place of the necessary pendular rings is already significantly lower. Typical calculations then give a maximum extension from the contact point of $0.02d$, which, being an upper boundary, seems much too low to help forward the continuous meniscus. Moreover, experiments with water containing 1 mol salinity did not show a behaviour different from that for double distilled water. If we may assume that the water condensed in pendular rings is virtually free from salinity this excludes significant capillary condensation.

The above more theoretical considerations, together with the existence of class IIb *and* IIa for the same systems under identical conditions, lead to the conclusion that, according to the classical theory, capillary condensation has no influence on class behaviour.

3.5.3. Condensation of anomalous liquids. There is an extensive literature on the properties of so-called anomalous water (and other liquids containing OH-groups), sometimes present in the neighbourhood of polar surfaces. See for ample references [103, 104]. Even older are the reported deviations from the Kelvin equation, eq (1.12), recently reported again [348] for toluene in glass capillaries, in which case the existence of anomalous toluene has been hypothesized. The evidence for the hypothesis that at

least part of these anomalous phenomena can be ascribed to very high concentrations in the liquid of material from the solid surface or other sources, is becoming more and more convincing [349-351]. This would explain, inter alia, the reported condensation at vapour pressures much below saturation (e g [352,353]). If the latter takes place above the wetting liquid front the arguments against capillary condensation, given in the preceding sub-section, have to be abandoned. Moreover, the systems that display IIb behaviour are more or less comparable to those for which anomalous condensation has been observed.

Because anomalous condensation of water and toluene in glass or quartz capillaries has been reported most often, experiments were performed to test this hypothesis with respect to our porous media. A small sintered porous medium of 150 μm glass beads was placed in a saturated atmosphere at constant temperature.[9] The kinetics of capillary condensation yielded the correct order of magnitude, assuming a driving force obtained by means of the Kelvin equation. We therefore conclude that anomalous condensation is not the explanation for the occurrence of class IIb.[10]

3.6. Experiments with counter-pressure

For IIb systems experiments were carried out in which the gas pressure above the meniscus front and above the free liquid surface is not equal, from a moment just after the commencement of capillary rise ($t \simeq 2$ sec). At $t < 0$ air is flowing through the porous medium. There were no indications that this complicated situation around $t=0$ has any influence on the results for $t > 5$ sec. For capillary rise under these conditions eq (1.33) transforms to

$$\epsilon \frac{dh}{dt} = \frac{k}{h}(h_c - \Delta P - h)$$

where ΔP is the counter-pressure, i e the pressure difference as described above.

---

9. More important than the constant temperature is the absence of temperature gradients. The latter were estimated to be below 0.002 K/cm.
10. The experiments were performed by Mr P.C. Steyne. Many special provisions are necessary to obtain reliable results. The details of the experimental procedure and other connected results (amongst these a probable solution to the reported [4,354] anomalous phenomenon that saturated macroporous media lose liquid in a saturated atmosphere) will be reported elsewhere.

TABLE 3.5

Comparison of experiments with and without counterpressure (experiments 3zc2e; capillary rise of water in 350 μm glass beads)

without counterpressure		with counterpressure		
h_c (cm)	k (10^{-4} m/sec)	h_c (cm)	k (10^{-4} m/sec)	ΔP (cm)
7	7.6	7.8	1.9	2
		7.5	1.5	3
7.3	2.7	7.6	1.1	4
8.7	0.76	8.9	0.27	3
9.1	0.11	10.3	0.08	6.5
		10.7	0.04	4
		11	0.012	7.4

In Table 3.5 an example is given of the results in a normal experiment and the results at different counter-pressures. This comparison is made by taking the slope of the dh/dt vs $1/h$ curve at different points and to characterize it by an apparent k and an apparent h_c. As can be seen, the capillary rise behaviour does not depend on the length of porous medium filled with liquid, h, but solely on the pressure difference between the two liquid levels, h_c-ΔP-h. From this it follows that the mechanism responsible for IIb behaviour is only dependent on the situation in the direct surroundings of the three-phase line and not on the previous history of the capillary rise, the situation in the saturated part of the porous medium (which excludes the influence of air entrapment), or unknown transport phenomena taking place over long distances (e g long distance diffusion of solutes in the liquid).

3.7. Conclusions

The experimental data presented in this chapter lead to the following conclusions, which are mostly to the effect that there is no empirical correlation between class behaviour and some other variable.

(i) There is no correlation between class behaviour and the properties of the porespace geometry; in particular the following parameters and potential disturbing factors do not influence class

behaviour: particle size, sieve fraction, porosity distribution of the packing, disturbance of the packing at the wall, disturbance of the packing by the wetting process, influence of the supporting filter.

(ii) Both capillary rise and non-capillary liquid transport in porous media follow the Kozeny equation, eq (1.23).

(iii) There is a correlation between class behaviour and surface treatment for the system sand-water. This suggests the hypothesis that a saturation gradient is observed when the contact angle is zero or almost zero and that no saturation gradient is observed when the contact angle is above some critical value.

(iv) For soda- and lead-glass beads there is no correlation between class behaviour and surface treatment. In particular there is no correlation between class behaviour and etching of the surface.

(v) There is no correlation between class behaviour and phenomena involving the presence of the displaced phase (air). When a saturation gradient is present both the liquid and the displaced phase are continuous.

(vi) Evaporation of the wetting liquid may cause an apparent equilibrium for systems that reach equilibrium relatively slow, but it does not interfere with class behaviour.

(vii) Class behaviour cannot be explained with reference to capillary condensation of either normal or anomalous liquid.

(viii) The mechanism responsible for the occurrence of relatively slow capillary rise is dependent only on the situation in the direct surroundings of the three-phase line.

CHAPTER 4

CONTACT ANGLE AND CAPILLARY RISE

4.1. Introduction

This chapter and the next treat the relation between the mechanism of capillary rise and the contact angle. There are two hypotheses:

(i) A wide saturation gradient at equilibrium after capillary rise, as observed for class Ia, corresponds to a contact angle of about zero. The absence of a saturation gradient, as observed for class IIa and IIb, corresponds to a contact angle larger than some critical value.[1]

(ii) The relatively slow capillary rise, as observed for class IIb (and Ib), is caused by the fact that the contact angle decreases during capillary rise.

The first part of the present chapter is devoted to the possibility of a priori estimation of the contact angle. Partly because the contact angle cannot often be determined experimentally. Partly because some systems apparently display a contact angle larger than zero in cases for which this would not be expected (e g glass-hexane).

The interpretation of hypothesis (i) is the subject of chapter 5. Possible mechanisms that might explain hypothesis (ii) are discussed in the second part of the present chapter.

4.2. Contact angle of IIa and IIb systems: Introduction

4.2.1. General remarks. If it is assumed that the porespace configuration and the surface tension, γ_{LV}, are the same, any difference in class behaviour has to be ascribed to a difference in θ. We have noted in chapter 2 that the equilibrium heights of systems that come under both class Ia and IIa or IIb, are always higher for the Ia case. Further, in section 3.3.1, we have noted that the combination sand-water changes its Ia into IIa or IIb behaviour when the sand is deliberately contaminated. On this basis it seems reasonable to suppose that for class Ia, $\theta \simeq 0$, and that for classes IIa/IIb, θ is above some critical value. It is, however, not an easy matter to prove this hypothesis because there is no method to determine the

1. See sections 1.9.1 and 2.3 for the meaning of "saturation gradient".

contact angle of particles independent of the subject under investigation.

Secondly, many systems display IIa or IIb behaviour, while it is not at all clear why they should have $\theta > 0$. In this section some basic equations and concepts are introduced. In the next section indirect methods to calculate θ are discussed. This knowledge is then applied to the principal systems studied in sections 4.4-6.

4.2.2. The Young-Dupré equation. When γ_{LV}, γ_{SV}, γ_{SL}, and γ_S are the surface tensions for the interfaces liquid-vapour, solid-vapour, solid-liquid, and solid-vacuum, respectively, and π is the film pressure (in Gibbs' terminology the superficial surface tension) we have:

$$\gamma_{LV} \cos\theta = \gamma_{SV} - \gamma_{SL} \tag{4.1}$$

$$\pi_{SV} \equiv \gamma_S - \gamma_{SV} \tag{4.2a}$$

$$\pi_{SL} \equiv \gamma_S - \gamma_{SL} \tag{4.2b}$$

$$\gamma_{LV} \cos\theta = \pi_{SL} - \pi_{SV} \tag{4.3}$$

There is some controversy as to the validity of eq (4.1), in which we will not enter [R361]. It is, however, of importance to note that γ is, in general, not equal to the surface free energy [362,363].

4.2.3. The Gibbs equation. For a system at equilibrium consisting of an inert solid phase and a one component vapour, which adsorbs on the solid surface, Gibbs' adsorption equation can be written as [cf [364], eq (5.39)]:

$$\left(\frac{\partial\gamma}{\partial\mu'}\right)_T = -\Gamma \tag{4.4}$$

where Γ is the surface concentration (mol/cm^2) and μ' is the chemical potential per mol. This provides the possibility of calculating π_{SV} from a measured adsorption isotherm [365]:

$$\pi_{SV} = kT \int_0^{\Gamma} \Gamma \, d(\ln p_v) \tag{4.5}$$

It should be noted that the integration is not straightforward because of the uncertainty in the region $\Gamma \approx 0$ [366].

4.2.4. The disjoining pressure. This concept has been introduced by Deryagin [R104,R367]. Its status is not altogether clear [76]. We will define the disjoining pressure in terms of the chemical potential per unit volume of adsorbed film, μ. With ℓ the thickness of the film (defined for molecular as well as for thick films) eq (3.3) can be written as:

$$\left(\frac{\partial \gamma}{\partial \mu}\right)_T = -\ell \tag{4.6}$$

Using the boundary condition

$$\ell \to \infty \qquad \gamma_{SV}(\ell) \to \gamma_{SL} + \gamma_{LV} \tag{4.7}$$

integration of eq (4.6) yields [368]:

$$\gamma_{SV}(\ell) = \gamma_{SL} + \gamma_{LV} + \int_{\ell}^{\infty} \ell \frac{d\mu}{d\ell}\, d\ell \tag{4.8}$$

The disjoining pressure, p_d, can then be defined as

$$p_d \equiv \ell \frac{d\mu}{d\ell} \tag{4.9}$$

The reason to introduce the concept of a pressure is (i) the analogy with the capillary pressure, p_c, both obeying a Kelvin equation, and (ii) the mechanical model for the stability of thick films, seen as a disjoining pressure counterbalancing the hydrostatic forces tending to diminish the filmthickness.

The more basic parameter μ is a complicated function of ℓ. It contains contributions of (i) van der Waals forces, (ii) specific long-range interactions, such as caused by structured multilayers, and (iii) electrostatic repulsion in electric double layers. The film is thermodynamically stable if

$$\left(\frac{\partial \mu}{\partial \ell}\right)_T > 0 \tag{4.10}$$

If p_d is positive for all ℓ, we have a duplex film and $\theta=0$ for all values of ℓ. If $\theta < 0$ there is a region of unstable film thicknesses, for which p_d is negative. This implies that

$$\mu(\ell) = \frac{kT}{\ell} \ln Q \tag{4.11}$$

stating the equilibrium between the film and the vapour phase, is satisfied by more than one value of ℓ for some Q [368] ($Q \equiv p_v/p_s$).

4.3. Indirect methods of calculating θ

4.3.1. Critical surface tension. Zisman introduced (i) the distinction between low- and high-energy surfaces, for pure solids corresponding to low- and high-melting solids, and (ii) the critical surface tension, γ_c, as a characterizing parameter of low energy surfaces [R369,R370]. It appears that for low-energy solids (such as polystyrene) there exists a linear relationship between $\cos\theta$ and γ_{LV} for members of a homologous series. The intersection of this line and $\cos\theta = 1$ is γ_c. Hence, with b a constant,

$$\begin{aligned} \cos\theta &= 1 + b(\gamma_c - \gamma_{LV}) && \gamma_{LV} > \gamma_c \\ \cos\theta &= 1 && \gamma_{LV} < \gamma_c \end{aligned} \qquad (4.12)$$

Moreover, it appears that different homologous series yield about the same γ_c and b. Therefore it was proposed to consider γ_c as an empirical parameter characterizing the surface. For polystyrene γ_c=33 [371]. (All values for surface tensions and film pressures given in this chapter are in dynes/cm.) This method gives the possibility of estimating θ for a liquid on a low-energy surface when some values of θ for other liquids on the same surface are known.

4.3.2. Calculation from the work of adhesion. Eq (4.2) can be rewritten as

$$\cos\theta = 1 - \frac{\pi_{SV}}{\gamma_{LV}} + \frac{W_A}{\gamma_{LV}} \qquad (4.13)$$

where W_A, the work of adhesion, is given by

$$W_A = \gamma_L + \gamma_S - \gamma_{SL} \qquad (4.14)$$

The work of adhesion contains various kinds of interactions: van der Waals, H-bonding, π-bonding, electric double layers. Good and Girifalco suggested [372,373]:

$$W_A = 2\Phi\sqrt{\gamma_S\gamma_L} \qquad (4.15)$$

There is, however, some controversy about the meaning of the term Φ [374,375] and we still need the values of Φ and γ_S for a calculation of θ, assuming that γ_{LV} and π_{SV} pose no problems.

In case only dispersion forces act, Fowkes [376,377] obtained (summing the dispersion energies between the atoms on the basis of London's theory):

$$W_A^d = 2\sqrt{\gamma_S^d \gamma_L^d} \tag{4.16}$$

where the superscripts d indicate the contribution of the dispersion forces to the parameter concerned and hence

$$\cos\theta \approx -1 - \frac{\pi_{SV}}{\gamma_{LV}} + 2\,\frac{\sqrt{\gamma_S^d \gamma_L^d}}{\gamma_L} \tag{4.17}$$

Values of π_{SV}, γ_{LV}, γ_S^d, and γ_L^d can, in principle, be measured or calculated from first principles [377-379]. Some values, relevant to the systems studied here, are given in Table 4.1. However, eq (4.17) is only valid when there are no adsorbed films (i e $\pi_{SV} \simeq 0$) [375,380]. More strict derivations, in terms of Hamaker constants, have been given [368,380], but this approach as yet does not give a possibility of a priori calculation of θ for a certain system. It is, however, of importance that these derivations [related to the specification of the function $\mu(\ell)$] have shown that finite values of θ are possible for a bulk liquid on its own adsorbed film, also in the case that only dispersion forces operate [368,380,381]. It may be noted that there is nothing strange to a liquid having a

TABLE 4.1

Some values of the vanderWaals contribution to the solid surface tension

system	γ_S^d	γ_L^d	reference
polystyrene	44		[378]
copper-heptane	60	20	[458]
silica-heptane	78	20	[451]
silica-water	123	22	[378,459]
hydrated silica	22-30		[377]

finite θ and π_{SV}. Physically the molecules in the film may have a solid phase induced orientation, which gives the film a structure strongly different from the bulk liquid.

4.3.3. Calculation from adsorption isotherms. When $\theta > 0$ the bulk liquid coexists with an adsorbed film of finite thickness. This implies that the adsorption isotherm intersects the Q=1 axis one or more times. This was probably realized for the first time by Freundlich in 1922 [382].

Combination of eqs (4.1), (4.8), and (4.11) gives

$$\gamma_{LV}(\cos\theta - 1) = kT \int_{\Gamma=\Gamma_0}^{\infty} \Gamma \, d(\ln p_v) \qquad (4.18)$$

where Γ_0 is the lowest surface concentration for Q=1. (Eq (4.18) can also be obtained from eq (4.4) using the appropriate boundary conditions.) Adamson [383] discusses the possibility of making reasonable assumptions regarding the mathematical form of $\Gamma(Q)$, or, what is in fact the same, $\mu(\ell)$. Although one may dispute the reliability of applying parameters, obtained by curve-fitting over the region Q=0.8 to Q=0.98, to the region $\Gamma=\Gamma_0$ to $\Gamma=\infty$, the application of eq (4.18) to availbale data gives the right order of magnitude for $\gamma_{LV}(\cos\theta - 1)$. Hence, it would be possible to calculate θ from measured adsorption isotherms.

4.4. Contact angles on polystyrene.

In Table 4.2 values of θ are given for several C-H low-energy surfaces and different organic liquids. The data given for polyethene support the view that for low-energy surfaces reproducible values of θ are found, which is, in general, not the case for high-energy surfaces.

In Table 4.3 some results are given of the experiments performed with polystyrene spheres. To compare the data, we introduce the parameter Λ (cf section 5.1.2),

$$\Lambda \equiv \frac{4\gamma_{LV}}{\rho g h_c d} \qquad (4.19)$$

The estimated values for θ are obtained from eq (4.12) and by interpolation on the continuous curve of $\cos\theta$ vs γ_{LV}, both constructed from the data for polystyrene in Table 4.2. Although

TABLE 4.2

Contact angles on polymer surfaces

liquid	γ_{LV}	contact angle, θ			
		polystyrene [371,384]	polyethene [385]	polyethene [387]	naphtalene, anthracene [386]
water	73	91	94	94	94
glycerol	63	80	79		79
formamide	58	74	77	77	73
glycol	48			61	63
methylene iodide	51	35	52		
α-bromonaphtalene	45	15	35	34	
benzene/toluene	28		<5		
octane/hexane	18-22		0		

TABLE 4.3

Class behaviour and contact angle for polystyrene (γ_c = 33)

liquid	γ_{LV}	θ	Λ	class
water	73	91	no capillary rise	
formamide	58	74	no capillary rise	
methylene iodide	51	35	pstyr dissolves	
α-bromonaphtalene	45	15	pstyr dissolves	
glycol	48	25-50	3.1	IIa
nitromethane	37	10-25	2.1	IIb
acetonitril	29	0	0.5-0.6	Ib
ethanol	23	0	0.4-0.6	Ia
heptane	20	0	0.4-0.6	Ia

there is, of course, some doubt as to the estimates of θ, the correlation between θ and Λ is so good that it seems certain that Ia/Ib behaviour corresponds to $\theta \simeq 0$ and IIa/IIb behaviour to $\theta >$ 10-25 degrees.[2] From Table 4.3 it can further be concluded

2. Both methylene iodide and α-bromonaphtalene dissolve the polystyrene to an extent that no reliable data can be obtained. The data for acetonitril are uncertain because it slowly dissolves the polystyrene, thus blocking any further capillary rise. The data given are based on an experiment in which there is a layer of silicagel below the polystyrene packing.

that there is no capillary rise when θ is above some value between 50^0 and 70^0.[3]

4.5. Contact angle glass-water

For a long time it has been known that water on glass, in general, shows a finite θ [176,193,357,389-392]. (In this and the next sections it is always the advancing contact angle that is discussed.) To explain this there are roughly two possibilities: contamination of the surface or an aggregated adsorbed phase. Certainly contamination cannot be excluded. It is virtually impossible to obtain water that is free of impurities of some sort [393], the atmosphere is contaminated with oil, and severe cleaning methods seem to result more often than not in higher, less reproducible, contact angles [389]. There are, however, several reasons that make the contamination hypothesis improbable, when reasonable precautions are taken to avoid contaminations.

(i) We find $\theta>0$ for untreated sand and water (i e class IIb). Sand, yielding $\theta=0$ for water, gives $\theta>0$ after rinsing with reagent toluene or acetone. Hence the surface is easily contaminated. However, when the sand is heated at 600^0C, it yields $\theta=0$ with normally distilled water, whereas no special precautions are taken to exclude contact between the sand and atmospheric air. Again, the cases in which $\theta=0$ has been reported for glass-water do not seem to be more careful experiments than those in which $\theta\neq0$. Therefore, to explain that some glasses never yield $\theta=0$ by referring to contamination, one has to invoke the ad hoc hypothesis that some glasses are more sensitive to contamination than others.

(ii) In all cases in which a finite advancing contact angle is reported for capillary rise in cylinders, the receding contact angle is zero. One may wonder why, in case it is assumed that the (hydrated) glass is contaminated easily, this does not happen to the liquid-vapour interface.

(iii) It is an often reported fact that, in general, heating of glass or silica results in an increase in θ, while boiling in water yields a decrease in θ [176,357,395]. (However, exceptions

3. Cf section 5.5.3. This value should be distinguished from the value of $\theta=73^0$ reported for the wetting cycle in a suction experiment [388], because in the latter case pendular rings are present in the porous medium.

exist [392,396].) The supported explanations for such phenomena, invoking destruction and formation of a silicagel surface layer or irreversible dehydration phenomena [392,395,396,483], their consistency with different pre-treatment procedures, and the reproducibility of surfaces yielding a certain θ, seem to exclude contamination.

(iv) Finite θ's for water on glass have been observed, and ascribed to contamination, in systems in which extreme care had been taken to prevent contamination [397]. This might seem to oppose the above, but the argument may as well be reversed.

Now, as to the possibility of a non-duplex film of water on glass, there is rather strong, though not conclusive, evidence that water can form a multilayer film on glass or silica, and this film has other properties than water. This aggregated phase (Deryagin's α-phase) displays a finite θ to liquid water and can be compared in this respect with ice, which also shows a finite θ to water [R398]. Experimental evidence for the existence of this phase can be found in [399-401,R402]. The thickness of the film would be about 60 Å and the difference is contributed to a difference in the value of the long range interaction forces (cf section 4.2.4).[4] We therefore conclude that the finite θ for the IIb system glass beads - water is not due to contamination, but has to be ascribed to the presence of an aggregated adsorbed film.

4.6. Contact angle glass-toluene/hexane

4.6.1. Introduction. In relation to gas chromatography, the poor wettability of organic liquids on glass surfaces has been recognized for many years [346,412], though not for liquid paraffins, and it is therefore possible that the main cause is autophobicity (see below). Glass is considered to be a high-energy surface. Therefore

4. These aggregated films should be distinguished from the stable thick films (500-2000 Å) of polar liquids above a draining meniscus in a glass or quartz capillary [R367,R381,403,404]. These films are not formed from the vapour phase [405]. There is no agreement as to whether they occur only for θ=0 [406-409]. Above these thick films the above mentioned aggregated films would be present [411]. It is a point of discussion whether the thick films are due to surface tension gradients [367] (i e Marangoni films) or stabilized by an electric double layer [381,397].

one would not expect that liquids such as toluene and hexane display a finite θ on glass. Nevertheless, most experiments with these liquids and glass belong to class IIb.

In what follows we mainly confine ourselves to hexane and toluene and we subsequently discuss: (i) the γ_c of hydrated glass, (ii) autophobicity, (iii) impurities, (iv) calculation of θ using eq (4.17), and (v) arguments for the existence of a non-duplex film.

4.6.2. Critical surface tension of glass. The physically adsorbed water on glass (2-20 monolayers) decreases the surface tension of the solid phase. It is therefore possible that the surface is a low-energy surface for non-polar liquids. In that case it is possible to apply the γ_c approach (cf section 4.3.1). In Table 4.4 the data reported for the γ_c of glass are given. Although there is a large scatter and not all necessary information is available, we may note: (i) There is a significant influence of the cleaning procedure. (ii) For pyrex-toluene we have always found a Ia behaviour ($\gamma_{LV} = 28$). (iii) The reported values of γ_c are too high to expect a finite θ, in particular not for hexane ($\gamma_{LV} = 18$).

TABLE 4.4

Critical surface tension for hydrated glass surfaces

glass	treatment	γ_c	reference
?	?	30	[413]
soda (?)	not modified	19-28	[414]
soda (?)	acid	40-44	[414]
?	?	30-40	[415]
pyrex	acetone	28	[416]
pyrex	S-Cr acid	44	[416]

4.6.3. Autophobic liquids. This concept, which also stems from Zisman [396,417], refers to the fact that polar organic liquids can give an oriented monolayer on a high-energy surface. This monolayer has a γ_c smaller that the γ_{LV} of the liquid; thus a finite θ is observed. Aliphatic alcohols (from C_3 onwards) are typical examples [366,399,410], but it can be expected that all molecules containing a long aliphatic chain and a polar end-group will be autophobic on high-energy surface.

4.6.4. Impurities. Small concentrations (< 0.1 ppm) of, e g , aliphatic amines or monocarboxylic acids present in organic liquids will adsorb on high-energy surfaces and will show a low-energy surface to the wetting liquid [417,418]. However, from the extensive studies of Zisman it follows that all low-energy surfaces, except fluorinated compounds, have $\gamma_c > 22$ [R370] and yield $\theta=0$ for hydrocarbons below nonane [419,420]. The possibility that the reagent toluene we used contains an impurity causing $\gamma_c < 28$ is not to be excluded. On the other hand, there was observed no difference in the IIb (and Ia) behaviour of glass-toluene and glass-hexane.[5]

Furthermore, the experiments with toluene and hexane were reproducible for the same batch of glass and different batches of liquid (in the case of toluene: different suppliers). These two points, together with the fact that the presence of fluorinated contaminants is improbable, leads to the conclusion that it is not very plausible that the IIb behaviour for glass-toluene and glass-hexane is caused by impurities.

4.6.5. Calculation of θ. If we assume that for glass-hexane only dispersion forces are present, we can apply eq (4.17). Assuming for the moment $\pi_{SV}\simeq 0$, we have

$$\cos\theta = -1 + 2\frac{\sqrt{\gamma_S^d \gamma_L^d}}{\gamma_L} \qquad (4.19)$$

For hexane $\gamma_L^d=\gamma_L=18$ and hence a finite θ is predicted when $\gamma_S^d < 18$.[6] For silica, γ_S^d has been reported to be 76, but for one monolayer of water this already decreases to 26.5, and with three monolayers to 22, to be compared with $\gamma_L^d=21.8$ for liquid water [377]. (There is evidence that θ increases with water adsorption on silica [422].) These values are not beyond doubt. For example, other calculations [380] yield for water a γ_L^d between 17.4 and 21.4. Nevertheless, on

---

5. The hexane used is chromatographically pure for more than 99.5 %, and it seems improbable that it contains polar compounds (other than water). Polar traces in reagent alkanes, even after seeping through adsorption columns, have been reported [421], but these impurities may well have come from other sources.

6. This, incidentally, shows that $\gamma_S^d=\gamma_c$, when $\pi_{SV}=0$ and $\gamma_L=\gamma_L^d$ and throws some doubt upon both eq (4.12) and (4.17).

the basis of eq (4.19) we should expect $\theta=0$ for hexane on hydrated glass.[7]

4.6.6. Non-duplex films. The calculation in the preceding subsection are restricted to $\pi_{SV}\simeq 0$. There is a lot of confusion about the question whether the value of π_{SV} is significant for systems that show a finite contact angle[8], but the evidence for the contention that $\pi_{SV} >> 1$ seems to be growing rapidly. It is not until quite recently that it has been realized that there is no a priori connection between θ and π_{SV} [106,366,383,426]. We propose that there is enough evidence, now, to suppose that hydrocarbons can display significant film pressures and contact angles on hydrated surfaces:

(i) Long ago [399,427,430] it was already observed that many organic liquids, inter alia hexane, benzene, and glycol, do not spread on mica in air (glass behaving similar but less reproducible).

(ii) Using the data of [400], and eq (4.18), Adamson [383,428] found finite contact angles for several polar liquids on glass (for which aggregated or autophobic films are much more probable than for hydrocarbons), but also $\theta\simeq 17^0$ for hexane.[9]

(iii) Induced polarization, caused by the electrostatic field of the solid, has been observed for hexane on hydrated-oxidized-metal surfaces [421], as well as for benzene adsorbed on water [423]. There is some H-bonding between benzene or hexane and the surface hydroxyl groups on silica [484]. Clearly the adsorbate does not interact with the adsorbent by dispersion forces only.

(iv) Several organic vapours, among these hexane and toluene, form multilayers (up to four, assuming vertical orientation) on liquid water [R423]. It has been suggested that the lower alkanes

---

7. Two things may be noted in this connection: (i) The γ_S^d for polystyrene has been reported as 44 [377]. Hence polystyrene is wetted much better by hydrocarbons than hydrated surfaces. (ii) It does not follow from the above that toluene should yield $\theta>0$ because $\gamma_S^d < \gamma_L$. Aromatics interact with oxide or water surfaces also via the phenyl ring [379,423,483]. The contribution of the π-bonds to the adhesion forces has been estimated to be 15-20 [378] and this term should be added to W_A.
8. Cf [367,372,373,375,376,395,424,425].
9. Adamson found $\theta=0$ for CCl_4 ($\gamma_{LV}=27$), which shows IIb behaviour as well. However, non-duplex films for CCl_4 seem possible; cf [429].

can form incipient clatherates or hydrates yielding an extensively modified surface [383,431].

(v) Most adsorption isotherms are determined on powders. Therefore conclusions as to multilayers are not possible due to capillary condensation [432]. An exception is [410,426]. Orientated multilayers of the lower alkanes were found on a pentanol layer, adsorbed on an oxidized aluminium surface.

(vi) Also in case only dispersion forces are present, a negative disjoining pressure is, a priori, possible [368,380,381], in particular for very different molecules. A region of negative p_d has been reported for benzene-mercury [433].

4.7. Possible mechanisms causing IIb behaviour

4.7.1. Introduction. In chapter 3 it has been shown that the mechanism causing IIb behaviour is influenced only by the situation in the surroundings of the three-phase line. Then there remain three possible sources for IIb behaviour: increasing γ_{LV}, decreasing effective meniscus circumference, decreasing θ. The first two possibilities are discarded in the two following sub-sections.

4.7.2. Increasing liquid surface tension. The equilibrium height for IIb systems is about twice $h_c|_{t\to 0}$ (cf Table 3.4). This excludes the hypothesis that γ_{LV}, the surface tension of the liquid-vapour interface, increases during capillary rise.[10]

4.7.3. Decrease of effective meniscus circumference. It can be imagined that IIb behaviour is caused by the fact that the effective circumference of the meniscus that acts as the driving force decreases during capillary rise. That is to say: at each moment the meniscus moves only at a few points; this has an effect on the curvature at other points, which then come in a favourable position to move; etcetera. In terms of the porespace models this means that the number of tubes in which transport takes place decreases with h, while yet all tubes are filled by the rising front. In terms of eq (1.33) it means that h_c increases and k decreases with h.

This mechanism will not be analyzed in detail because there

10. The slow drainage of water from toluene rinsed sand can be ascribed to a decrease in γ_{LV} caused by impurities (surfactants) moving from the solid-liquid to the solid-vapour interface.

are a number of reasons that make it improbable for the homogeneous media studied.[11]

(i) IIb behaviour has also been observed in cylindrical capillaries for which the above mechanism is not possible (see section 4.8.1).

(ii) The same particle packings show IIa as well as IIb behaviour. This implies that the porespace geometry as such does not induce the mechanism under discussion.

(iii) It seems reasonable to expect that, given a sharp front, the apparent k will not decrease by more than a factor equal to the number of particles in a horizontal layer of the porous medium. For the same reasons one would expect the capillary rise in a packing of smaller particles to take much longer than for large particles. None of these is observed.

(iv) It has often been reported that when $\theta \neq 0$ the liquid front in a capillary [355,356], or a particle packing [96,357], moves irregularly, jumping from one point to another. This, however, does not support the mechanism under discussion. In the case of capillaries the effect is only observed when $\theta \neq 0$, and will be caused by a surface that is energetically or geometrically inhomogeneous. In the case of a particle packing the microscopic movement is irregular for the same reason as it is in tubes with constrictions (cf Fig 1.2, models *151*).

4.8. Decreasing contact angles

4.8.1. General remarks. In this section mechanisms are discussed that might explain a decrease of θ with h. In the next section this knowledge is applied to the systems that show IIb behaviour. No convincing explanation for the decrease in θ is always possible. It should however be noted that the experimental fact that θ can decrease during capillary rise is not in doubt: IIb behaviour has been observed in cylindrical glass capillaries with several liquids.[12]

---

11. It is expected that the mechanism does play a role in the wetting of strongly heterogeneous porous media (also in the sense of not being homogeneously wettable) and during the formation of a saturation gradient.

12. For octanol [434], di-*n*-butyl phtalate [356] and water [390]. For glass-water we too observed IIb behaviour (r = 0.15 mm; equilibrium time about 200 hr). Attempts to obtain a IIb behaviour for glass-toluene failed because in all cases $\theta \simeq 0$.

According to eq (4.3), assuming γ_{LV} to be constant (cf section 4.7.2), a decrease in θ corresponds to an increase in $\pi_{SL}-\pi_{SV}$. We will not attempt to describe the mechanisms below in terms of surface tensions or film pressures, nor will we attempt to justify the thermodynamic possibility of these mechanisms, because the meaning of γ_S, γ_{SL}, and γ_{SV}, and to a less extent π_{SL} and π_{SV}, is obscure for an inert surface and a pure liquid, not to mention the systems under discussion.

4.8.2. Liquid penetrates solid or film. Probably this is the most common cause when hydrocarbon surfaces show a decrease of θ with time [435]. It would also explain the hysteresis in θ [436]. Penetration of water in polymer surfaces is well-known [437-439]. And the same phenomena occur when a high-energy surface has been covered with a monolayer of a polar compound changing the surface in a paraffin-like [421]. Small alkane molecules penetrate between C-H chains, and probably all small molecules will do this [370,420].

4.8.3. Dissolving surface. For high-energy surfaces the ζ-potential or surface potential or contact potential will influence the surface tensions and hence θ [397,440]. From the phenomena observed with model porous electrodes (mostly cylindrical capillaries), which we will not discuss here, it is clear that electrochemical processes occurring at the surface may result in an increase as well as a decrease of θ (see [440-444]). Further, it is well known that the ζ-potential of mineral surfaces depends strongly on the pre-treatment of the surface and, in general, displays a time effect when aged in water [R445]. This should be ascribed to ions going into or out of solution. For example, it has been observed that when hydrated silica is brought into contact with water, hydrated silicon or silanol groups leave the surface and form a double layer [446]. These processes can be very slow.[13]

4.8.4. De- or replacement of adsorbed films. If the solid phase is (partly) covered with an adsorbed film of a surfactant, the latter may move to the other interfaces in the system. This effect, causing a decrease in θ, has been observed, e g , in the wetting of contaminated soils [448]. A general description is difficult, because θ may be a complicated function of the concentrations of the different

13. We may note in this connection that the formation (from the vapour phase) of hydration layers on oxides may take months [447].

surfactants present [449]. Further, it is possible that some adsorbed film just dissolves in the liquid [421,424]. When these phenomena occur, we may expect them to be rather slow. The desorption itself can be a slow process [450]; then diffusion has to take place from the three-phase line.

If a hydrated surface is wetted by an organic liquid, equilibrium between the adsorbed water and the water in solution has to be established. It is expected that this is a rather rapid process and that it will hardly change the surface.

4.8.5. Evaporation from the film. When a meniscus is in equilibrium with an adsorbed film, evaporation can cause a decrease in θ, because the evaporation increases π_{sv} [106,399,482]. However, this mechanism cannot occur during capillary rise.

Evaporation may further cause a change in film properties when there is more than one component present in the film. These effects can be compared with and could be aggravated by the Marangoni phenomena caused by preferential evaporation [452,453], temperature gradients [453,454] and electro-osmotic gradients [442,443,455]. Probably, the phenomena reported by Hardy [456] and Bangham [399,427], concerning the sensitivity of θ to the presence of a second adsorbable compound, fall into this class. Typical examples are that acetic acid does not spread on glass in the (relative) absence of water vapour [456] and that most organic liquids (such as toluene, hexane, glycol) show an increase in θ (on mica) when methanol vapour is added to the system [399].

4.8.6. Film jumps. When liquids display a finite θ on their own adsorbed film there exist two or more (meta)stable film thicknesses at $Q=1$, corresponding to different contact angles. Bangham [399] reports a decrease in θ for a lens of, e g , benzene on mica, when the atmosphere is being supersaturated with this liquid. It is possible that this corresponds to a jump over an unstable part of the function $\mu(\ell)$, passing a region where p_d is negative (cf section 4.2.4). Further it is possible that, during capillary rise, changes in the temperature (or concentration of dissolved compounds) may, temporarily and locally, cause a discontinuous jump of a high-θ film to a low-θ film. (Because porous media, contrary to cylindrical capillaries, display structural hysteresis, rupture of a low-θ film cannot cause a decrease of a certain height of capillary rise.) This mechanism can then sustain a mechanism as described in section 4.7.3.

TABLE 4.5

Possible IIb explaining mechanims

++ most probable mechanism; + possible mechanism; 0 mechanism cannot be excluded; - mechanism is impossible or highly improbable

mechanism	polystyrene	glass - water	glass - polar organic liquids	glass- non-polar organic liquids
surface penetration	++	-	-	-
solution of surface	-	++	0	-
desorption contamination	0	-	-	-
replacement water film	-	-	++	0
evaporation of film	-	-	-	-
change in film constitution	-	+	+	+
film jumps	-	+	0	++

4.9. Interpretation IIb behaviour

4.9.1. Introduction. Because in most cases the mechanism causing a finite θ is not fully understood, any interpretation of IIb behaviour has to be highly speculative. This is amplified by the fact that most mechanisms, described in the preceding section, cannot easily be subjected to experimental test. In Table 4.5 we present a judgement regarding the plausibility of these IIb explaining mechanisms for some of the systems studied. A few remarks for the different groups are given below.

4.9.2. Polystyrene. Heptane and ethanol yield a Ia behaviour. Acetonitril displays a Ib behaviour, but it is possible that this is due to blocking by dissolved polystyrene. Glycol comes under class IIa. Nitromethane belongs to class IIb. It is possible that polar contaminations, of which some are always present on the surface [435,457], interact with nitromethane. The best hypothesis seems penetration of the surface by nitromethane molecules.

4.9.3. Glass-water. We assume that the meniscus is in equilibrium with a non-duplex film and that there is no interference of organic impurities (desorption of contaminants is anyway implausible, because these would decrease γ_{LV}). The most probable mechanism seems solution of the surface. That this happens is not the point, as appears from the fact that after some weeks in water the glass

beads are strongly sintered together, but such media, after being dried, have not lost their IIb behaviour.[14]

4.9.4. Glass-apolar liquids. Replacement of the waterfilm, which might occur for glass and polar liquids, seems improbable for apolar liquids. Experiments were performed with toluene and heptane dried over molecular sieves and with toluene and heptane saturated with water. No difference was found. Assuming that the menisci of toluene and hexane are in equilibrium with a non-duplex film, both a change in film properties by preferential evaporation and the film-jump hypothesis are possible.[15]

4.10. Concluding remarks

The main conclusion of this chapter is that there is a correlation between class behaviour and contact angle. More detailed the considerations of this chapter can be summarized as follows.

(i) For irregular dense rotund particle packings, the occurrence of a wide saturation gradient at equilibrium corresponds to a contact angle approximately equal to zero. A sharp liquid front at equilibrium corresponds to a contact angle above some critical value.[16] The interpretation of this experimental law is the subject of chapter 5.

---

14. In the case of soda glass there is an irreversible decrease of $\theta(h)$ after the first one or two experiments with the same packing. From the third experiment onwards $h(t)$ is reproducible.

15. Paraffin oil - glass beads belongs to class IIa. This may correspond to the absence of a (primary) film in this case [456].

16. The evidence for this conclusion is scattered over chapters 2-5. The conclusion is included here because the experimental results for polystyrene, the only system for which estimates of the contact angle are possible, is considered to be conclusive evidence for this hypothesis. The other evidence includes: (i) The equilibrium height of a system that shows Ia as well as IIa or IIb behaviour is always higher in the Ia case (section 2.3.2). (ii) The system sand-water changes its Ia to IIa or IIb behaviour when the sand surface is deliberately contaminated (section 3.3.1). (iii) All Ia systems yield the same values for Λ_h (section 5.4.2), while the upper boundary of the saturation gradient is equal to the value predicted for $\theta=0$ by the theory offered in chapter 5.

(ii) The system water - glass beads may display a finite contact angle.[17] This can be ascribed to the existence of an aggregated adsorbed water film with other properties than bulk water.

(iii) The systems toluene - glass beads and hexane - glass beads may display a finite contact angle. It is hypothesized that apolar liquids may also form non-bulk-liquid resembling phases on glass surfaces.

(iv) The occurrence of relatively slow capillary rise is due to the fact that during capillary rise the contact angle slowly decreases, thus increasing the curvature of the liquid front. Depending on the nature of the interacting solid-liquid combination a decrease in the contact angle can be ascribed to several of a number of mechanisms such as: liquid penetrates solid surface, surface dissolves, adsorbed film properties change. However, at present more specific conclusions are not possible.

17. It may be noted that this and the following conclusion are not minor conclusions because, if they were not true, this would be conclusive evidence against both conclusions (i) and (iv).

CHAPTER 5

CONCAVE AND ANTICLASTIC MENISCI

5.1. Introduction

5.1.1. General remarks. It has been concluded in chapter 4 that, qualitatively, the presence of a wide saturation gradient after capillary rise corresponds to a contact angle of about zero, whereas the absence of a saturation gradient corresponds to a contact angle above some critical value. The subject of this chapter is the presentation of a theory of capillary rise which accounts for this experimental fact.

In chapter 1 it has been shown that none of the existing porespace or other models can account for the phenomena observed during capillary rise in macroporous media. More specifically, none of the existing theories on capillary liquid transport can account for the fact that the same system, i e the same particle packing and the same liquid, sometimes yields a wide saturation gradient and sometimes no saturation gradient at all. (The failure to account for this anomaly is, of course, partly explained by the fact that the problem has not, so far, been recognized and reported.) In fact, knowledge on the mechanism of capillary rise is virtually non-existent. This knowledge can be summarized by Haines' contention [215] that 'The rise of the water front will be checked by the widest section of the pore whereas in drainage the check is the narrowest section.' - the first clause of which is, under any reasonable interpretation, definitely not true.

The experiments and considerations given in chapter 3 exclude the possibility that the problem, regarding the presence or absence of a saturation gradient, is simply caused by some extraneous factor, e g the homogeneity of the packing. Therefore it is necessary to make a more detailed analysis of the mechanism of moving interfaces. The basic feature of the theory presented here is that it is necessary to recognize that a liquid-vapour interface in a porous medium contains concave and anticlastic parts. (Anticlastic means that the two principal radii of curvature are of opposite sign.) The anticlastic parts or α-menisci are contained by two particles. The concave parts or γ-menisci are contained by three or more particles. If the porespace is visualized as consisting,

of cavities connected by windows, then the transport mechanism can be seen as a continuous merging and generation of α- and γ-menisci. The theory analyzes the contribution of the α- and γ-menisci to the continuity of transport and the dependency of this mechanism on the contact angle.

As basic premises the theory requires data on the curvature of α- and γ-menisci and on the (statistical) properties of irregular packings. The available data in the literature on these subjects are rudimentary, because of the extreme complexity of the mathematical problems involved. Therefore, at present, the theory yields only a few quantitative predictions. It should, however, be noted that it is, at present, the only theory that can explain the phenomena observed during capillary rise.

5.1.2. Terminology. The considerations in this chapter are confined to irregular, dense, monosized sphere packings, i e the porespace geometry is a more or less fixed parameter. Distances, curvatures, and heights of capillary rise are expressed in terms of a dimensionless length parameter, Λ, with the particle radius as the unit of length. Thus for some distance L in a particle packing,

$$\Lambda \equiv \frac{2L}{d} \tag{5.1}$$

and for the curvature of some meniscus:

$$\Lambda \equiv \frac{4}{Cd} \tag{5.2}$$

and hence for a meniscus at equilibrium after capillary rise [cf eqs (1.10) and (1.11)]:

$$\Lambda \equiv \frac{4\gamma_{LV}}{\rho g h_c d} \tag{5.3}$$

The porespace of a sphere packing (regular or irregular) consists of cavities connected by windows. Each window connects two cavities. A window is bounded by curved lines on the surface of three or four spheres. These lines meet at the contact-points of the spheres or are connected by part of the lines connecting sphere centers at near-contacts. What a near-contact is depends on conventions chosen. Equilateral windows have the form of an equilateral

concave triangle or concave square. See Fig 5.1, top. Windows between three spheres are called ∇-windows, between four spheres ◇-windows. One of the parameters to characterize a window or a cavity is the radius, Λ_r, of the largest sphere, that can pass through the window, respectively just fits into the cavity.

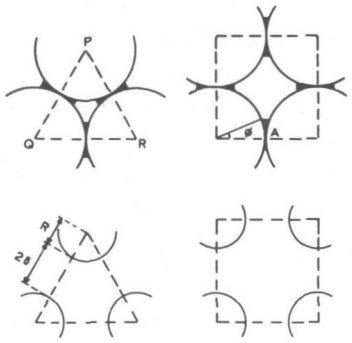

Fig 5.1. Top: Concave equilateral triangle and concave square. The α-meniscus at a contact point A is characterized by the angle ϕ. Bottom: Intersection parallel to the plane through the sphere centers, P, Q, and R; $d = 2(\delta+R)$.

A pendular ring at a contact-point of two spheres has an anticlastic meniscus, for short: α-meniscus, with curvature Λ_α. An α-meniscus fills one of the angles of several windows. (A ∇-window has three ∇-angles; a ◇-window has four ◇-angles.) The value of Λ_α at which a number of filled angles merge, and close a window, is Λ_w. The merging α-menisci yield a concave lense of liquid in the window, or, if we consider only one side of the window, a principally concave meniscus, for short: γ-meniscus, with curvature Λ_γ.

Isolated menisci are not considered. There is, as said before, only one meniscus at the liquid front, consisting of concave parts separated by anticlastic parts. The term meniscus will, however, be used as follows:

meniscus ≡ a more or less confined mainly concave, or mainly anticlastic, part of the continuous liquid-vapour interface coterminous with a small number of spheres, usually two, three, or four.

The curvature at which a cavity fills is Λ_c. The value of Λ_c depends mainly on the number of windows closed and the height of

the γ-menisci in the windows, i e , the height above the plane through the sphere centers constituting the window. When a cavity fills, this generates a number of new α- and γ-menisci.

At equilibrium after capillary rise or drainage, for each height, $\Lambda_\alpha=\Lambda_\gamma$. This value will be denoted by Λ_h and we will say, e g , that such and such a system yields a saturation gradient of Λ_h = 0.4-0.6 (cf Table 4.3).

5.1.3. Existing knowledge. The available knowledge relevant to the present problem can be divided into five parts, three of which we shall use.

(i) The most common approach to capillary liquid transport is to specify Haines' statement quoted above by contending that drainage is governed by the Λ_r distribution for the windows and that wetting is governed by the Λ_r distribution for the cavities (see e g [18], p 37). As to drainage this is not entirely uncorrect, but for wetting it is certainly not true, for regular as well as irregular packings. (This statement is substantiated in the sections that follow.)

(ii) Laborous calculations have been made on models for the wetting cycle of a suction experiment [216,347]. It is assumed that the wetting cycle is determined by the curvature at which advancing γ-menisci meet isolated α-menici (of the pendular rings that remain after the draining cycle of a suction experiment). The assumptions imply either that for menisci rising in a window we may assume $\Lambda_\gamma=\Lambda_r$, which is not permitted (see below), or the absence of capillary rise in case no isolated pendular rings are present.

(iii) The α-meniscus at a contact point is part of a nodoid. The exact equations for Λ_α are known, but they are difficult to solve. See further section 5.2.2.

(iv) The equations for a γ-meniscus between spheres, even for the most simple geometry, are not known. The Λ_γ of the meniscus between regularly spaced solid cylinders can be calculated [460] and these will be used. See section 5.2.3.

(v) To describe capillary rise in an irregular sphere packing we need its properties. For an irregular dense monosized sphere packing, some knowledge on its statistical geometry is available. This is discussed in section 5.3.1.

5.1.4. Outline of the argument. The argument of this chapter is based on the knowledge mentioned under (iii)-(v) in the preceding

sub-section and considers the relative importance of α- and γ-menisci in maintaining transport. As will appear, it is the difference in the functions $\Lambda_\alpha(\theta)$ and $\Lambda_\gamma(\theta)$ that can explain the presence or absence of a saturation gradient as a function of θ, for a given porespace geometry.

In section 5.2 we discuss the mechnism of capillary liquid transport in two regular sphere packings. This is not to give an exact account of the capillary rise in such packings[1], but to introduce the characteristics of capillary liquid transport using rather simple systems. In section 5.3 the capillary rise in irregular dense sphere packings is considered for θ=0. The packing is characterized by means of a Delauney graph (cf section 1.6.3). These a priori considerations are then compared with the experimental data for Ia and Ib systems in section 5.4. This provides further information on the contribution of the α- and γ-menisci to the movement of the wetting front. Finally, in section 5.5, the influence of θ on the wetting mechanism is discussed.

5.2. Menisci in regular sphere packings

5.2.1. Regular sphere packings. The use of regular sphere packings as a model for porous media has been reviewed in section 1.6.1. Since 1935 [11,12] the knowledge on regular sphere packings is more or less established. The six basic packing structures (there are more [218,461]) considered by Graton and Fraser [11] are given in Fig 5.2 and some data are given in Table 5.1. The six possibilities of packing spheres reduce to four if we do not consider the orientation. Although rotund-particle packings have porosities of 36-40%, the use of regular packings for analyzing capillary liquid transport has been restricted to the cubic and the rhombohedral packing.[2]

The cubic packing (see Fig 1.4, model *311*, and Fig 5.2a) has a rather simple porespace geometry. The cubic unit cell is formed by passing planes through the centers of eight contiguous spheres

---

1. Because h_c, depending strongly on the orientation of the packing in the field of gravity, is in general equal to zero.
2. Cf section 1.6.1. The historical reason for this choice is, probably, the fact that Haines used them. A more rational reason is that these two packings present the extremes for a (meta)stable monosized packing of spheres in a gravity field.

TABLE 5.1

Some properties of regular sphere packings [11,218]

packing	porosity (%)	number of contact-points	Λ_r cavities	Λ_r windows
cubic	47.64	6	0.7320	0.4142
orthorhombic	39.54	8	0.5275	0.4142 0.1547
body-centered tetragonal	30.18	10	0.2910	0.2649 0.1547
rhombohedral	25.95	12	0.2247 0.4142	0.1547

and consists of a cuboidal cavity bounded by six ◇-windows (concave squares, e g BFKE in Fig 5.2a).

The rhombohedral packing (see Fig 1.4, model *312*, and Fig 5.2c and 5.2f) is more difficult to visualize. In Fig 5.3 a photograph is presented of the unit cell (from [338]). In Fig 5.4 a number of photographs are given of a casting of the rhombohedral cell, taken from different directions at points in the same plane.

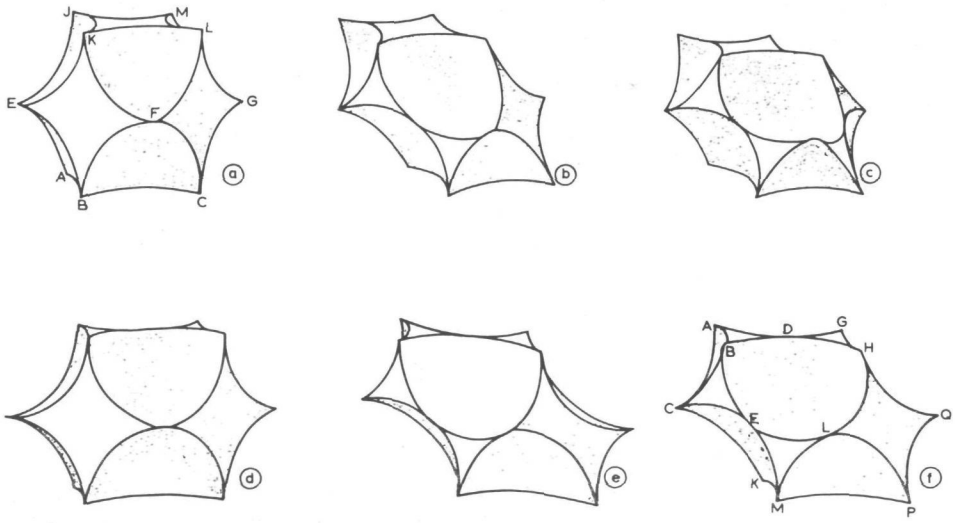

Fig 5.2. Regular sphere packings (from [11]): (a) cubic; (b) and (d) orthorhombic; (c) and (f) rhombohedral; (e) body-centered tetragonal.

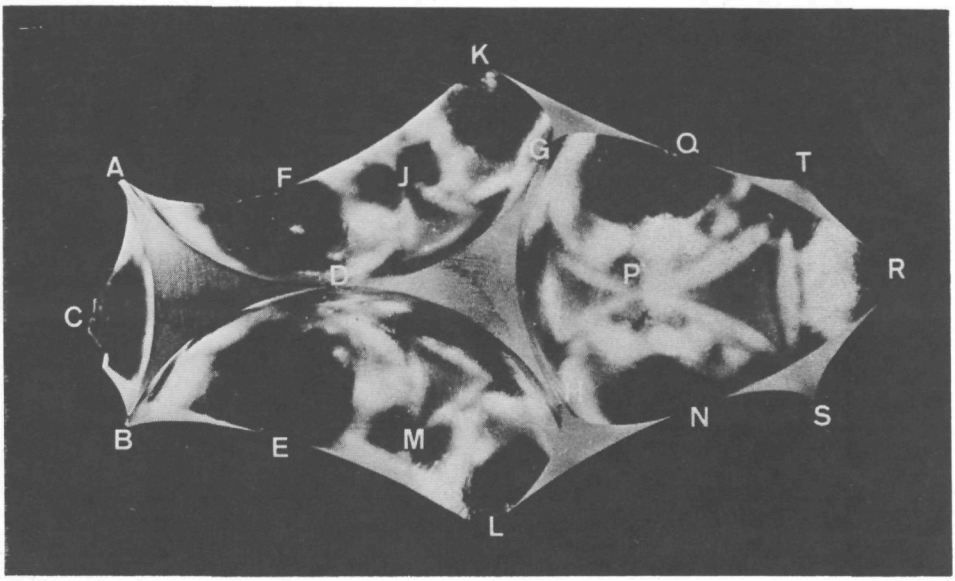

Fig 5.4a. Photograph of a casting of the porespace in a unit rhombohedron.

The rhombohedral cell consists of two tetrahedral and one octahedral cavity connected by ∇-windows (concave equilateral triangles).[3]

5.2.2. Anticlastic menisci. Liquid present around the contact-point of two spheres forms a wheel-rim meniscus, the mathematical form of which is nodoidal. It is usual to express the properties

3. In more detail the configuration of the porespace can be described as follows (cf Figs 5.2-4):

tetrahedral cavity ABC-DEF	bounded by ∇-windows		ABD BCE CAF	DEF	
octahedral cavity DEF-GHJKLM-NPQ	bounded by ∇-windows	DEF	DGH ELM FJK	HLN MJP KGQ	NPQ
tetrahedral cavity NPQ-RST	bounded by ∇-windows		NPQ	NRS PST QRT	

One rhombohedral cell corresponds to one sphere, six contact-points, and eight windows. One contact-point forms part of four ∇-windows (hence one α-meniscus forming part of four ∇-angles). Each window connects a tetrahedral to an octahedral cavity.

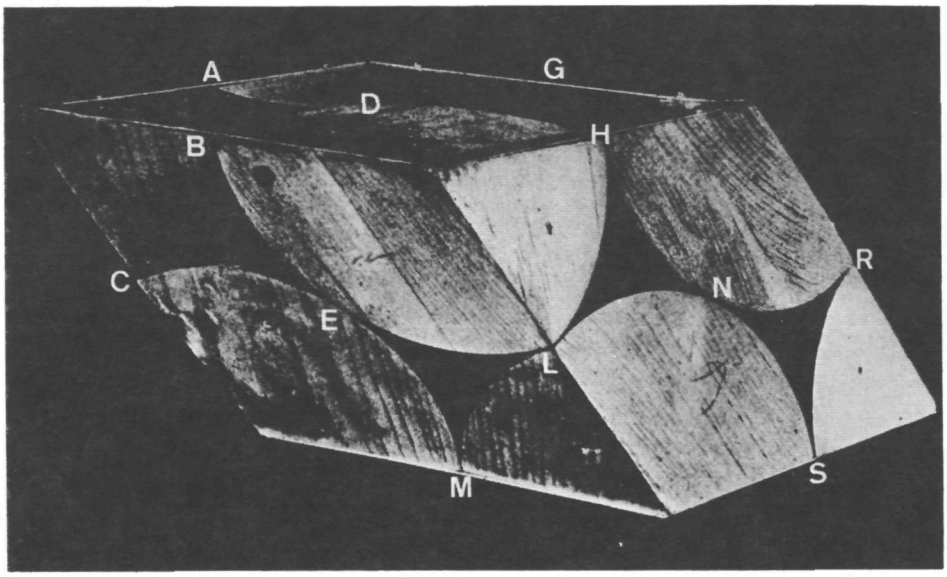

Fig 5.3. Unit rhombohedron formed by passing planes through the centres of eight contiguous spheres in a rhombohedral packing (from [338]).

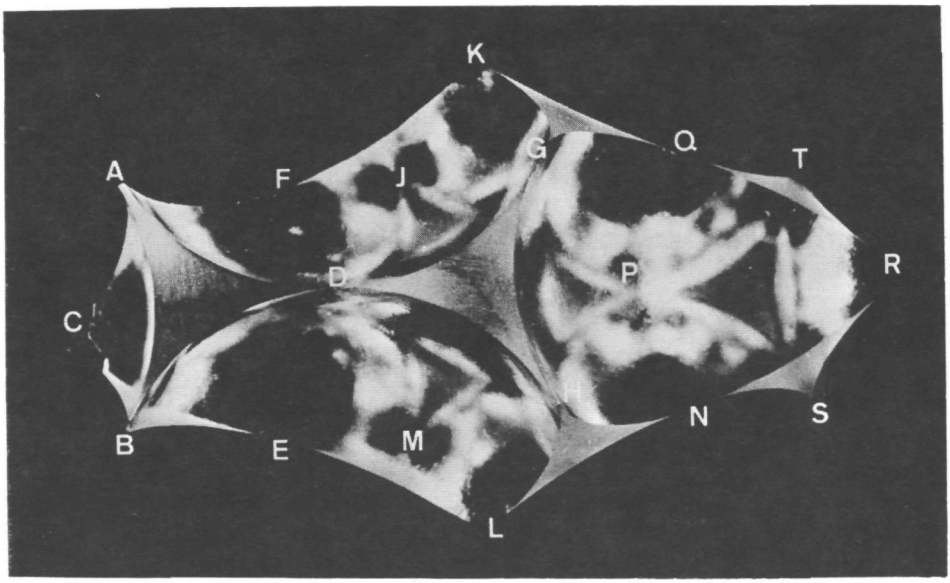

Fig 5.4b. Photograph of a casting of the porespace in a unit rhombohedron.

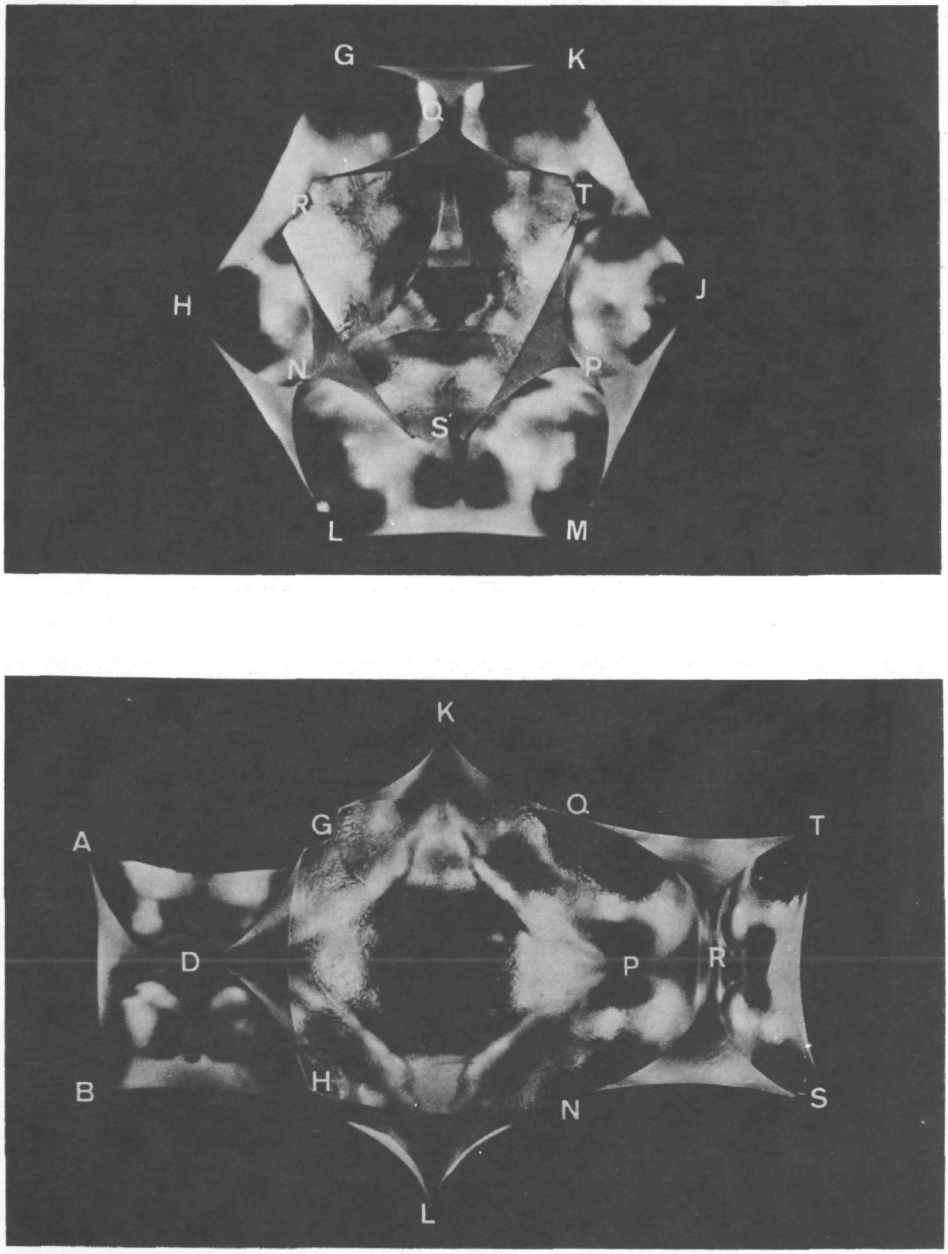

Fig 5.4c. Photograph of a casting of the porespace in a unit rhombohedron.

TABLE 5.2

Values of Λ_α as a function of ϕ and θ [218,468]

ϕ	$\theta = 0$	$\theta = 13^0$	$\theta = 20^0$	$\theta = 30^0$	$\theta = 40^0$
25	0.268	*0.32*	0.380	*0.53*	0.936
27.5		*0.43*	*0.52*	*0.77*	*1.66*
30	0.440	*0.57*	0.710	*1.16*	3.79
32.68	*0.57*				$\pm\infty$
35	0.715	(1.1)	1.42		
40	1.18	(2.3)	3.70		
45	2.11		$\pm\infty$		
55.64	$\pm\infty$				

of the pendular ring as a function of ϕ, the angle contained by the line connecting the sphere centers and the line connecting a sphere center with the three-phase line (see Fig 5.1). If an equilateral ∇-window contains two or three α-menisci, they merge at $\phi = 30^0$. If an equilateral $\diamond$-window contains three or four α-menisci, they merge at $\phi = 45^0$.

The exact equations to find $\Lambda(\phi,\theta)$ are known [462-464], but they are extremely difficult to solve, especially for $\theta \neq 0$, and only a few points have been calculated (and reported). Various approximate solutions have been used, but in general the deviations, in particular for high values of ϕ, are too large to be useful for the present purpose [224,263,347,465-467]. We need Λ_α in the range $\phi = 30\text{-}45^0$. In Table 5.2 the available data are given. The figures given in normal type are reported to be exact [464,468], but they differ slightly from older exact data [462,463]. The figures in italic type have been obtained by approximating the nodoid by a hyperboloid of revolution, which yields a good approximation for $\theta=0$ [218]. The figures in curved brackets are interpolated. Estimates for Λ_α of the meniscus between unequal spheres have shown that the values differ hardly from those for monosized spheres [469].

5.2.3. Concave menisci. Even for the most simple configurations, such as the meniscus in the window between three or four contiguous spheres (sphere centres in one plane), no exact solution for Λ_γ is

known. We will use the values of Λ for the γ-meniscus between solid cylinders as an estimate for Λ_γ.[4]

For the configuration given in Fig 5.1, bottom, Princen [460] calculated Λ_γ for the meniscus between three of four solid cylinders as a function of θ and δ/R, R being the cylinder radius and 2δ the distance between any two neighbouring cylinders . Princen also derived the (more simple) equations to calculate Λ_γ for the infinite extension of these cylinder configurations (above some critical δ/R, Λ_γ is different for a few isolated cylinders and for an infinite array). We surmise that these results can be applied to γ-menisci in sphere packings as follows. Consider a window between, e g , three contiguous spheres. The three-phase lines of the γ-meniscus will have a complex form. If we assume that they are lying approximately in a plane parallel to that through the sphere centres then, cf Fig 5.5, the configuration is the same as that for the meniscus between three solid cylinders, with $2(\delta+R) = d$ and an apparent contact angle, β, given by $\cos\beta = R/(\delta+R)$. When a γ-meniscus rises in a window both δ/R and β increase. Some values of Λ_γ for equilateral windows are given in Table 5.3 as a function of δ/R, for different configurations, and for $\theta=0$ and $\theta=20^0$. As to the applicability of the data for cylinders to spheres two points may be noted:

(i) Any deviation of the three-phase line on a sphere from a plane of latitude increases Λ_γ, but it has been shown that this

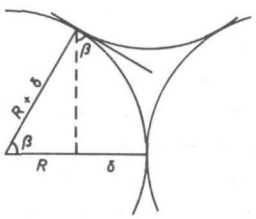

Fig 5.5. Model for a γ-meniscus rising in a window: cylinders of radius R, on a distance 2δ; β is the apparent contact angle.

4. Usually Λ_γ is taken equal to Λ_r of the window concerned. This value is always too low and progressively so when the window edges contain a smaller part of the three-phase lines. Other approaches, e g using the hydraulic radius, also give large deviations of the true values when applied to geometries for which the true values are known [470].

TABLE 5.3

Approximate values of Λ_γ for a window meniscus at different heights above the minimum window cross section

δ/R	β	$\theta = 0$				$\theta = 20^0$			
		∇-window		◇-window		∇-window		◇-window	
		isolated	array	isolated	array	isolated	array	isolated	array
0	0	0.18	0.18	0.45	0.45	0.18	0.18	0.47	0.47
0.05	17.8	0.24	0.24	0.51	0.51	0.27	0.27	0.58	0.58
0.07	20.8	0.27	0.26	0.54	0.54	0.34	0.32	0.62	0.62
0.10	24.6	0.36	0.33	0.58	0.58	0.49	0.43	0.71	0.69
0.12	26.8	0.43	0.38	0.61	0.61	0.62	0.50	0.84	0.78
0.14	28.7	0.51	0.43	0.67	0.67	0.78	0.58	0.97	0.87
0.16	30.4	0.58	0.48	0.76	0.71	0.96	0.65	1.15	0.96
0.18	32.1	0.68	0.54	0.85	0.77	1.17	0.74	1.38	1.07
0.20	33.6	0.80	0.59	0.97	0.83	1.46	0.83	1.63	1.17
0.24	36.2	1.04	0.70	1.20	0.96	2.2	1.01	2.3	1.39

deviation is, in general, very small [471].[5]

(ii) As said, the theoretical value of the lowest Λ_γ for a concave meniscus between three spheres (corresponding to the break-through pressure) is not known. But the experimental value is known rather accurate, reported values being 0.174-0.177 [215], 0.175 [472], and 0.171-0.180 [470]. The corresponding theoretical value for three cylinders is 0.177 [460]. For four spheres an experimental value of 0.437 has been reported [472], to be compared with the theoretical value of 0.445 for cylinders [460]. This case is a rather strong test because, for δ=0, the difference between α-menisci between spheres and those between cylinders is largest. Above δ/R = 0.05-0.1 a three-phase line will not deviate much from a parallel of latitude, both for spheres and cylinders.

5.2.4. Capillary rise in a cubic packing. In this section reference is made to the cuboidal cavity as depicted in Fig 5.2. If the direction of gravity is along the vertical, there is no capillary rise, because the meniscus in the lower plane, i e the window ABCD, can never reach the next layer. After drainage a sharp front between

5. Theoretically by assuming several analytic functions for the three-phase line and calculating the difference in the vertical force. Experimentally by comparing the influence of adjacent spheres on the force necessary to pull a sphere from a liquid.

the capillary and the pendular stage will be present at $\Lambda_h=0.45$ ($=\Lambda_\gamma$ for break-through of an array of concave squares).

As a hypothetical experiment we will consider a "haphazard cubic packing", whose elements have the same properties as a regular cubic packing but are connected in an irregular way. (To be sure, this is not physically possible.)

A window, e g BEKF, will close when three α-menisci at, say, B, E and F merge. This occurs for $\phi=45^0$, for which $\Lambda_\alpha=2.11=\Lambda_w$. The closure generates a new α-meniscus at K. Each α-meniscus is divided over four angles in four different windows. Hence, we have the following scheme of continuity of transport, where '→' stands for 'generates' or 'gives rise to',

3 angles → 1 window → 1 α-meniscus → 3 angles

The number of angles necessary to close a window is equal to the number of new angles generated. This is, in general, not enough to guarantee continuity of transport because of the overlap in the new angles generated. The symmetry of a regular cubic packing is such that there is so much overlap that there is no transport at all.

As to the filling of the cuboidal cavity, it is easily seen that this cannot occur when only one or two windows are filled. For three filled windows, having one sphere in common, closure of the cavity is perhaps possible. Assume that windows ABCD, AHEJ, and DHGM are filled. The meniscus is then, for the greater part, supported by spheres JEK, MLG and BCF. The cavity will be closed when this meniscus reaches sphere KLF. Using the assumptions underlying Table 5.3, one finds for this configuration $R=\delta$ and $\beta=45^0$, yielding a Λ_c between 2.4 and ∞ depending on the presence of menisci in adjacent cavities.

When three windows of the cavity, not having one sphere in common, are filled, the configuration of the γ-meniscus in the cavity is very complicated. If we assume that the cavity closes when the γ-menisci in the windows touch the inscribed sphere of the cavity, this yields $1.5 < \Lambda_c < 2.9$. It is expected that this estimate is on the low side. The other three windows are closed anyway at $\Lambda=2.11$, because each of them has, or obtains, three angles filled. Therefore we may expect that for this variant $\Lambda_c \simeq 2.1$, and that the closure of the cavity does not add to the continuity of transport.

Thus, depending on the connectivity of the windows, there are three possibilities:

(i) No capillary rise, as in the regular cubic packing.

(ii) Λ_h=2.11, and no saturation gradient, when there is no overlap of generated angles.

(iii) Λ_h having some value between 2.4 and ∞ when the closure of the cuboidal cavity by three windows, having one sphere in common, is needed to maintain continuity of transport. A saturation gradient is possible in this case.

5.2.5. Capillary rise in a rhombohedral packing. In this sub-section we refer to the rhombohedral cell as depicted in Figs 5.2-4. This cell contains ∇-windows as well as $\diamond$-windows, in a proportion 8:3.[6] An equilateral concave triangle with one angle filled cannot close because, in reaching the opposite sphere, the α-meniscus would have $\phi=60^0$, for which Λ_α is negative. Two filled angles will close a window at Λ=0.44 ($\phi=30^0$). For this case the scheme of continuity is:

$$2\ \nabla\text{-angles} \rightarrow 1\ \nabla\text{-window} \rightarrow 3\ \nabla\text{-angles}$$

Hence, two merging angles generate three new ones and when the overlap is not too large this mechanism can maintain transport for $\Lambda_h > 0.44$. For $\Lambda > 2.11$ the $\diamond$-windows may add to this. Each contact-point forms part of four ∇-angles and two $\diamond$-angles. Hence, for the scheme of continuity

$$2\ \nabla\text{-angles} \rightarrow 1\ \nabla\text{-window} \rightarrow \begin{matrix} 3\ \nabla\text{-angles} \\ 2\ \diamond\text{-angles} \end{matrix}$$

$$1\ \diamond\text{-angle} \rightarrow \tfrac{1}{3}\diamond\text{-window} \rightarrow \begin{matrix} 1\ \nabla\text{-angle} \\ \tfrac{1}{3}\ \diamond\text{-angle} \end{matrix}$$

This scheme will break down only for a very high amount of overlap.

A tetrahedral cavity cannot be closed by one window. When two windows are filled it seems reasonable to suppose that the cavity is filled when the two γ-menisci touch the inscribed sphere of the cavity. For this configuration we find $0.30 < \gamma_c < 0.35$. Of course, with two windows filled, the cavity closes anyway at Λ=0.44.

---

6. The ∇-windows have been mentioned in note 3. The concave squares are FGNM, DLPK, and EHQJ. A rhombohedral cell contains (2+½.12)=8 ∇-windows and 3 $\diamond$-windows.

Because the tetrahedral cavities are separated from each other by octahedral cavities they do not contribute to the continuity of transport. It appears that octahedral cavities do not close before a configuration is reached that displays continuity of transport by ∇- and ◇-windows only.[7] Therefore the cavities do not change the above mentioned scheme of continuity for transport by windows only.

There is some dispute as to whether air bubbles can remain in octahedral cavities, all windows being closed [216,470]. Experiments have shown that, with one window open (seven filled), an octahedral cavity closes at about $\Lambda=0.3$ [215]. Therefore, when the windows close one after another at $\Lambda=0.44$ (or 2.11) there will be no air entrapment.

The above considerations show that it is not some Λ related to the geometry of the cavities that governs capillary rise in particle packings but only, or first and for all, the merging of α-menisci in the windows. When enough windows have been closed, the cavities, in general, just follow. It is possible that the filling of the cavities contributes to the continuity of transport but we always have $\Lambda_h > \Lambda_w$.

5.3. Capillary rise in irregular sphere packings ($\theta=0$)

5.3.1. Properties of irregular packings. For the present problem, given the available knowledge and also a priori, the best approach seems

---

7. To consider the closure of the octahedral cavity as a function of the number of windows filled, this cavity is best visualized as contained by four contiguous spheres in one plane with two spheres placed in the ◇-window. The cavity will certainly not be filled when one up to three windows are filled. When four windows are filled there are two possibilities:

   (i) PQN, FJK, HJP, and KGQ are filled.

   (ii) PQN, FJK, HJP, and ELM are filled.

   In the first variant we have a meniscus rising between four spheres, which has to reach the overlying sphere. This is not possible. The cavity will close at $\Lambda=2.11$ when window EHQJ is filled. For the second variant we may assume that the cavity will close when the γ-menisci reach the inscribed sphere. This yields $1.2 < \Lambda_c < 3.5$. However, this situation is not reached because in this variant all ∇-windows have or obtain two angles filled, thus closing the cavity at $\Lambda=0.44$.

to describe the statistical geometry of an irregular sphere packing by means of a Delauney graph, thus dividing the porous medium in tetrahedra (cf section 1.6.3). Hence, all cavities are accessible by four windows and there are only ∇-windows. The edge length of a tetrahedron is denoted by Λ_e.

In an irregular dense sphere packing (ε = 36-37 %), a sphere has, on the average, 6-7.5 true contacts (i e Λ_e=2) and about 14 neighbours for $\Lambda_e < 2\sqrt{2}$. Many experimental as well as computer based data that confirm these figures are available [R10,R232, R481]. Hence it seems obvious to use them as input data for a tetrahedral model.

We will use the data of Mason [233], who calculated the properties of 1000 tetrahedra from the edge length distribution, $f(\Lambda_e)$, as measured by Scott [473,474]. This $f(\Lambda_e)$, which predicts 7.5 contacts for $\Lambda_e < 2.04$ and 13.75 contacts for $\Lambda_e < 2.80$, was obtained on a packing with a porosity of 36.3 %. Computer generated packings yield, at $\varepsilon \simeq 37\%$, roughly the same distribution [475,476]. For example, 6.8 contacts for $\Lambda_e < 2.04$, and 14.1 contacts for $\Lambda_e < 2.80$. The sphere packings used in our experiments had porosities in the range 34.9-36.3 % [318]. Although our packings are constructed from sieve fractions, we shall assume that the statistical properties of our packings are not much different from that of Scott. That all irregular dense sphere packings with ε = 35-38 % have, approximately, the same statistical geometry is supported by the reproducibility of the experimental $f(\Lambda_e)$ for numerous different packings [232]. The assumptions of Mason's model are the following:

(i) There are no neighbours for $\Lambda_e > 2.80$. (Bernal [276] reports 2 out of 24.000 edges greater than 3.2.)

(ii) The $f(\Lambda_e)$ for individual tetrahedra is identical to that for an assembly of tetrahedra.

(iii) The values of Λ_e are independent of each other.

The tetrahedra so constructed yield ε=36.5%. In the sequel we will mainly use two results from Mason's calculations. In both cases part of the data is supported by independent evidence.

(i) Mason finds that one sphere forms part of 23.3 tetrahedra. From this it follows that there are 23.3/4 tetrahedra per sphere. There are 6.9 edges per sphere. Hence one edge forms part of 6x23.3/(6.9x4) = 5.1 tetrahedra, and, because space is completely

filled by tetrahedra, one edge forms part of 5.1 windows. This value is also found by [277].

(ii) Mason has calculated $f(\Lambda_r)$ for the cavities as well as the windows. We are interested mainly in the latter. It appears that for 19% of the windows $0.143 < \Lambda_r < 0.16$, which is the window between three touching spheres. This result can be compared with the experimental value of 26% [245].[8]

5.3.2. Capillary rise in the tetrahedra model. From section 5.2 two points emerge: (i) the anticlastic menisci are the principal agents governing transport, and (ii) it is of the utmost importance to know the connectivity of the tetrahedral structure, because the amount of overlap in freshly generated menisci determines how many menisci are necessary to maintain continuity of transport. Nevertheless, we do not go into statistical considerations of the latter problem. We will use the simple working hypothesis that there will be some overlap, but not much, and we will then see how the predictions compare with the experimental data.[9]

To obtain $f(\Lambda_w)$ *from* $f(\Lambda_r)$ *we use model 313 (cf Fig* 1.4) *and* the calculations of [224] which yield $\phi(\Lambda_r)$. This implies that it is assumed that each window is characterized by one Λ_w only, no matter which two angles are filled. The $f(\Lambda_w)$ obtained in this way certainly yields too low values of Λ_w for isolated filled angles. This error is compensated by the fact that each filled angle is connected to at least one closed window which will decrease $\Lambda_\alpha(\phi)$ and hence Λ_w.

---

8. This value of 26 % is not given as such in [245]. Data are reported on the number of concave polygons found in an irregular sphere packing when considering only true contacts. These data were recalculated by dividing all polygons in ∇-windows and making a correction for the number of near-contacts so obtained. It should be noted that the argument in the next sections becomes stronger when the value of 26%, in stead of 19%, is assumed.
9. The nature of the connectivity of the windows and cavities *is* of the utmost importance but it is not opportune to consider the problem here: It is still a matter of dispute what can be considered as random parameters in an irregular sphere packing. (We do not speak of a random sphere packing because it is not the distribution of the spheres in space that is random (because they cannot overlap) and it is unclear what it is then, that is random.) Moreover there are indications that irregular sphere packings are anisotropic [477].

From section 5.2 it is clear that there cannot be any significant capillary rise for $\Lambda_h < 0.44$, corresponding to the closure of the smallest ∇-windows. If we consider transport by windows only the scheme of continuity is:

2 angles → 1 window → 1 α-meniscus → 4.1 angles

If there is not much overlap, this implies that continuity of transport is maintained by only 50% of the windows (filling all contactpoints but not necessarily all windows). These windows have Λ_r = 0.15-0.28, yielding Λ_w = 0.44-0.68. Hence we will observe a saturation gradient for Λ_h = 0.44-0.68, or to still higher values of Λ when at these values of Λ_w not all cavities are closed. If the majority of the cavities is not closed before three windows are filled, it appears that, in the range for which 75-90 % of the windows fill, the maximal Λ_r is of the order of that of a concave square. Hence the porous medium will be completely saturated to at least Λ_h=2.11. These predictions are well within the boundaries set by the considerations for regular sphere packings.

To close a cavity at least two γ-menisci are needed, a closure yielding two new γ-menisci. Because of some overlap and a number of large cavities, which will never be filled by two γ-menisci, this mechanism cannot maintain transport to any appreciable height. If all, or almost all, cavities would always easily close when two windows are filled we need less windows to maintain transport. A typical scheme of continuity is:

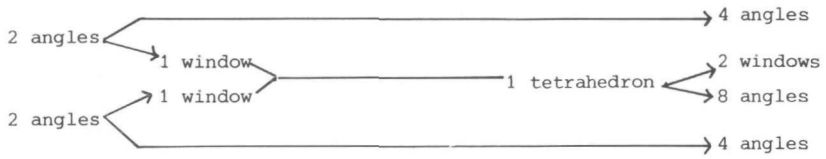

This scheme, in which the larger windows are closed via tetrahedra that are filled by their smaller windows, suggests that 20% of the windows might be enough to maintain transport. Because for 20% of the windows Λ_w=0.44, we may expect no saturation gradient and Λ_h= 0.44 in that case.

Many intermediate cases are possible. For the moment it is enough to state the extremes for Λ_h of an irregular sphere packing and θ=0 (and still under the assumption of little overlap):

(i) If the cavities are always easily closed when two windows are filled, continuity of transport is maintained by 20% (or less) of the windows. No saturation gradient will be observed and $\Lambda_h=0.44$.

(ii) If the cavities are not filled before three windows are closed the transport is maintained by 50-90% of the windows. A saturation gradient will be observed for which $\Lambda_h=0.44-z$, with $0.68 < z < 2.1$.

We now turn to a comparison with the experimental results.

5.4. Comparison with the experimental data for θ=0

5.4.1. Digression on drainage. Because the mechanism of drainage is much simpler than that of capillary rise, drainage experiments can be used as a rough check on the reliability of the tetrahedra model and, more in particular, on the $f(\Lambda_r)$ of the windows.

After drainage the equilibrium saturation gradient will be governed by the distribution of the larger windows in the packing, because, to empty a cell only two windows are necessary. Using some appropriate assumptions regarding the connectivity (cf section 1.6.3) Mason [233] predicts for the saturation zone after drainage $\Lambda_h = 0.28-0.34$. This can be compared with some of our experimental results given in Table 5.4. Although there is some scatter, the prediction is rather well confirmed for Ia systems, for the average height as well as for the width of the saturation gradient.

TABLE 5.4

Saturation gradient at equilibrium after drainage

experiment	system	class	Λ_h	
			30% < u < 90%	u=50%
3fp33td	350 μm glass beads - toluene	Ia	0.31 - 0.37	0.34
3fp34td	350 μm glass beads - toluene	Ia	0.29 - 0.35	0.32
3S43td	360 μm sand - toluene	Ia	0.25 - 0.33	0.26
9Sw2ed	925 μm sand - water	Ia	0.28 - 0.33	0.30
3n14td	350 μm glass beads - toluene	IIb	0.38 - 0.39	0.38
3n8td	350 μm glass beads - toluene	IIb	0.33 - 0.39	0.37
3n91td	350 μm glass beads - toluene	IIb	0.40 - 0.44	0.43
9st2ed	925 μm sand - water	IIa	0.42 - 0.52	0.45

TABLE 5.5

Equilibrium saturation gradient after capillary rise for Ia systems

experiment	system	Λ_h	
		$10\% < u < 90\%$	$u=50\%$
3fi22tx	350 μm glass beads - toluene	0.44 - 0.61	0.53
3fp32tx	350 μm glass beads - toluene	0.46 - 0.61	0.55
3fp41hx	350 μm glass beads - hexane	0.46 - 0.61	0.54
3z1ts	350 μm glass beads - toluene	0.40 - 0.64	0.54
2Pk4kx	215 μm polystyrene - heptane	0.40 - 0.63	0.54
4C1tx	360 μm crushed glass - toluene	0.39 - 0.55	0.46
3S33tx	360 μm sand - toluene	0.32 - 0.51	0.43
3S42tx	360 μm sand - toluene	0.32 - 0.59	0.48
5Sw2ex	550 μm sand - water	0.32 - 0.65	0.50
5Sw3ex	550 μm sand - water	0.31 - 0.72	0.53
9Sw6ex	925 μm sand - water	0.32 - 0.57	0.43

TABLE 5.6

Values of δ/R for which $\Lambda_\gamma \simeq \Lambda_\alpha \simeq \Lambda_h$ for several configurations

θ	pendular rings		isolated ∇-windows		array ∇-windows	
	ϕ	Λ_α	δ/R	Λ_γ	δ/R	Λ_γ
0	30	0.44	0.12	0.43	0.14	0.43
	35	0.71	0.18	0.68	0.24	0.70
20^0	30	0.71	0.12	0.62	0.14	0.58
	35	1.42	0.18	1.17	0.24	1.01

θ	pendular rings		isolated $\diamond$-windows		array $\diamond$-windows	
	ϕ	Λ_α	δ/R	Λ_γ	δ/R	Λ_γ
0	30	0.44	0	0.45	0	0.45
	35	0.71	0.15	0.71	0.16	0.71
20^0	30	0.71	0	0.47	0	0.45
	35	1.42	0.15	1.06	0.16	0.96

The results for IIb (and IIa) systems show higher values for Λ_h. It can therefore be concluded that for IIa/IIb systems not only the advancing but also the receding θ is greater than zero.

5.4.2. Saturation gradient Ia systems. In Table 5.5 values of Λ_h (after capillary rise) are given for some Ia systems. The fact that very different systems give the same Λ_h range further supports the hypothesis that $\theta \simeq 0$ for these systems. If we compare these figures with the data given in section 5.3.2 the following points emerge.

(i) As predicted there is no capillary rise for $\Lambda_h < 0.44$ in the case of sphere packings. The lower values for angular particles may be due to (α) a more pronounced effect of the particle size distribution, (β) the fact that smaller windows can occur.

(ii) The porous medium is completely saturated for $\Lambda_h > 0.64$. At this value about 40-50% of the windows are filled. Hence, the closure of the cavities contributes to the continuity of transport for $\Lambda_h > 0.64$, that is to say, a number of windows are closed by two windows at $\Lambda_\gamma = \Lambda_c > 0.64$.

(iii) Because filled windows contribute only a small part to the saturation, it is to be expected that in the region $0.44 < \Lambda_c < 0.64$ a number of cavities is closed, partly from a configuration with three windows filled, partly with two windows filled.

The cavities are closed by γ-menisci rising in the windows. In Table 5.6 the values of δ/R are given for several configurations when $\Lambda_\gamma \simeq 0.44$ and $\Lambda_\gamma \simeq 0.71$. Although the model used is defined to contain only ∇-windows, the values for $\diamond$-windows are included because, for a somewhat distorted concave square, which the model divides into two ∇-windows, it seems reasonable to assign to both of these ∇-windows the Λ_γ value of the $\diamond$-windows.

As can be seen from Table 5.6 the values of δ/R are in the range 0.1-0.2. This is the order of magnitude one would expect for two windows closing a cavity, noting that

(i) For a γ-meniscus in a window of a regular tetrahedral cavity (cf section 5.2.5), touching the inscribed sphere, $\delta/R \simeq 0.07$. This value might be used as setting the lower boundary for Λ_h at which cavities are closed.

(ii) The median of the $f(\Lambda_r)$ of the cavities is at about $\Lambda_r = 0.375$. Assuming this tetrahedron to be formed by four equidistant spheres this yields $\delta/R \simeq 0.12$ for the γ-meniscus touching the inscribed sphere.

TABLE 5.7

The values of Λ_h for some Ib systems

experiment	system	class	$\Lambda_h\|_{t\to 0}$	Λ_h
2Pk2rx	215 μm polystyrene - acetonitril	Ib	1.6	0.52-0.62
3P'1a	360 μm polystyrene - ethanol	Ib	1.1	0.57
4f1g	360 μm glass beads - glycol	Ib	1.6	0.49-0.57
3n1d	350 μm glass beads - dichloro-acetic acid	Ib	1.9	0.62
5Bc11e21	215 μm glass beads - water	Ib	0.93	0.47-0.54
3fp32tx	350 μm glass beads - toluene	Ia	0.60	0.46-0.61
2S23tx	325 μm sand - toluene	Ia	0.42	0.30-0.45
Cammerer [171]	250 μm glass beads - water	Ib	3	0.62-1.00
Heizmann [72]	680 μm glass beads - water	Ib		0.44-0.73

5.4.3. Saturation gradient Ib systems. It has been remarked in chapter 2 that we did not succeed in finding Ib systems of which the saturation gradient at equilibrium could be or was measured by means of X-ray absorption. It has now been established that all Ia systems show a saturation gradient in the region $\Lambda_h = 0.4\text{-}0.7$, while all IIa and IIb systems yield $\Lambda_h > 0.7$ (see Tables 5.5 and 5.9). It may therefore be hypothesized that systems that show a relatively slow capillary rise and $\Lambda_h < 0.7$ belong to class Ib. In Table 5.7 some of these systems, thus classified as Ib, are given. (It may be noted that in most cases the saturation gradient was observed visually.) It is on this basis that these systems have been included under class Ib in Table 2.1.

5.4.4. Comparison with suction experiments. In section 1.10.5 it has been remarked that one should distinguish:

(i) Capillary rise and the wetting cycle in a suction experiment, because of the pendular rings present in the latter.

(ii) Drainage and the drying cycle in a suction experiment, because of the difference in kinetics.

These remarks were based on a priori considerations. From the comparison of experimental data, it appears, that, at least for spheres and $\theta=0$, the difference, if any, is not large. In Table

TABLE 5.8

Comparison of suction with capillary rise and drainage (θ=0)

description	Λ_h for u = 50 %	
	imbibition	draining
Mason's model [233]		0.31
typical drainage experiment (cf Table 5.4)		0.33
typical capillary rise experiment (cf Table 5.5)	0.54	
capillary rise in partly saturated medium (cf Fig 5.6)	0.54	
suction; this laboratory		0.36
suction; Haynes [470]	0.51	0.33
suction; Morrow & Harris [478]	0.59	0.37

5.8, Λ_h at u=50% is given for a number of imbibition and draining situations. The differences seem to be within experimental error.[10]

For drainage and the drying cycle the correspondence is not unexpected. For the two imbibition cases the unexpected result can be explained with reference to the merging of α-menisci, which governs transport. The presence of (small) pendular rings has no influence. They are too far away from the nearest γ- and α-menisci to contribute to the continuity of transport. This is further illustrated by the fact that capillary rise in partly saturated media results in a normal Ia behaviour. In Fig 5.6 the equilibrium saturation gradient is given for such a system (the values of Λ_h for this experiment are included in Tables 5.5 and 5.8). The presence of the initial saturation has no significant effect on the mechanism of capillary rise.

10. Although very many suction experiments have been reported in the literature the number of reliable sources, reporting complete data for the wetting and the drying cycle of an irregular sphere packing, are scarce. Therefore, only two sources can be mentioned in Table 5.8. Large differences between Λ_h for capillary rise and Λ_h for the wetting cycle, which have been reported, e g by Haines, can be ascribed to differences in θ.

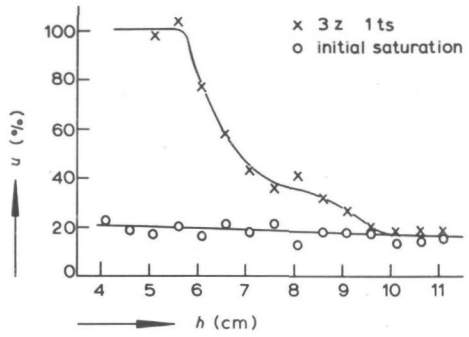

Fig 5.6. Capillary rise of toluene in 350 μm glass beads. The porous medium has an initial saturation of $u \simeq 20\%$.

5.5. Comparison with the experimental data for $\theta >> 0$

5.5.1. Mechanism for IIa/IIb systems. All IIa/IIb systems yield $\Lambda_h > 0.7$. Some typical values are given in Table 5.9. The values of $\Lambda_h|_{t\to 0}$ are included to illustrate the difference between IIa and IIb systems. IIa systems tend to give higher values of Λ_h than IIb systems.[11]

Given the mechanism of capillary rise developed in the previous sections, the absence of a saturation gradient strongly suggests that, for IIa and IIb systems, 20% of the windows are enough to maintain transport, the greater part of the cavities closing when two windows are filled. Although no detailed arguments can be given that this is always true when $\Lambda_h > 0.7$, the weaker hypothesis that with increasing θ the filling of cavities becomes more favourable relative to the filling of the windows, is certainly correct. This is exemplified in Table 5.6 for $\theta = 20^0$. It can be seen, e g , that Λ_w for the 20% smallest windows is 0.44 for $\theta = 0$ and 0.71 for $\theta = 20^0$. The same change in θ gives for Λ_γ, and hence Λ_c, a much smaller change, especially for the ◇-windows. Thus, as it were, more cavities become available to assist the windows in maintaining transport. This effect will become more pronounced at still higher θ.

11. It might be of interest that for $\Lambda_h|_{t\to 0}$ (which is equal to Λ_h for IIa systems) we have never found values between 0.7 and 1.1. Explicit attempts to obtain values in this region did not succeed (cf Table 5.10).

TABLE 5.9

Λ_h for some typical IIa and IIb systems

experiment	system	$\Lambda_h \mid_{\to 0}$	Λ_h	eqilibrium time (days)	number of days after which no further readings were taken
1s1t	125 μm glass beads - toluene	2.2	0.82	15	62
3n5t	350 μm glass beads - toluene	1.3	0.87	5	40
3np1ex	350 μm glass beads - water	1.7	0.77	60	144
3S3e	360 μm sand - water	2.2	1.13	66	114
2Pk1nx	215 μm polystyrene - nitromethane	2.8	<2.1		3
5Sa2e	550 μm sand - water	1.2	1.2	<<1	3
7Sa4e	780 μm sand - water	1.5	1.5	<<1	3
5St1ex	550 μm sand - water	6.1	6.1	<<1	3
6St1e	655 μm sand - water	2.5	2.5	<<1	3
2Pk1g	215 μm polystyrene - glycol	4.1	4.1	<1	60
$3f'_e2p$	350 μm glass beads - paraffinic oil	2.1	2.1	<1	40

TABLE 5.10

Capillary rise of water in 550 µm sand, subjected to various surface treatments

Class Ia/IIa

experiment	treatment	Λ_h
5Sw3ex	24 hours at 500°C	0.31-0.72
5Sw2ex		0.32-0.65
5Sa4e	rinsed several times with reagent acetone and dried at 80°C	0.52-0.64
5Sa3e		0.57-0.72
5Sa2e		1.16
5St2e	rinsed with 1:1 acetone/toluene	1.4
5St1ex	rinsed with reagent toluene	6.1

TABLE 5.11

Capillary rise of toluene in mixtures of 350 µm IIb glass beads and 360 µm Ia sand (cf Fig 5.7)

experiment	% sand	Λ_h 10 % < u < 90 %	Λ_h u = 50 %
3n92t	0	0.68-0.71	0.68
1M1t	10	0.63-0.66	0.63
2M1t	20	0.50-0.63	0.56
5M2t	50	0.40-0.58	0.51
7M1t	75	0.31-0.49	0.42
3S31t	100	0.31-0.49	0.42

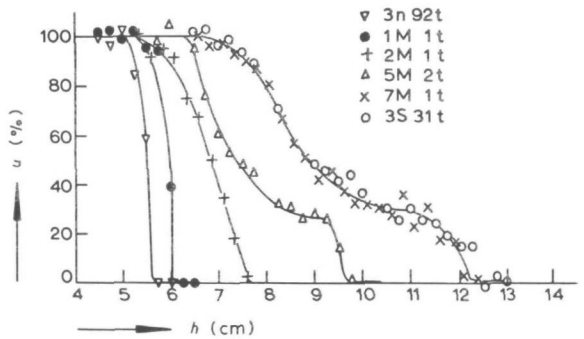

Fig 5.7. Capillary rise of toluene in different mixtures of sand and glass beads. Cf Table 5.11.

We therefore conclude that for IIa/IIb systems:

(i) Λ_h is equal to Λ_w for the smallest windows, i e , Λ_γ for $\phi=30^0$, as given in Table 5.2.

(ii) For most cavities, with two windows closed, $\Lambda_c < \Lambda_w$.

(iii) These cavities plus the smallest windows maintain transport.

5.5.2. Intermediate cases. For reasons of clarity the existence of intermediate cases between Ia/Ib and IIa/IIb systems has not been mentioned in the previous chapters and sections. Of course they exist, but for some reason they seem to be rare. Just by way of illustration two examples of provoked intermediate cases are given. In Table 5.10 for capillary rise of water in sand, of which the surface had been treated in different ways. In Table 5.11 and Fig 5.7 for mixtures of IIb glass beads and Ia sand.

5.5.3. Value of θ *for* $\Lambda_h = \infty$. Most porespace models imply that h_c is proportional to $\cos\theta$. It is only incidentally recognized that this is not true [347,479,480]. The mechanism of capillary rise described in this chapter implies that the value of θ for which $h_c=0$ corresponds to that for which $\Lambda_\alpha(\phi=30^0) = \infty$. It is estimated that for that configuration $47^0 < \theta < 53^0$.[12] This compares rather well with the experimental results for polystyrene spheres (see Table 4.3).

5.6. Concluding remarks

In this chapter a theory has been developed, describing the mechanism of capillary rise in dense irregular sphere packings. This theory explains the possibility of a saturation gradient of varying widths (including the absence of a saturation gradient) depending on the value of the contact angle. The general features of the theory can be stated a priori and can be summarized as follows.

(i) In analyzing the mechanism of capillary rise, it is of crucial importance to recognize the existence and role of two kinds of menisci: the concave γ-menisci in the windows and the wheel-rim α-menisci at the contact-points of the spheres.

(ii) The mechanism of capillary rise is characterized by a continuous merging and generation of α- and γ-menisci. Both kinds

12. The exact value of Λ_α for $\theta=40^0$ is known, being 3.8 [468]. An approximate calculation method, which gives $\Lambda_\gamma=3.0$ for $\theta=40^0$, yields $\theta=45^0$ for $\Lambda_w = \infty$.

of menisci contribute to the advancement of the liquid front, but the α-menisci are the main agents.

(iii) The maximum height of capillary rise is determined by the merging of α-menisci in the smallest windows.

(iv) The dependence on the contact angle is different for the curvature of the α-menisci and that of the γ-menisci. Therefore, the relative contribution of α- and γ-menisci to the continuity of transport changes as a function of the contact angle. This may cause, in principle, significant differences in the nature of capillary rise as a function of the contact angle.

(v) In general, a saturation gradient has to be expected at equilibrium, depending on the size distribution of cavities and windows. (Roughly speaking the windows are filled by the α-menisci and the cavities are filled by the γ-menisci.)

(vi) However, under certain conditions, the capillary rise is determined completely by the α-menisci in the smallest windows. Because there is a large number of equal-sized smallest windows, in this case no saturation gradient is formed.

Because of the extreme difficulties involved in establishing the exact curvature of various menisci at the liquid front and the exact statistical properties of irregular packings, the theory does not give quantitative predictions, except for conclusion (iii), which is in fact verified.[13] From a comparison of the theory with the experimental data the following conclusions emerge, which give a posteriori support for the theory.[14]

---

13. See section 5.4.2 and Table 5.5. The following minor conclusions contribute further to the experimental verification of the theory: (i) The theory gives the correct prediction for drainage (section 5.4.1). (ii) The predictions of the theory for the wetting cycle of a suction experiment are verified by the experimental data reported in the literature (section 5.4.4). (iii) The theory predicts that no capillary rise will take place for a contact angle larger than about 50 degrees. As to the order of magnitude this is confirmed by the experimental results for polystyrene (section 4.4).

14. The theory contains about 16 important assumptions. These assumptions are supported all by a priori arguments or independent evidence, with the exception of one: The working hypothesis that there is not much overlap in the menisci generated after closing of a window or cavity (see section 5.3.2). This hypothesis is ad hoc in the sense that only under this assumptions the theory contains conclusion (vi), and hence (ix).

(vii) For systems that display a saturation gradient (contact angle approximately zero) the continuity of transport is mainly maintained by the α-menisci and the saturation gradient is mainly a function of the size distribution of the windows.

(viii) When the contact angle increases, the contribution of the γ-menisci to the continuity of transport becomes more and more significant.

(ix) For systems that display no saturation gradient at equilibrium the height of capillary rise follows from conclusion (iii).

APPENDIX

Symbols used in naming the experiments

The name of an experiment αβγδεξ consists of five symbols containing one or more signs.

α consists of a numeral and/or a capital and indicates the solid phase and the particle size

β consists of a small letter (with subscripts and/or superscripts) and refers to the applied pre-treatment of the solid surface

γ consists of a small letter and denotes other properties of the porous medium

δ consists of one or two numerals; the first numeral is a sequence number for experiments on identical systems; the second is a sequence number for experiments with one and the same porous medium

ε consists of a small letter and designates the wetting phase

ξ consists of a small letter or a numeral and refers to special experimental conditions

The symbols β, γ, and ξ can be absent. For all β and γ, $\beta \neq \gamma$.

α *solid phase*

1 glass beads "Strahlperlen", soda glass, ρ = 2490 kg/m^3; Glass- und Spiegel Manufaktur, 465 Gelsenkirchen, West-Germany; 100-150 μm

2 see 1, 150-300 μm

3 see 1, 300-400 um

4 glass beads "Ballotini", lead glass, ρ = 2930 kg/m^3; Tamson, Zoetermeer, Holland; 300-420 μm

8 soda glass beads, unknown source, 800-900 μm.

1A alumina silicate glass beads, ρ = 2800 kg/m^3; Corning Glass Works, Corning, N.Y. 14830; 100-150 μm

1B see 4; 53-65 μm

2B see 4; 90-103 μm

3B see 4; 105-125 μm

4B see 4; 125-175 μm

5B see 4; 175-250 μm

6B see 4; 250-300 μm

4C crushed lead glass, 300-420 μm

1E soda glass beads; Englass, Scudamore Road, Leicester LE 3 1UG; 100-150 μm

3E see 1E; 300-400 μm

5G fused silica particles, 420-500 μm

3K copper beads, 300-420 μm

1M mixture of glass beads 3 and sand 3S; 10% 3S

2M see 1M; 20% 3S

3M see 1M; 30% 3S

5M see 1M; 50% 3S

7M see 1M; 75% 3S

P polystyrene spheres "Vestyron", ρ = 1040 kg/m^3; Chemische Werke Hüls; 350-500 μm

2P see P; 175-250 μm

3P see P; 250-300 μm

3P' polystyrene spheres, unknown source; 300-420 μm

1S burnt sand; Zand en Grintzifterij "De Combinatie", Papendrecht-Holland; 150-250 μm

2S see 1S; 250-400 μm

3S see 1S; 300-420 μm

3S' sand taken from the shore at Kijkduin, The Netherlands; 300-420 μm

5S see 1S; 500-600 μm

6S see 1S; 600-710 μm

7S see 1S; 710-850 μm

9S see 1S; 850-1000 μm

1U glass beads, ρ = 2370 kg/m^3; unknown source; 90-105 μm

2U see 1U; 105-125 μm

3U see 1U; 125-175 μm

1X pyrex glass beads, ρ = 2900 kg/m^3; Pulles & Hanique, Eindhoven, Holland, 125-175 μm

β *pre-treatment solid surface* (cf Table 3.2)

a heat, water, acetone

e water

f detergent, 5% HF (30 min), water, acetone

f^1 detergent, 5% HF (2x30 min), water, acetone

f^2 detergent, 5% HF (3x30 min), water, acetone

f^3 detergent, 65% HF (15 min), water

f_e^1 detergent, 5% HF (2x30 min), water

f_s detergent, 5% HF (30 min), water, acetone, toluene, sulfo-chromic acid, water, acetone

f_f as f_s followed by: toluene, acetone, 5% HF (30 min), water, acetone

k heptane

n detergent, warm nitric acid (30-60 min), water, acetone

s detergent, boiling sulfo-chromic acid (10-60 min), water, (acetone)

t reagent toluene

t' impure toluene

w heat (500-600^{0}C)

γ *properties porous medium*

(void) particle packing supported by a Jena glass filter PO (160-250 μm)

b particle packing supported by a filter made from the same particles that constitute the packing

c consolidated porous medium

d diameter of porous medium 15 mm (usually it is 23 mm)

i particle packing supported by unknown filter

p particle packing supported by a Jena glass filter P4 (10-16 μm)

r rectangular porous medium

ε *wetting phase* (reagent quality if not otherwise specified)

a ethanol 100%

b α-bromonaphtaline; Merck

c acetone; Merck

d di-chloroacetic acid; Brocades

e water, double distilled

e' water with surface active agent

f formamide; Merck

g glycol; UCB

h *n*-hexane, chromatographically pure for 99.5+ %

k *n*-heptane, impure; Phillips

m methylene iodide; BDH

n nitromethane; Merck

p paraffin oil (medicinal)

r acetonitril; Fisher

t toluene; UCB; M&B; BDH; Baker

ξ *special experimental conditions*

(number) the number indicates the counter pressure in cm H_2O (cf section 3.6)

d drainage experiment

e the experiment was performed in an atmosphere saturated with the wetting liquid

s capillary rise in a partly saturated porous medium

v the experiment was performed at low pressure (cf section 3.4.1)

x the saturation gradient was measured by means of X-ray absorption.

LIST OF SYMBOLS

C	sum of inverse radii of curvature, cf eq (1.10)	$[1/L]$
d	particle diameter	$[L]$
$\mathbb{D}_{AB}$	molecular diffusion coefficient of species A in species B	$[L^2/\theta]$
$\mathbb{D}_{eff}$	effective diffusion coefficient, cf eq (1.2)	$[L^2/\theta]$
$\mathbb{D}_u$	moisture diffusivity, cf eq (1.17)	$[L^2/\theta]$
g	acceleration of gravity	$[L/\theta^2]$
h	height, vertical coordinate	$[L]$
h_c	equilibrium height of capillary rise	$[L]$
I	intensity of X-rays, cf section 2.2.4	-
j_A	diffusional mass flux of component A (relative to the mass-average velocity of the gas mixture), cf eq (1.2)	$[M/L^2\theta]$
k	permeability, cf eq (1.7)	$[L/\theta]$
k	Boltzmann constant (in sections 4.2 and 4.3)	$[ML^2/\theta^2T]$
l	length of a tube	$[L]$
ℓ	film thickness, cf section 4.2.4	$[L]$
L	distance	$[L]$
M	molecular weight	-
p_b	break-through pressure, cf eq (1.20)	$[M/L\theta^2]$
p_c	capillary pressure, cf eq (1.10)	$[M/L\theta^2]$
p_d	disjoining pressure, cf eq (4.9)	$[M/L\theta^2]$
p_s	saturated vapour pressure	$[M/L\theta^2]$
p_v	vapour pressure	$[M/L\theta^2]$
ΔP	pressure dificiency	$[L]$ or $[M/L\theta^2]$
q	liquid flux, filter velocity, cf eqs (1.5-7)	$[L/\theta]$
q_h	heat flux, cf eq (1.1)	$[M/\theta^3]$
Q	diffusibility (in chapter 1), cf eq (1.3)	$[M/\theta^3]$
Q	$\equiv p_v/p_s$ (in chapter 4)	-
r	tube radius	$[L]$
r_h	hydraulic radius, cf eq (1.19)	$[L]$
R	gas constant	$[L^2/\theta^2T]$
R	cylinder radius (in chapter 5), cf section 5.2.3	$[L]$
s	specific surface, (m^2 solid surface)/(m^3 solid mass)	$[1/L]$

t	time	$[\theta]$
T	temperature	$[T]$
u	liquid content, %vol porespace filled	-
W_A	work of adhesion, cf eq (4.14)	$[M/\theta^2]$
x	coordinate in transport direction	$[L]$
α	angle between vertical and transport direction	-
β	number of tubes to which a certain tube is connected (chapter 1)	-
β	apparent contact angle (chapter 5), cf section 5.2.3	-
γ	surface tension	$[M/\theta^2]$
γ_c	critical surface tension, cf section 4.3.1	$[M/\theta^2]$
Γ	surface concentration, cf eq (4.4), mol/cm^2	$[1/L^2]$
δ	constrictivity factor (chapter 1), cf section 1.4.5	-
δ	distance (chapter 5), cf section 5.2.3	$[L]$
ε	porosity	-
η	dynamic viscosity	$[M/L\theta]$
θ	contact angle	-
Λ	see eqs (5.1-3)	-
Λ_c, Λ_h, Λ_r, Λ_w, Λ_α, Λ_γ	see section 5.1.2	-
Λ_e	see section 5.3.1	-
μ	chemical potential per unit volume of adsorbed film, cf section 4.2.4	$[M/L\theta^2]$
ξ	cf eqs (1.21-28)	-
π	film pressure, cf eq (4.2)	$[M/\theta^2]$
ρ	density	$[M/L^3]$
ρ_A	mass concentration of component A	$[M/L^3]$
τ	tortuosity, cf section 1.4.1	-
ϕ	angle, cf section 5.2.2	-
Ψ	capillary potential, pressure height, cf eqs (1.7) and (1.9)	$[L]$

subscripts

L	liquid
LV	liquid-vapour interface
S	solid
SL	solid-liquid interface
SV	solid-vapour interface

superscript

d	contribution of the dispersion forces

other symbols

$\equiv$	is defined as, is equivalent to
$\propto$	is proportional to
$\simeq$	is approximately equal to
$\rightarrow$	generates, gives rise to (in chapter 5)

BIBLIOGRAPHY

1. R.E. Collins, The Flow of Fluids through Porous Materials, Reinhold, New York (1961).
2. J. Bear, Dynamics of Fluids in Porous Media, Elsevier, New York (1972).
3. A.E. Scheidegger, The Physics of Flow through Porous Media, Univ. Toronto Press, Toronto (1960).
4. A.V. Luikov, Heat and Mass Transfer in Capillary-Porous Bodies, Pergamon, London (1966).
5. E. Manegold, Kapillarsysteme, Band I, Chemie & Technik Verl., Heidelberg (1955).
6. E. Manegold, Kapillarsysteme, Band II, Chemie & Technik Verl., Heidelberg (1960).
7. A.W. Lykow, Transporterscheinungen in kapillarporösen Kõrpern, Akademie Verl., Berlin (1958).
8. W.A. Gray, The Packing of Solid Particles, Chapman & Hall, London (1968).
9. F.A.L. Dullien and V.K. Batra, Ind. Eng. Chem. 62 (10) (1970) 25.
10. D.P. Haughey and G.S.G. Beveridge, Can. J. Chem. Eng. 47 (1969) 130.
11. L.C. Graton and H.J. Fraser, J. Geol. 43 (1935) 985.
12. J. Hrubísek, Kolloid Beih. 53 (1941) 385.
13. K.E. Zimens, in: Handb. der Katalyse, Springer, Vienna, 4 (1943) 153.
14. Methoden der Strukturuntersuchung an hochdispersen und porösen Stoffen, H. Witzman, Ed., Akademie Verl., Berlin (1961).
15. J.M. Dalla Valle, Micromeritics, Pitman, London (1948).
16. P.C. Carman, Flow of Gases through Porous Media, Butterworth, London (1956).
17. J. Happel and H. Brenner, Low Reynolds-number Hydrodynamics, Prentice Hall, New Jersey (1965).
18. R.B. Keey, Drying Principles and Practice, Pergamon, Oxford (1972).
19. P.C. Carman, Trans. Inst. Chem. Engrs. 15 (1937) 151.
20. O. Krischer, Die wissenschaftliche Grundlagen der Trocknungstechnik, Springer, Berlin (1963).
21. A.W. Lykow, Experimentelle und theoretische Grundlagen der Trocknung, VEB, Verlag Technik, Berlin (1955).
22. F. Moore, Trans. Brit. Ceram. Soc. 60 (1961) 517.
23. G.D. Fulford, Can. J. Chem. Eng. 47 (1969) 378.
24. A.V. Lykov, Int. Chem. Eng. 10 (1970) 599.
25. C.N. Satterfield, Mass Transfer in Heterogeneous Catalysis, MIT, Cambridge (1970).
26. G.R. Youngquist, Ind. Eng. Chem. 62 (8) (1970) 52.
27. Poristaya Struktura Katalizatorov i Protsessy Perenoso v Geterogennom Katalize, G.K. Boreskov, Ed., Novosibirsk (1970).
28. P.S. Eagleson, Dynamic Hydrology, McGraw Hill, New York (1970).
29. R.J.M. de Wiest, Flow through Porous Media, Academic Press, New York (1969).
30. M. Muskat, The Flow of Homogeneous Fluids through Porous Media, J.W. Edwards, New York (1946).
31. V.I. Aravin and S.N. Numerov, Theory of Fluid Flow in Undeformable Porous Media, IPST (Israel Program of Scientific Translations), Jerusalem (1965).
32. Soil Sci. 113 (4) (1972).
33. E.C. Childs, Soil Water Phenomena, Wiley, London (1969).
34. Water in the Unsaturated Zone, IASH, Unesco, Paris (1968).
35. B.A. Keen, The Physical Properties of the Soil, Butterworth, London (1931).
36. A.N. Puri, Soils: their Physics and Chemistry, New York (1949).
37. Transfer of Water in Porous Media, Rilem Symp., Paris (1964).
38. Final Report 2nd CIB/RILEM Symp., Bouwcentrum, Rotterdam (1974).
39. L. Addleson, Materials for Building, Iliffe, London (1972).
40. G.S.G. Beveridge and D.P. Haughey, Int. J. Heat Mass Trsf. 14 (1971) 1093.
41. C.K. Chan and C.L. Tien, Trans. ASME 95 (1973) 302.
42. A.C. Chen and D.R. Heldman, Trans. ASAE 15 (1972) 951.

43. G.H. Neale and W.K. Nader, A.I.Ch.E.J. 19 (1973) 112.
44. J.P. Breton, Physics Fluids 12 (1969) 2019.
45. J.P. Breton, J. Physique 31 (1970) 613.
46. H.G. Kessler, Thesis, Darmstadt (1961).
47. H.O. Pfannkuch, in: Fund. Trsp. Phen. Por. M., Elsevier, Amsterdam (1972) 42.
48. D.A. de Vries, Meded. Landb. Hogesch. Wageningen 52 (1952) 1.
49. J. van Brakel and P.M. Heertjes, Int. J. Heat Mass Trsf. 17 (1974) 1093.
50. G. Deininger, Ber. Bun. Ges. 77 (1973) 145.
51. J.G. Savins, Ind. Eng. Chem. 61 (10) (1969) 18.
52. H. Darcy, Les Fontaines Publiques de la Ville de Dijon, V. Dalmont, Paris (1856).
53. S. Whitaker, Ind. Eng. Chem. 62 (10) (1970) 54.
54. W.B. Fulks, R.B. Guenther, and E.L. Roetman, Acta Mech. 12 (1971) 121.
55. A. Marmur and E. Rubin, Ind. Eng. Chem. Fund. 11 (1972) 497.
56. L.J. Snyder and W.E. Stewart, A.I.Ch.E.J. 12 (1966) 167.
57. R.A. Greenkorn and D.P. Kessler, Ind. Eng. Chem. 61 (9) (1969) 14.
58. E. Wicke, Ber. Bun. Ges. 77 (1973) 160.
59. A.E. Scheidegger, J. Appl. Phys. 25 (1954) 994.
60. G. de Josselin de Jong, Trans. Am. Geophys. Union 39 (1958) 67.
61. J.W. Hiby, Symp. Interaction Fluids & Particles, Butterworth, London (1962) 312.
62. A. Klute, Soil Sci. 113 (1972) 264.
63. N.R. Morrow, J. Can. Petr. Techn. 10 (Jan.) (1971) 38, 47.
64. L.K. Thomas, D.L. Katz, and M.R. Tek, Soc. Petr. Eng. J. 8 (1968) 174.
65. F.F. Craig, The Reservoir Engineering Aspects of Waterflooding, Am. Inst. Mining, New York (1971).
66. W. Batel, Chem. Ing. Tech. 33 (1961) 541.
67. G.H. Fricke, D. Rosenthal, and G.A. Welford, A.I.Ch.E.J. 19 (1973) 991.
68. T. Katan and E.A. Grens, J. Electrochem. Soc. 118 (1971) 1881.
69. E.W. Otto, Chem. Eng. Progr., Symp. Series 62 (61) (1966) 158.
70. A.M. Schwartz, Ind. Eng. Chem. 61 (1) (1969) 10.
71. H. Künzel and B. Schwarz, Berichte Bauforschung (51) (1968) 99.
72. P. Heizmann, Holz Roh. Werkst. 28 (1970) 295.
73. D.N.R. Smith and W.B. Banks, Proc. Roy. Soc. Lond. B 177 (1971) 197.
74. E. Buckingham. U.S. Dept. Agr., Bureau of Soils, Bull. (38) (1907).
75. N.R. Morrow, Ind. Eng. Chem. 62 (6) (1970) 32.
76. J.C. Melrose, J. Colloid Interf. Sci. 38 (1971) 212.
77. L.M. Skinner and J.R. Sambles, Aerosol Science 3 (1972) 199.
78. J.R. Philip, Adv. Hydroscience 5 (1969) 215.
79. R. Lucas, Kolloid Z. 23 (1918) 15.
80. E.W. Washburn, Phys. Rev. 17 (1921) 273.
81. J.M. Bell and F.K. Cameron, J. Phys. Chem. 10 (1906) 659.
82. J. Kozeny, Sitz. Ber. Akad. Wiss. Wien, Abt. IIA, 136 (1927) 271.
83. G. Pickett, J. Appl. Phys. 15 (1944) 623.
84. A.P. Porhaev, Kolloid Zh. 11 (1949) 346.
85. J. Szekely, A.W. Neumann, and Y.K. Chuang, J. Colloid Interf. Sci. 35 (1971) 273.
86. R.J. Good, J. Colloid Interf. Sci. 42 (1973) 473.
87. D. Croney, J.D. Coleman, and P.M. Bridge, Road Res. Techn. Paper no. 24, Dept. Sci. & Ind. Res., London (1952).
88. N.R. Morrow and C.C. Harris, Soc. Petr. Eng. J. 5 (1965) 15.
89. W. Fischer and D. John, Messtechnik 76 (1968) 309.
90. H.L. Ritter and L.C. Drake, Ind. Eng. Chem., Anal. Ed. 17 (1945) 782.
91. H.M. Rootare, Perspect. Powder Met. 5 (1970) 225.
92. W.K. Bell, Mercury Penetration and Retraction Hysteresis in Closely Packed Spheres, Univ. Technol. Delft (1972).
93. P.M. Heertjes and W.C. Witvoet, Tenside Detergents 8 (1971) 248.
94. P.M. Heertjes and W.C. Witvoet, Powder Technol. 3 (1969/70) 339.

95. D.R. Oliver and D.L. Clarke, The Chem. Eng. (2) (1971) 58.
96. F.W. Crawford and G.M. Hoover, J. Geophys. Res. 71 (1966) 2911.
97. A. Endo, M. Suzuki, and S. Ohtani, Kag. Kog. 34 (1970) 299.
98. M. Suzuki and S. Maeda, J. Chem. Eng. Japan 1 (1968) 26.
99. J.C.P. Broekhoff and B.G. Linsen, Phys. & Chem. Aspects Adsorbents & Catalysts (B.G. Linsen, Ed.), Academic Press, London (1970) 1.
100. D.A. Rose, Bull. Rilem (29) (1965) 119; J. Soil Sci. 22 (1971) 490.
101. N.V. Churaev, Inzh. Fiz. Zh. 23 (1972) 807.
102. Water in the Unsaturated Zone, IASH, Unesco, Paris (1968) 761-800.
103. W. Drost-Hansen, in: Chemistry and Physics of Interfaces (S. Ross, Ed.), Am. Chem. Soc., Washington, 2 (1971) 203.
104. B.V. Deryagin, Ed., Research in Surface Forces, vol. 3, Consultants Bureau, New York (1971).
105. H. Sawistowski, Chem. Ing. Tech. 45 (1973) 1093.
106. P.C. Wayner, Int. J. Heat Mass Trsf. 15 (1972) 1851; 16 (1973) 1777.
107. E. Buckingham. U.S. Dept. Agr., Bureau of Soils, Bull. (25) (1904).
108. H. Rumpf and A.R. Gupte, Chem. Ing. Tech. 43 (1971) 367.
109. E.G. Youngs, Soil Sci. 86 (1958) 117, 202; 97 (1964) 307.
110. G.E. Laliberte, A.T. Corey, and R.H. Brooks, Hydrol. Papers Colorado State Univ. (17) (1966).
111. D.H. Lester, Thesis, Rochester (1969).
112. Ch. Marle, R. Albert, and M. Sardé, Rev. I.F.P., hors série 18 (1963) 162.
113. O. Molerus, M.H. Pahl, and H. Rumpf, Chem. Ing. Techn. 43 (1971) 376.
114. W.H. Gauvin and S. Katta, A.I.Ch.E.J. 19 (1973) 775.
115. J. Happel, A.I.Ch.E.J. 4 (1958) 197; 5 (1959) 174.
116. S. Kuwabara, J. Phys. Soc. Japan 14 (1959) 527.
117. N. Epstein and J.H. Masliyah, Chem. Eng. J. 3 (1972) 169.
118. R.B. Evans, G.M. Watson, and E.A. Mason, J. Chem. Phys. 35 (1961) 2076; 36 (1962) 1894; E.A. Mason, A.P. Malinouskas, and R.B. Evans, J. Chem. Phys. 46 (1967) 3199.
119. S. Irmay, Bull. Rilem (29) (1965) 37.
120. A.E. Scheidegger and K.H. Liao, in: Fund Trsp. Phen. Por. M., Elsevier, Amsterdam (1972) 3.
121. J. Bear and C. Braester, in: Fund. Trsp. Phen. Por. M., Elsevier, Amsterdam (1972) 177.
122. J.C. Slattery, A.I.Ch.E.J. 16 (1970) 345.
123. M.D. Burghardt and W.W. Bowley, Powder Technol. 6 (1972) 51.
124. S.R. de Groot and P. Mazur, Non-Equilibrium Thermodynamics, North-Holland, Amsterdam (1962).
125. P.H. Groenevelt and G.H. Bolt, J. Hydrol. 7 (1969) 358.
126. J. Valchár. Proc. 3rd Int. Heat Trsf. Conf., 1 (1966) 409.
127. W.E. Ranz, Colloq. Int. C. Nat. Rech. Sci. 160 (1966) 47.
128. J.R. Philip and D.A. de Vries, Trans. Am. Geophys. Union 38 (1957) 222; 39 (1958) 909.
129. D. Hansen, W.H. Breyer, and W.J. Riback, Trans. ASME, J. Heat Trsf. 92 (1970) 520.
130. D. Berger and D.C.T. Pei, Int. J. Heat Mass Trsf. 16 (1973) 293.
131. S.V. Shishkov, J. Appl. Chem. USSR 38 (1965) 304.
132. A.V. Luikov, Colloq. Int. C. Nat. Rech. Sci. 160 (1966) 21.
133. A.V. Luikov, J. Eng. Phys. 9 (1965) 189.
134. S.A. Tanaeva, J. Eng. Phys. 9 (1965) 589.
135. S.A. Tanaeva, J. Eng. Phys. 10 (1966) 32.
136. N. Bjerrum and E. Manegold, Kolloid Z. 43 (1927) 5.
137. C.S. Slichter, 19th Annual Report U.S. Geol. Survey, part II, (1899) 295.
138. F.E. Bartell, Ind. Eng. Chem. 19 (1927) 1277.
139. J. Letey, J. Osborn, and R.E. Pelishek, Soil Sci. 93 (1962) 149.
140. D. Renzow, W. Tanner, W. Leiner, and P.J. Sell, Farbe Lack 79 (1973) 1158.
141. P.C. Carman, Soil Sci. 52 (1941) 1.

142. A. Mitscherlich, Bodenkunde, P. Parey, Berlin (1905) 169.
143. D. Brauns and K. Schneider, Chem. Ing. Techn. 38 (1966) 38.
144. B.V. Deryagin, Kolloid Zh. 8 (1946) 27.
145. N.U. Koida and M.A. Bukhbinder, Russ. J. Phys. Chem. 35 (1962) 1205.
146. L.I. Kuzmin and G.P. Postnikov, Ind. Lab. 35 (1969) 1800.
147. B.V. Deryagin, M.K. Melnikova, and V.I. Krylova, Coll. J. USSR 14 (1952) 459.
148. E.H. Lucassen-Reynders, Thesis, Utrecht (1962); J. Phys. Chem. 67 (1963) 969.
149. P.C. Carman, Disc. Far. Soc. (3) (1948) 72.
150. F.C. Blake, Trans. Am. Inst. Chem. Engrs. 14 (1922) 415.
151. G.M. Fair and L.P. Hatch, J. Am. Water Works Ass. 25 (1933) 1551.
152. M.J. Boussinesq, J. de Math. (2) 13 (1868) 377.
153. D.S. Scott and F.A.L. Dullien, A.I.Ch.E.J. 8 (1962) 113.
154. L.B. Rothfeld, A.I.Ch.E.J. 9 (1963) 19.
155. A. Wheeler, Catalysis 2 (1955) 105.
156. W. Rose and W.A. Bruce, Trans. AIME 186 (1949) 127.
157. M.R.J. Wyllie and W.D. Rose, Trans. AIME 189 (1950) 105.
158. W. Rose and M.R.J. Wyllie, Trans. AIME 186 (1949) 329.
159. O.F. Thornton, Trans. AIME 186 (1949) 186.
160. M.A. Bukhbinder, Kolloid Zh. 27 (1965) 661.
161. A.J. de Bethune and R.L. Rowell, J. Phys. Chem. 67 (1963) 2065.
162. E.A. Floot, R.H. Tomlinson, and A.E. Seger, Can. J. Chem. 30 (1952) 348.
163. W.R. Purcell, Trans. AIME 186 (1949) 186.
164. M.R.J. Wyllie and M.R. Spangler, Bull. Am. Assoc. Petrol. Geol. 36 (1952) 359.
165. I. Fatt and H. Dijkstra, Trans. AIME 192 (1951) 249.
166. J. Paczirszky, Comptes Rendus 2ième Colloq. ARTFP, (1965) 247.
167. N.T. Burdine, L.S. Gournay, and P.P. Reicherts, Trans. AIME 189 (1950) 195; 198 (1953) 71.
168. M.R.J. Wyllie and A.R. Gregory, Ind. Eng. Chem. 47 (1955) 1379.
169. G.A. Turner, Chem. Eng. Sci. 7 (1958) 156; 10 (1959) 14.
170. M.F.L. Johnson and W.E. Stewart, J. Cat. 4 (1965) 248.
171. A.N. Braslavskii, J. Appl. Chem. USSR 34 (1961) 769; 35 (1962) 2141; 36 (1963) 2648.
172. W.F. Cammerer, V.D.I. Forschungsh. (500) (1962).
173. S. Ohtani, M. Suzuki, and S. Maeda, Chem. Eng. Japan 2 (1964) 38.
174. S. Ohtani and S. Maedo, Chem. Eng. Japan 2 (1964) 220.
175. F. Kastanek, J. Hydrol. 14 (1971) 213; 16 (1972) 267; 17 (1972) 247.
176. E. Sommer, Thesis, Darmstadt (1971).
177. H. Adzumi, Bull. Chem. Soc. Japan 12 (1937) 199, 285, 292, 304.
178. R.N. Foster and J.B. Butt, A.I.Ch.E.J. 12 (1966) 180.
179. M.R.J. Wyllie and G.H.F. Gardner, World Oil, April (1958) 210.
180. E.C. Childs and N. Collis George, Proc. Roy. Soc. Lond. A201 (1950) 392.
181. T.J. Marschall, J. Soil Sci. 9 (1958) 1.
182. R.J. Millington and J.P. Quirk, Nature 183 (1959) 387.
183. R.J. Millington and J.P. Quirk, Trans. Far. Soc. 57 (1961) 1200.
184. R.J. Millington, Science 130 (1959) 100.
185. T.J. Marshall, Symp. Interaction Fluids & Particles, Butterworth, London (1962) 299.
186. R.J. Millington and R.C. Shearer, Soil Sci. 111 (1971) 372.
187. N.F. White, D.K. Sunada, H.R. Duke, and A.T. Corey, Soil Sci. 113 (1972) 7.
188. J.P. Herzig, D.M. Leclerc, and P. Le Goff, Ind. Eng. Chem. 62 (5) (1970) 8.
189. J.A. Currie, Brit. J. Appl. Phys. 11 (1960) 314, 318.
190. A.S. Michaels, A.I.Ch.E.J. 5 (1959) 290.
191. E.E. Petersen, A.I.Ch.E.J. 4 (1958) 343.
192. J.H. de Boer, Proc. 10th Symp. Colston Res. Soc., Butterworth, London (1958) 68.
193. W.O. Smith, P.D. Foote, and P.F. Busang, Physics 1 (1931) 18; W.O. Smith, Physics 4 (1933) 184, 425.

194. M.M. Kusakov and D.N. Nekrasov, Dokl. AN SSSR 119 (1958) 107; D.N. Nekrasov and M.M. Kusakov. Dokl. AN SSSR 133 (1960) 1379.
195. M. Svatá, Powder Technol. 5 (1971/72) 345.
196. W.R. Purcell, Trans. AIME 189 (1950) 369.
197. N.F. Astbury, Trans. Brit. Ceram. Soc. 67 (1968) 319; 79 (1971) 77.
198. A.C. Paytakes, C. Tien, and R.M. Turian, A.I.Ch.E.J. 19 (1973) 58, 67.
199. W. Batel, Chem. Ing. Tech. 31 (1959) 388.
200. P.B. Weisz and A.B. Schwartz, J. Cat 1 (1962) 399.
201. R. Aris, Chem. Eng. Sci. 11 (1959) 194.
202. A.N. Braslavskii, V.V. Darvin, E.S. Roskin, and S.N. Ivanova, Russ. J. Phys. Chem. 43 (1970) 1814.
203. I. Fatt. J. Petrol. Technol. 8 (1956) 144.
204. I. Fatt, Science 131 (1960) 158.
205. R.M. Weinbrandt and I. Fatt, J. Petrol. Technol. 21 (1969) 543.
206. I. Fatt, J. Inst. Petroleum 52 (1966) 231.
207. I. Fatt, J. Phys. Chem. 63 (1959) 751; 64 (1960) 1162; 65 (1961) 1709.
208. I. Fatt, Symp. Interact. Fluids & Particles, Butterworth, London (1962) 304.
209. C.G. Dodd and O.G. Kiel, J. Phys. Chem. 63 (1959) 1646.
210. C.C. Harris, Nature 205 (1965) 353.
211. H. Schubert, Chem. Ing. Tech. 45 (1973) 396.
212. N. Wakao and J.M. Smith, Chem. Eng. Sci. 17 (1962) 825.
213. K.P. Stark, in: Fund. Trsp. Phen. Por. M., Elsevier, Amsterdam (1972) 86.
214. E.F. Adams, Thesis, Rensselaer Polytechnic Inst., Troy, N.Y. (1962).
215. W.B. Haines, J. Agric. Sci. 17 (1927) 264; 20 (1930) 97.
216. E.C. Sewell and W.W. Watson, Bull. Rilem (29) (1965) 125.
217. D. Dollimore and G.R. Heal, J. Colloid Interf. Sci. 42 (1973) 233.
218. S. Kruyer, Trans. Far. Soc. 54 (1958) 1758.
219. N.H. Ceaglske and O.A. Hougen, Trans. Am. Inst. Chem. Engrs. 33 (1937) 283.
220. J.F. Pearse, T.R. Oliver, and D.M. Newitt, Trans. Inst. Chem. Engrs. 27 (1949) 1; T.R. Oliver and D.M. Newitt, ibid 27 (1949) 9.
221. W.O. Smith, P.D. Foote, and P.F. Busang, Phys. Rev. 24 (1929) 1271.
222. W.O. Smith, Physics 3 (1932) 139.
223. R.P. Mayer and R.A. Stowe, J. Colloid Sci. 20 (1965) 893.
224. R.P. Mayer and R.A. Stowe, J. Phys. Chem. 70 (1966) 3867.
225. L.K. Frevel and L.J. Kressley, Anal. Chem. 35 (1963) 1492.
226. K. Yamaguchi, Kag. Kog. 29 (1965) 83.
227. H.M. Princen, J. Colloid Interf. Sci. 30 (1969) 69, 359; 34 (1970) 171.
228. D.H. Everett, Proc. 10th Symp. Colston Res. Soc., Butterworth, London (1958) 95.
229. M.E. Wise, Philips Res. Rep. 7 (1952) 321; 15 (1960) 101.
230. M.J. Hogendijk, Philips Res. Rep. 18 (1963) 109.
231. J.D. Bernal and J. Mason, Nature 188 (1960) 910.
232. R. Ben Aïm and P. Le Goff, Powder Technol. 2 (1968) 1.
233. G. Mason, J. Colloid, Interf. Sci. 35 (1971) 279; 41 (1972) 208.
234. R. Ben Aïm, P. Le Goff, and P. Le Lec, Powder Technol. 5 (1971/72) 51.
235. R.N. Foster, J.B. Butt, and H. Bliss, J. Cat. 7 (1967) 191.
236. O.S. Ksenzhek, Russ. J. Phys. Chem. 37 (1963) 691.
237. D. Nicholson, Trans. Far. Soc. 64 (1968) 3416; 66 (1970) 1713.
238. D. Nicholson and J.H. Petropoulos, J. Phys. D4 (1971) 181.
239. W. Rose, Illinois State Geol. Survey, Circ. 237, Urbana (1957).
240. J.G. Owen, Trans. AIME 195 (1952) 169.
241. T. Tabuchi, Soil Sci. 102 (1966) 161, 329; 112 (1971) 448.
242. R.P. Iczkowski. Ind. Eng. Chem. Fund. 6 (1967) 263.
243. R.P. Iczkowski. Ind. Eng. Chem. Fund. 7 (1968) 572.
244. R.P. Iczkowski, Ind. Eng. Chem. Fund. 9 (1970) 674.
245. P. Le Goff and J. Delachombre, Rev. Franç. Corps Gras 12 (1) (1965) 3.
246. L.M. Pis'men, Soviet Electrochem. 9 (1973) 251, 388.

247. R.E. Peck, D.A. Max, and M.S. Ahluwalia, Chem. Eng. Sci. 26 (1971) 389.
248. G. de Josselin de Jong, in: Fund. Trsp. Phen. Por. M., Elsevier, Amsterdam (1972) 259.
249. P.G. Saffman, J. Fluid. Mech. 6 (1959) 321; 7 (1960) 194.
250. R.E. Haring and R.A. Greenkorn, A.I.Ch.E.J. 16 (1970) 477.
251. R.J. Pakula and R.A. Greenkorn, A.I.Ch.E.J. 17 (1971) 1265.
252. G. Matheron, Eléments pour une Théorie des Milieux Poreux, Masson, Paris (1967).
253. J.A. Guin, D.P. Kessler, and R.A. Greenkorn, Ind. Eng. Chem. Fund. 11 (1972) 477.
254. J.A. Guin, D.P. Kessler, and R.A. Greenkorn, Chem. Eng. Sci. 26 (1971) 1475.
255. R.S. Schlechter and J.L. Gidley, A.I.Ch.E.J. 15 (1969) 339.
256. D.E. Lamb and R.H. Wilhelm, Ind. Eng. Chem. Fund. 2 (1963) 173.
257. H. Balduin, Tonind. Ztg. 92 (1968) 353.
258. Z. Horák and P. Schneider, Chem. Eng. J. 2 (1971) 26.
259. O.S. Ksenzhek, E.A. Kalinovskii, S.A. Petrova, and V.I. Sitvinova, Russ. J. Phys. Chem. 41 (1967) 856.
260. R.M. Barrer and D. Nicholson, Brit. J. Appl. Phys. 16 (1965) 1377.
261. F.A.L. Dullien and M.I.S. Azzam, A.I.Ch.E.J. 19 (1973) 222.
262. W. Rose and P.A. Witherspoon, Illinois State Geol. Survey, Circ. 224, Urbana (1956).
263. W. Rose, Bull. Ill. Geol. Survey (80) (1957) 147.
264. R. Ehrlich and F.E. Crane, Soc. Petr. Eng. J. 9 (1969) 221.
265. N.R. Morrow, Chem. Eng. Sci. 25 (1970) 1799.
266. D.H. Everett and J.M. Haynes, J. Colloid Interf. Sci. 28 (1972) 125.
267. A. Reverbei, G. Ferraiolo, and A. Peloso, Ann. Chim. 56 (1966) 1552.
268. G.C. Topp and E.E. Miller, Soil Sci. Soc. Am. Proc. 30 (1966) 156.
269. G. Vachaud and J.L. Thony, Water Res. Res. 7 (1971) 111.
270. A. Poulovassilis and E.C. Childs, Soil Sci. 112 (1971) 301.
271. A. Poulovassilis, Soil Sci. 93 (1962) 405.
272. J. Mualem, Water Res. Res. 9 (1973) 1324.
273. F.A. Dullien, in: Fund. Trsp. Phen. Por. M., Elsevier, Amsterdam (1972) 67.
274. M.A. Al'tschuler, Kolloid Zh. 23 (1961) 646.
275. R.H. Beresford, in: A Course on Particle Technology, Loughborough Univ., Noordwijk (1970).
276. J.D. Bernal, S.V. King, and J.L. Finney, Disc. Far. Soc. (43) (1967) 60,75.
277. J.L. Finney, Proc. Roy. Soc. Lond. A 319 (1970) 479.
278. J.A. Dodds and P.J. Lloyd, Powder Technol. 5 (1971/72) 69.
279. R.T. De Hoff, in: Characterization of Ceramics (L.L. Hench and R.W. Gould, Eds.), Dekker, New York (1971) 530.
280. H. Rumpf, S. Debbas, and K. Schönert, Chem. Ing. Tech. 39 (1967) 126.
281. A.R. Gupte, Chem. Ing. Tech. 43 (1971) 754.
282. S. Debbas, Thesis, Karlsruhe (1965).
283. H. Robel and E. Wiegand, Chem. Tech. Leipzig 25 (1973) 550.
284. J.R.F. Arthur and T. Dunstan, Nature 223 (1969) 464.
285. H. Brusset, J.R. Donati, and B. Pascal, C.R.Ac. Sci. Paris B 264 (1967) 175.
286. A.I. Aganov, Zh. Tekhn. Fiz. 6 (1936) 1601.
287. L.A. Plotnikov, Zav. Lab. 15 (1949) 494.
288. H.O. Pfannkuch, Int. Geol. Congr., section 11 (1972) 191.
289. M.E. Lago, U. Böhm, and F. Plachco, Int. J. Heat Mass Trsf. 14 (1971) 813.
290. D.E. Felch and F.O. Shuck, Ind. Eng. Chem. Fund. 10 (1971) 299; 11 (1972) 282.
291. Humidity and Moisture, A. Wexler, Ed., 4 (1965).
292. D.P. Litevchuk and M.F. Kazanskii, Inzh. Fiz. Zh. 23 (1972) 294.
293. J.C. Calhoun, M. Lewis, and R.C. Newman, Trans. AIME 186 (1949) 189.
294. J. van Brakel and P.M. Heertjes, paper 2.1.3 of ref. (38).
295. B. Schindler, Thesis, Stuttgart (1973).
296. R.R. Goddard, G.H.F. Gardner, and M.R.J. Wyllie, Symp. Interact. Fluids & Part., Butterworth, London (1962) 326.

297. M. Vilain and J.P. Druelle, C.R. Ac. Sci. Paris D 271 (1970) 2269.
298. M. Svatá, Powder Technol. 2 (1969) 311.
299. M. Svatá and Z. Zábranský, Powder Technol. 2 (1968) 159.
300. M.R.J. Wyllie and W.D. Rose, Nature 165 (1950) 972.
301. W. Lohre, Tonind. Ztg. 83 (1959) 334.
302. F.E. Hackett, Trans. Far. Soc. 17 (1921) 260.
303. K.A. Smith, A.F. Sarofin, and G. Margolis, Report No. 295-14, DSR 70877, M.I.T., Cambridge (1970).
304. B. Schindler and P.-J. Sell, Chem. Ing. Tech. 45 (1973) 583.
305. W.W. McLaughlin, U.S. Dept. Agric., Bull. (835) (1920); (1221) (1924).
306. S. Krawkow, J. Landw. (1900) 209.
307. A. Attenberg, Land. Vers. Sta. 69 (1918) 93; Chem. Zeitung 29 (1905) 196.
308. H.A. Wadsworth, Soil Sci. 32 (1931) 417.
309. R.L. Peck and D.A. McLean, Ind. Eng. Chem., Anal. Ed. 6 (1934) 85.
310. to be published.
311. C.B. Orr, Powder Technol. 3 (1969/70) 117.
312. L.J. Klinkenberg, Trans. AIME 210 (1957) 366.
313. M.C. Leverett, Trans. AIME 142 (1941) 152.
314. A. Houpeur, Rev. Inst. Fr. Pétrole 14 (11-12) (1959).
315. H.I. Meyer, J. Appl. Phys. 24 (1953) 510.
316. G. Bockstiegel, Proc. (1965) Int. Powder Met. Conf., 1 (1966) 155.
317. K.K. Watson, Water Res. Res. 2 (1966) 709.
318. J. van Brakel and P.M. Heertjes, Powder Technol. 9 (1974) 263.
319. M. Svatá and Z. Zábranský, Powder Technol. 3 (1970) 296.
320. G.P. Wotzak, A.I.Ch.E.J. 20 (1974) 197.
321. E.A. Flood, Proc. 10th. Symp. Colston Res. Soc., Butterworth, London (1958) 151.
322. F.A. Soeiro, Bull. Rilem (29) (1965) 137.
323. J.A. Guin, D.P. Kessler, and R.A. Greenkorn, Phys. Fluids 14 (1971) 181.
324. D.P. Litevchuk, M.F. Kazansky, and P.P. Lutzik, Inzh. Fiz. Zh. 23 (1972) 145.
325. A. Arbhabhirama and Z.U. Ahmed, Water Res. Res. 9 (1973) 401.
326. A.V. Bautin, N.S. Lidorenko, I.B. Rubashov, and V.M. Smirnov, Dokl. Phys. Chem. 211 (1973) 570.
327. F.A.L. Dullien and G.K. Dhawan, J. Colloid Interf. Sci. 47 (1974) 337.
328. J. Versluys, Thesis, Amsterdam (1916); Int. Mitteil. f. Bodenk. 7 (1917) 117.
329. E.W. Washburn, Proc. N.Y. Acad. Sci. 7 (1921) 115.
330. L.M. Pismen, Chem. Eng. Sci. 29 (1974) 1227.
331. E.E. Underwood, Quantitative Stereology, Addison-Wesley, Reading, Mass. (1970).
332. D.A. Farrell and W.E. Larson, Water Res. Res. 8 (1972) 699.
333. J.R. Philip, Ann. Rev. Fluid Mech. 2 (1970) 177.
334. G.H. Neale and W.K. Nader, A.I.Ch.E.J. 20 (1974) 530.
335. A.N. Braslavskii, J. Appl. Chem. USSR 35 (1961) 2141.
336. E. Wollny, Forsch. Agrik.-Physik 7 (1884) 269.
337. E.W. Hilgard, Soils, Macmillan, London (1906).
338. O.E. Meinzer, U.S. Dept. Interior, Geological Survey, Water-Supply Paper 489, Washington (1923).
339. J.S. Cammerer, Tonindustrie Z. 78 (1954) 199.
340. A.W. Neumann and R.J. Good, J. Colloid Interf. Sci. 38 (1972) 341.
341. V.R. Gray, Wetting, S.C.I. Monograph (25) (1967) 99.
342. R.E. Johnson and R.H. Dettre, Adv. Chem. Series 43 (1964) 112.
343. A.W. Neumann, D. Renzow, H. Reumuth, and I.E. Richter, Fortschr. Kolloide Polymere 55 (1971) 49.
344. R.N. Wenzel, Ind. Eng. Chem. 28 (1936) 988.
345. Y. Tamai and K. Aratani, J. Phys. Chem. 76 (1972) 3267.
346. M. Novotný and A. Zlatkis, Chromatogr. Rev. 14 (1971) 1.

347. J.C. Melrose, J. Soc. Petr. Eng. 5 (1965) 259.
348. N.L. Coleburn and J.L. Shereshefsky, J. Colloid Interf. Sci. 38 (1972) 84.
349. B.F. Howell and J. Lancaster, J. Colloid Interf. Sci. 38 (1972) 633.
350. B.V. Deryagin and N.V. Churaev, Colloid J. USSR 35 (1973) 762; J. Colloid Interf. Sci. 46 (1974) 437.
351. W.J. O'Brien, Surface Sci. 19 (1970) 387; 23 (1970) 427; 25 (1971) 298.
352. G.K. Swinzov, Kolloid Zh. 34 (1972) 396.
353. A.E. Afanas'ev, N.J. Gamayunov, N.V. Churaev, and N.E. Yashenko, Inzh. Fiz. Zh. 22 (1972) 627.
354. Yu.L. Kavkazov, Vzaimodeistviye Kozhi c Vlagoi, Moscow (1952) 77-89.
355. D.D. Eley and D.C. Pepper, Trans. Far. Soc. 42 (1946) 697.
356. T.D. Blake, D.H. Everett, and J.M. Haynes, Wetting, S.C.I. Monograph (25) (1967) 164.
357. S. Wladitchensky, ref. (34) p. 360.
358. V. Ludviksson and E.N. Lightfoot, A.I.Ch.E.J. 14 (1968) 674.
359. R.J. Hansen and T.Y. Toong, J. Colloid Interf. Sci. 37 (1971) 196.
360. H.M. Scholberg, Surface Sci. 28 (1971) 229.
361. A.W. Adamson, Physical Chemistry of Surfaces, Interscience, New York (1967).
362. R.E. Johnson, J. Phys. Chem. 63 (1959) 1655.
363. R.J. Good, Wetting, S.C.I. Monograph (25) (1967) 328.
364. R. Defay and I. Prigogine, Surface Tension and Adsorption, Longmans, London (1966).
365. ref.(361) pp. 350-352.
366. T.D. Blake and W.H. Wade, J. Phys. Chem. 75 (1971) 1887.
367. J.F. Padday, Special Disc. Far. Soc. (1) (1970) 64.
368. I.E. Dzyaloshinskii, E.M. Lifshitz, and L.P. Pitaevskii, Adv. Physics 10 (1961) 165.
369. W.A. Zisman, Ind. Eng. Chem. 55 (10) (1963) 19.
370. W.A. Zisman, Adv. Chem. Series 43 (1964) 1.
371. A.H. Ellison and W.A. Zisman, J. Phys. Chem. 58 (1954) 503.
372. L.A. Girifalco and R.J. Good, J. Phys. Chem. 61 (1957) 904.
373. R.J. Good, Adv. Chem. Series 43 (1964) 74.
374. J.F. Padday, Wetting, S.C.I. Monograph (25) (1967) 345.
375. M.C. Phillips and A.C. Riddiford, Wetting, S.C.I. Monograph (25) (1967) 31.
376. F.M. Fowkes, Adv. Chem. Series 43 (1964) 99.
377. F.M. Fowkes, Wetting, S.C.I. Monograph (25) (1967) 3, 42.
378. F.M. Fowkes, Ind. Eng. Chem. 56 (12) (1964) 40.
379. F.M. Fowkes, in: Treatise on Adhesion and Adhesives (R.L. Patrick, Ed.), Dekker, New York, 1 (1967) 325.
380. J.N. Israelschvili, J. Chem. Soc., Far. Trans. II 69 (1973) 1729.
381. A.D. Read and J.A. Kitchener, Wetting, S.C.I. Monograph (25) (1967) 300.
382. H. Freundlich, Kapillarchemie, Akademische Verl., Leipzig (1922).
383. A.W. Adamson, J. Colloid Interf. Sci. 27 (1968) 180.
384. N.L. Jarvis, R.B. Fox, and W.A. Zisman, Adv. Chem. Series 43 (1964) 317.
385. H.W. Fox and W.A. Zisman, J. Colloid Sci. 7 (1952) 428.
386. H.W. Fox, E.F. Hare, and W.A. Zisman, J. Colloid Sci. 8 (1953) 194.
387. A.M. Schwartz, C.A. Rader, and E. Huey, Adv. Chem. Series 43 (1964) 250.
388. N.R. Morrow and N. Mungan, Rev. Inst. Fr. Pétrole 26 (1971) 629.
389. E.A. Romanov, D.T. Kokorev, and N.V. Churaev, Int. J. Heat Mass Trsf. 16 (1973) 549.
390. G. Quincke, Ann. Physik Chemie 52 (1894) 1.
391. G. Quincke, Ann. Physik Chemie (Pogg. Ann.) 160 (1877) 337, 560.
392. P. Volkmann, Ann. Physik Chemie 53 (1894) 633.
393. W. Kaye, J. Colloid Interf. Sci. 46 (1974) 543.
394. C.L. Watson and J. Letey, Soil Sci. Soc. Am. Proc. 34 (1970) 814.
395. R.G. Frieser, J. Electrochem. Soc. 121 (1974) 669.

396. E.F. Hare and W.A. Zisman, J. Phys. Chem. 59 (1955) 335.
397. A.D. Read and J.A. Kitchener, J. Colloid Interf. Sci. 30 (1969) 391.
398. J. Kloubek, J. Colloid Interf. Sci. 46 (1974) 185.
399. D.H. Bangham and Z. Saweris, Trans. Far. Soc. 34 (1938) 554.
400. B.V. Derjaguin and Z.M. Zorin, Proc. 2nd Int. Congr. Surface Activity, Butterworth, London, 2 (1957) 145.
401. V.D. Sobolev and Z.M. Zorin, ref. (104), p. 29.
402. B.V. Deryagin and L.M. Shcherbakov, Colloid J. USSR 23 (1961) 33.
403. P.P. Zolobarev and N.V. Churaev, Zh. Fiz. Khim. 46 (1972) 1123.
404. N.V. Churaev, Inzh. Fiz. Zh. 23 (1972) 807.
405. B.V. Deryagin, S.V. Nerpin, and N.V. Churaev, Kolloid Zh. 26 (1964) 301.
406. B.V. Deryagin, S.V. Nerpin, and N.V. Churaev, Bull. Rilem (29) (1965) 93.
407. N.V. Churaev and I.G. Ershova, Kolloid Zh. 33 (1971) 771, 913.
408. V.G. Chalenko, Ukr. Khim. Zh. 38 (1972) 150.
409. N.V. Churaev, A.E. Afanas'ev, and N.I. Gamayunov, ref. (104) p. 342.
410. T.D. Blake and W.H. Wade, J. Phys. Chem. 76 (1972) 675.
411. N.V. Churaev, Inzh. Fiz. Zh. 19 (1970) 224.
412. M. Novotný and K. Grohmann, J. Chrom. 84 (1973) 167.
413. D.H. Kaelble, Physical Chemistry of Adhesion, Wiley-Interscience, New York (1971) 180.
414. K. Tesařík and M. Nečasová, J. Chrom. 65 (1972) 39.
415. A. Liberti, in: Gas Chromatography (A.B. Littlewood, Ed.), Elsevier, Amsterdam (1966) 95.
416. F. Farré-Rius, J. Henniker, and G. Guiochon, Nature 196 (1962) 63.
417. H.W. Fox, E.F. Hare, and W.A. Zisman, J. Phys. Chem. 59 (1955) 1097.
418. W.C. Bigelow, D.L. Pickett, and W.A. Zisman, J. Colloid Sci. 1 (1946) 513.
419. F. Schulman and W.A. Zisman, J. Colloid Sci. 7 (1952) 465.
420. E.G. Shafrin and W.A. Zisman, J. Colloid Sci. 7 (1952) 166.
421. K.W. Bewig and W.A. Zisman, J. Phys. Chem. 68 (1964) 1804.
422. M. Nečasová and K. Tesařík, J. Chrom. 79 (1973) 15.
423. M. Blank and R.H. Ottewil, J. Phys. Chem. 68 (1964) 2206.
424. A.W. Adamson and I. Ling, Adv. Chem. Series 43 (1964) 57.
425. J.C. Melrose, Adv. Chem. Series 43 (1964) 158.
426. T.D. Blake, J.L. Cayias, W.H. Wade, and J.Z. Zerdecki, J. Colloid Interf. Sci. 37 (1971) 678.
427. D.H. Bangham, S. Mosallam, and Z. Saweris, Nature 140 (1937) 237.
428. ref. (361) p. 375.
429. C. Pierce and B. Ewing, J. Phys. Chem. 71 (1967) 3408.
430. D.H. Bangham and R.I. Razouk, Trans. Far. Soc. 33 (1937) 1459.
431. ref. (361) p. 559.
432. W.H. Wade and J.W. Whalen, J. Phys. Chem. 72 (1968) 2898.
433. A. Sheludko and D. Platikanov, Kolloid Z. 175 (1961) 150.
434. Y. Murakami, Proc. Int. Congr. Rheol. (1968) 181.
435. N.K. Adam, Adv. Chem. Series 43 (1964) 52.
436. S.J. Gregg and R.I. Razouk, Disc. Far. Soc. (3) (1948) 94.
437. N.K. Adam, in: Waterproofing and Water Repellency (J.L. Moilliet, Ed.), Elsevier, Amsterdam (1963).
438. M.C. Phillips and A.C. Riddiford, J. Colloid Interf. Sci. 41 (1972) 77.
439. K. Kawasaki, J. Colloid Sci. 17 (1962) 169.
440. M. Bonnemay, G. Bronoël, and E. Levart, Electrochim. Acta 9 (1964) 727.
441. M. Shimokawa and T. Takamura, Electroan. Chem. Interf. Electrochem. 41 (1973) 359.
442. E.N. Lightfoot, J. Electrochem. Soc. 113 (1966) 614.
443. R.H. Muller, J. Electrochem. Soc. 113 (1966) 943.
444. F.G. Will, J. Electrochem. Soc. 110 (1963) 145.
445. P. Somasundaran, in: Clean Surfaces (G. Goldfinger, Ed.), Dekker, New York (1970).
446. L. Ter-Minassian-Saraga, Adv. Chem. Series 43 (1964) 232.
447. E.L. Fuller, J. Phys. Chem. 70 (1966) 1633.

448. R.D. van 't Woudt, J. Geophys. Res. 64 (1959) 263.
449. A.S. Michaels and S.W. Dean, J. Phys. Chem. 66 (1962) 1790.
450. L.O. Brockway and R.L. Jones, Adv. Chem. Series 43 (1964) 275.
451. G.E. Boyd and H.K. Livingston, J. Am. Chem. Soc. 64 (1942) 2383.
452. W.D. Bascom, R.L. Cottington, and C.R. Singleterry, Adv. Chem. Series 43 (1964) 355.
453. V. Ludviksson and E.N. Lightfoot, A.I.Ch.E.J. 17 (1971) 1166.
454. E.N. Lightfoot and V. Ludviksson, J. Electrochem. Soc. 113 (1966) 1325.
455. D.H. Gray, Nature 223 (1969) 371.
456. W.B. Hardy, Phil. Mag. 38 (1919) 49.
457. C.E. Schildknecht, Ed., Polymer Processes, Interscience, New York (1956).
458. W.D. Harkins and E.H. Loeser, J. Chem. Phys. 58 (1954) 236.
459. F.M. Fowkes, J. Phys. Chem. 67 (1963) 2538.
460. H.M. Princen, J. Colloid Interf. Sci. 30 (1969) 359.
461. J.A.R. Coutanceau Clarke, Nature 240 (1972) 408.
462. R.A. Fisher, J. Agric. Sci. 16 (1926) 492.
463. L.V. Radushkevich, Izv. Akad. Nauk SSSR (Khim.) 69 (1952) 1008.
464. J.C. Melrose, A.I.Ch.E.J. 12 (1966) 986.
465. W.O. Smith, P.D. Foote, and P.F. Busang, Phys. Rev. 36 (1930) 524.
466. W. von Engelhardt, Proc. 4th World Petr. Congr. (1955), section I/C, paper 4.
467. P.C. Carman, J. Phys. Chem. 57 (1953) 56.
468. J.C. Melrose and G.C. Wallick, J. Phys. Chem. 71 (1967) 3676.
469. W. Rose, J. Appl. Phys. 29 (1958) 687.
470. J.M. Haynes, Thesis, Univ. Bristol (1965).
471. W.O. Smith, P.D. Foote, and P.F. Busang, Physics 1 (1931) 18.
472. F.E. Hackett and J.C. Strettan, J. Agric. Sci. 18 (1928) 671.
473. G. Mason, Nature 217 (1968) 733.
474. G.D. Scott, Nature 194 (1962) 956.
475. G. Mason, Disc. Far. Soc. (43) (1967) 75.
476. D.J. Adams and A.J. Matheson, J. Chem. Phys. 56 (1972) 1989.
477. E.M. Tory, B.H. Church, M.K. Tam, and M. Ratner, Can. J. Chem. Eng. 51 (1973) 484.
478. N.R. Morrow and C.C. Harris, Soc. Petr. Eng. J. 5 (1965) 15.
479. C.C. Harris, A. Jowett, and N.R. Morrow, Trans. Inst. Mining Met. 73 (1964) 335, 519; 74 (1964) 30.
480. J.R. Philip, Soil Sci. Soc. Am. Proc. 35 (1971) 507.
481. H.S.M. Coxeter, Introduction to Geometry, Wiley, New York (1961) 405-412.
482. D.H. Bangham and R.I. Razouk, Trans. Far. Soc. 33 (1937) 1463.
483. L.D. Belyakowa, O.M. Dzhigit, and A.V. Kiselev, Proc. 2nd Int. Congr. Surface Activity, Butterworth, London 2 (1957) 213.
484. G. Curthoys, V. Ya. Davydov, A.V. Kiselev, S.A. Kiselev, and B.V. Kuznetsov, J. Colloid Interf. Sci. 48 (1974) 58.

SAMENVATTING

Het centrale onderwerp van dit proefschrift is een analyse van de verschijnselen die kunnen worden waargenomen wanneer een vloeistof opstijgt in een poreus medium (b.v. water in een stapeling van zandkorrels met een diameter in de orde van 0,4 mm). Deze verschijnselen zijn in twee opzichten problematisch:

(i) Als na de capillaire opstijging de evenwichtstoestand bereikt is, tussen de zwaartekracht en de capillairkracht, wordt soms een brede verzadigingsgradient waargenomen en soms niet. Dat wil zeggen, soms is er een scherpe scheiding en soms een zeer geleidelijke overgang tussen het geheel met vloeistof verzadigde en het droge gedeelte van het poreuze medium.

(ii) In sommige gevallen is na enige minuten evenwicht bereikt (voor de capillaire opstijging van water in grof zand). In andere gevallen echter kan het vele weken duren voordat een evenwichtstoestand bereikt wordt.

De vier combinatiemogelijkheden komen alle voor. Er zijn dus, bij wijze van spreken, in ieder geval vier soorten capillaire opstijging.

De inhoud van het proefschrift valt uiteen in twee delen. Het eerste hoofdstuk bevat de tekst van een overzichtsartikel betreffende het gebruik van capillairmodellen en andere methoden om transportverschijnselen in poreuze media te beschrijven. De nadruk ligt daarbij op capillair vloeistof transport. Het eerste hoofdstuk is enerzijds de inleiding tot de volgende vier hoofdstukken, welke bovengenoemde twee problemen behandelen; anderzijds de endogene verantwoording van het in de volgende hoofdstukken beschreven onderzoek. De belangrijkste conclusies van het eerste hoofdstuk zijn:

(i) De pogingen om capillair vloeistof transport in poreuze media te beschrijven zonder de geometrie van de porieruimte in de beschouwing te betrekken, zijn misplaatst.

(ii) Verschillende transportverschijnselen vereisen verschillende porieruimte modellen. Dit klemt des te meer, daar de in de modellen voorkomende parameters veelal bepaald worden via andere transportverschijnselen dan waarvoor het model gebruikt wordt.

(iii) Capillaire opstijging is het meest gecompliceerde transportverschijnsel in poreuze media. Dit blijkt onder meer uit het

feit, dat geen der in de literatuur voorgestelde porieruimte modellen de mogelijkheid biedt om de bij capillaire opstijging waargenomen verschijnselen zelfs maar kwalitatief te verklaren.

De volgende hoofdstukken zijn in hoofdzaak gewijd aan capillaire opstijging. In het tweede hoofdstuk worden de gebruikte experimentele methoden beschreven en de karakteristieken van de vier soorten capillaire opstijging toegelicht aan de hand van een groot aantal voorbeelden. De meeste experimenten werden uitgevoerd met als vaste fase glasbolletjes, zand of polystyreen bolletjes. Naast water werden verschillende organische vloeistoffen gebruikt als opstijgende vloeistof. In het derde hoofdstuk worden de meer voor de hand liggende hypothesen, welke de verschillende soorten capillaire opstijging zouden kunnen verklaren, geëlimineerd (b.v.: meer of minder homogene korrelstapelingen; insluiting van lucht; capillaire condensatie).

De poging tot een verklaring van de waargenomen verschijnselen wordt in het vierde hoofdstuk ingeleid met de vaststelling van twee empirische wetmatigheden:

(1) Het optreden van een brede verzadigingsgradient in de evenwichtstoestand correleert met een randhoek (bevochtigingshoek) van omstreeks nul graden. Een scherp vloeistoffront correleert met een randhoek die boven een bepaalde kritische waarde ligt.

(2) De langzame evenwichtsinstelling wordt veroorzaakt doordat tijdens de capillaire opstijging de randhoek daalt.

Een groot deel van het vierde hoofdstuk is gewijd aan a priori beschouwingen betreffende de randhoek van verschillende systemen. Het blijkt namelijk, dat een aantal systemen waarvan men dat op theoretische gronden niet zou verwachten een randhoek groter dan nul hebben (b.v. glas-hexaan). Eén van de conclusies is, dat polymoleculaire adsorptie films met een door de vaste fase geïnduceerde structuur vaker voorkomen dan in het algemeen wordt aangenomen. Tenslotte worden in dit hoofdstuk een aantal mechanismen besproken die een dalende randhoek kunnen verklaren. Bij de huidige stand van de wetenschap zijn definitieve conclusies ten aanzien van bovengenoemde wetmatigheid (2) echter nog niet mogelijk.

In het laatste hoofdstuk wordt ingegaan op het mechanisme van het zich voortbewegende vloeistoffront in een onregelmatige bolstapeling, teneinde te komen tot een interpretatie van bovengenoemde wetmatigheid (1). Op basis van a priori beschouwingen en de

experimentele resultaten wordt een verklaring gegeven voor het al dan niet optreden van een verzadigingsgradient. Deze verklaring omvat de volgende stappen:

(a) In het vloeistof-damp grensvlak moeten anticlastische en concave gedeelten onderscheiden worden. (Anticlastisch wil zeggen, dat de kromtestralen een tegengesteld teken hebben.) De anticlastische of α-meniscussen bevinden zich tussen twee bolletjes. De concave of γ-meniscussen bevinden zich tussen drie of meer bolletjes.

(b) Stelle men zich de porieruimte voor als holtes verbonden door vensters tussen drie of meer bolletjes dan kan het transportmechanisme gedacht worden als een continue samenvloeiïng en generatie van meniscussen. De continuïteit van het vloeistof transport wordt bewerkstelligd door twee elkaar ondersteunende mechanismen:
(i) Het vullen van vensters door α-meniscussen die samenvloeien.
(ii) Het vullen van holtes als een aantal vensters gevuld zijn.

(c) De capillaire opstijging is in de eerste plaats afhankelijk van de α-meniscussen. De γ-meniscussen vervullen een ondersteunende functie doch zijn, alleen, niet in staat de transportcontinuïteit te handhaven.

(d) In eerste benadering is de verzadigingsgradient in de evenwichtstoestand een functie van de venstergrootteverdeling. In een onregelmatige bolstapeling komen een groot aantal vensters voor van minimale grootte (te weten het venster tussen drie aanliggende bollen). Indien de α-meniscussen, die deze kleinste vensters vullen, samen met de γ-meniscussen, de transportcontinuïteit kunnen onderhouden zal er geen verzadigingsgradient worden waargenomen.

(e) De kromming van α- en γ-meniscussen hangt op verschillende wijze af van de randhoek. De bijdrage van de γ-meniscussen aan de transportcontinuïteit is groter bij grotere randhoeken. Boven een bepaalde waarde van de randhoek zal de maximale opstijghoogte uitsluitend bepaald worden door de vensters van minimale grootte.

STELLINGEN

1. Zowel voor een historische als voor een kennistheoretische analyse van het statistische waarschijnlijkheidsbegrip is het gewenst te onderscheiden de empirische noties "willekeurigheid" en "relatieve frequentie" en de theoretische notie "gelijkmogelijk".

2. In de literatuur wordt vaak gesteld, dat schrijvers zoals Aristoteles en Cicero het begrip statistische waarschijnlijkheid kenden. Dit is echter zeer de vraag.

   Aristoteles, Analytica Priora 70a3; Rhetorica 1357a34; Physica 196-198a; Metaphysica 1026b,1027a,1064-1065a.
   Cicero, De Divinatione, I,xiii,23; II,vi,16.
   Thomas van Aquino, Summa Contra Gentiles, III,74.
   W. Kneale, Probability and Induction, Oxford (1949) 150.
   F.N. David, Games, Gods & Gambling, Londen (1962) 21-26.
   E.F. Byrne, Probability and Opinion, Den Haag (1968) 189,203,etc.

3. De waarschijnlijkheidsrekening werd voor het eerst maatschappelijk toegepast in 1671, bij resolutie van de Heeren Staten van Hollandt en West-Vrieslandt, op voorstel van Johan de Witt en met een aanbeveling van Hudde.

   J. de Witt, Waerdye van Lyf-Renten naer Proportie van los-renten, D. Bierens de Haan (red.), Haarlem (1879).
   Bouwstoffen voor de Geschiedenis van de Levensverzekeringen en Lijfrenten in Nederland, Amsterdam (1897).
   E.S. Pearson en G. Kendall (red.), Studies in the History of Statistics and Probability, Londen (1970).
   F.N. David, Games, Gods & Gambling, Londen (1962).
   H. Westergaard, Contribution to the History of Statistics, Londen (1932).

4. Het is met de bestaande technieken voor de verwerking van korrel- en poedervormige materialen niet mogelijk om bollen volgens de dichtste stapeling te pakken. Het is daarom niet juist, althans onpraktisch, om voor willekeurige deeltjespakkingen in de praktijk (model: stapeling bollen van gelijke groote) aan te nemen dat de minimaal bereikbare porositeit 26% is. Deze minimaal bereikbare porositeit voor deeltjes van gelijke grootte ware te stellen op 36%.

   G.J. Kok en P.L. Zuideveld, Fysisch-Technische Scheidingsmethoden, Delft (1974) 279.
   S.V. Belov, O.G. Kartuesov en V.M. Polyaev, Soviet Powd. Met. Metal. Ceram. 11 (1972) 733.

5. Er bestaat geen betrouwbare methode om de randhoek van grofkorrelige materialen te bepalen. In het bijzonder kan hiervoor niet de Washburn vergelijking gebruikt worden.

P.M. Heertjes en N.F.W. Kossen, Powder Technology 1 (1967) 33.
W. Schicketanz, Powder Technology 9 (1974) 49.
J. van Brakel, Powder Technology 11 (1975) 91.

6. Waarschijnlijk liggen experimentele moeilijkheden ten grondslag aan de bevreemdende constatering dat verzadigde macroporeuze media uitdrogen in een verzadigde atmosfeer.

Yu.L. Kavkazov, Vzaimodeistviye Kozhi c Vlagoi, Moskou (1952) 77-89.
A.V. Luikov, Heat and Mass Transfer in Capillary-Porous Bodies, Londen (1966) 202,219.

7. Een boek als dat van Keey over drogen had niet gepubliceerd mogen worden. Niet uitgesloten moet worden dat dit een voorbeeld is van een meer algemeen verschijnsel veroorzaakt door de toenemende specialisatie.

R.B. Keey, Drying Principles and Practice, Oxford (1972).

8. Eén van de fundamentele wetten van het marxisme-leninisme, te weten het omslaan van kwantitatieve veranderingen in kwalitatieve, kan met behulp van een aantal eenvoudige experimenten weerlegd worden.

A.W. Lykow, Experimentelle und theoretische Grundlagen der Trocknungstechnik, Voorwoord, Berlijn (1955).
I.M. Bochenski, The Dogmatic Principles of Soviet Philosophy, Dordrecht (1963) 17.
Philosophisches Wörterbuch, art. Qualität und Quantität, Leipzig (1969).

9. Om de periode van constante droogsnelheid te verklaren is het niet nodig om, in strijd met de feiten, aan te nemen dat het oppervlak van het drogende capillair-poreuze materiaal verzadigd is met water.

10. De effectieve diffusiecoëfficiënt voor poreuze media is geen functie van de porositeit alleen.

L.M. Pis'men, Chem. Eng. Sci. 29 (1974) 1227.
J. van Brakel en P.M. Heertjes, Int. J. Heat Mass Trsf. 17 (1974) 1093.

11. Honderden publikaties zijn gewijd aan het verband tussen doorlatendheid, vochtpotentiaal en vochtgehalte van grond. Te betreuren is dat van de vele manjaren die hieraan besteed zijn er niet een aantal gebruikt is om deze grootheden nu eens onafhankelijk van elkaar te meten aan een homogene deeltjespakking.

12. In de taal waarin de resultaten van het natuurwetenschappelijk onderzoek geformuleerd worden komen egocentrische partikels (zoals 'ik', 'deze', 'hier') in het algemeen niet voor. Zo ze voorkomen dienen ze geëlimineerd te kunnen worden.

B.A.W. Russell, An Inquiry into Meaning and Truth, Harmondsworth (1969).

13. Het fundamentele onderscheid tussen, enerzijds het tellen van aanwijsbare entiteiten en anderzijds het meten van fysische grootheden met een, uiteraard, begrensde nauwkeurigheid, wordt verdoezeld door een definitie van meten te geven die georiënteerd is op de wijze waarop entiteiten in de formele wetenschappen geintroduceerd worden.

C.W. Churchman en P. Ratoosh (red.), Measurement: Definitions and Theories, New York (1959).
S. Kanger, Theoria 37 (1972) 1.
L. Tondl, Scientific Procedures, Dordrecht (1973).
D.H. Krantz, R.D. Luce, P. Suppes en A. Tversky, Foundations of Measurement, New York (1971).

14. Tegen Tarski's semantische definitie van het begrip ware volzin kan niet als bezwaar aangevoerd worden dat deze definitie als consequentie heeft dat uitspraken zoals "Als de spin een walvis is dan is de spin een zoogdier", aangeven wat het geval is.

A. Tarski, Logic, Semantics, Metamathematics, Oxford (1956) 152-278.
J.B. Ubbink, Rechtsgeleerd Magazijn Themis (1966) 432.

15. Op goede gronden is te verdedigen dat uitspraken als "De minutenwals van Chopin bestaat uit 140 maten" gelezen dienen te worden als een conjunctie van (i) een particuliere uitspraak met (existentieel) empirisch karakter en (ii) een universele uitspraak met analytisch karakter.

16. Bij een vergelijking van het anaerobe en het aerobe proces voor de zuivering van afvalwater dient de relatief langzame regeneratie van anaerobe microben als een voordeel van het anaerobe proces te worden uitgelegd.

17. In de literatuur is betoogd dat methanogene bacteriën niet op azijnzuur alleen kunnen leven. Dit is vermoedelijk onjuist.

P.H. Smith en R.A. Mah, Appl. Microbiol. 14 (1966) 368.
W.A. Pretorius, Water Res. 6 (1972) 1213.

18. Bunge's uitspraak dat de filosofie van de technologie een onderontwikkeld gebied is, is juist. Zijn eigen bijdrage aan dit onderwerp is een goede illustratie van dit feit.

M. Bunge, Scientific Research, Berlijn, 2 (1967) 121-150.

19. De conclusie van Mitroff en Turoff dat "technologische voorspelling" nooit een zuiver technische of wetenschappelijke aangelegenheid kan worden is misschien wel waar, doch berust op een onjuiste analyse.

I.I. Mitroff en M. Turoff, Technological Forecasting and Social Change 5 (1973) 113.

20. De systeemleer is de metafysica van de technocratie.

L. von Bertalanffy, General System Theory, Harmondsworth (1973).

21. Het serieus nemen van denkers die zich niet gebonden weten door de wetenschappelijke methode en deze vervolgens kritiseren wegens hun tekortschietende wetenschappelijke strengheid is "inconsistent".

R. Bakker, Wijsgerig Perspectief 3 (1962/63) 294.
J.A. de Jong, Een Wijsbegeerte van het Woord, Proefschrift, Amsterdam (1966).

22. Indien de technologie, althans in de huidige culturele context, een heersend karakter heeft, volgt daaruit niet dat ook de wetenschappelijke methode een inherent heersend karakter heeft.

M. Heidegger, Vorträge und Aufsätze, Pfullingen, 2 (1967) 5-62.
J. Habermas, Technik und Wissenschaft als "Ideologie", Frankfurt a/M (1968).

23. Het onderscheid tussen feiten (dat wat, waarschijnlijk, het geval is) en waarden (dat wat men behoort te doen) is fundamenteel. Daaruit volgt echter allerminst, noch is het zo, dat een scheiding tussen (i) de keuze van doelen en (ii) de verwezenlijking van deze doelen, mogelijk is.

Th.W. Adorno e.a., Der Positivismusstreit in der deutschen Soziologie, Neuwied (1969).
H. Krauch, Die organisierte Forschung, Neuwied (1970).

24. Aan de uitspraak dat wetenschap en technologie, in principe, in staat zijn om elk probleem op te lossen liggen tenminste twee, elk op zich hoogst onwaarschijnlijke postulaten ten grondslag: (i) Dat wat door verschillende personen en/of instituties als probleem ervaren wordt één probleem is. (ii) Dat wat als probleem ervaren wordt zonder verlies als wetenschappelijk probleem geformuleerd kan worden.

25. Diepgaande analyses van de wisselwerking tussen wetenschap en maatschappelijke structuren leiden te vaak naar de conclusie dat er meer autonomie en geld beschikbaar gesteld moet worden voor de discipline waarin de onderzoeker, die de conclusie trekt, werkzaam is.

I.L. Horowitz (red.), The Rise and Fall of Project Camelot, Cambridge, Ma. (1970).
G. van Benthem van den Bergh, J.P. Glastra van Loon en E.V.W. Vercruijsse, paper NUFFIC 20th Anniversary Conference (1972).

26. De onderzoekingen die geleid hebben tot de conclusie dat de citeringsgraad een goede maat is om concepties als "kwaliteit van het onderzoek" te meten, besteden, ten onrechte, geen aandacht aan (i) het verschil in publikatiemotivatie in verschillende academische subculturen en (ii) de moedertaal van de onderzoeker. Voorts is het zeer de vraag of de resultaten gegeneraliseerd mogen worden naar andere (sub)disciplines dan die welke onderwerp van onderzoek waren.

J.R. Cole en S. Cole, Social Stratification in Science, Chicago (1973) 21-36.

27. Van het wetenschappelijk personeel in vaste dienst bij de Universiteit kan en mag verlangd worden dat zij eenmaal in de vijf jaar een goed overzichtsartikel publiceren.

28. De bij het onderwijs aan de Universiteit betrokken stafleden dienen, gedurende de eerste jaren na hun indiensttreding, geschoold te worden in de methodologie van hun vakgebied.

29. Formuleringen die suggereren dat binnen het raam van een empirische wetenschap onbetwijfelbare kennis verworven kan worden dienen, met name uit educatief oogpunt, vermeden te worden.

30. Er klopt iets niet met de veel voorkomende gewoonte om in proefschriften wel diegenen te bedanken die, b.v., het proefschrift persklaar helpen maken, doch niet diegenen die, b.v., de spoedeisende bestellingen verzorgen, de apparatuur onderhouden of de begroting van het Instituut verdedigen.

Delft, 12 februari 1975.

J. van Brakel.